DROUGHT MONITORING IN THE SOUTHWESTERN UNITED STATES: ANALYSIS OF SEASONAL PRECIPITATION, MULTISCALAR INDICES, AND SOIL WATER

By

Trevor T. McKellar

A Dissertation Submitted to the Faculty of the

DEPARTMENT OF SOIL, WATER, AND ENVIRONMENTAL SCIENCE

In Partial Fulfillment of the Requirements
For the Degree of

DOCTOR OF PHILOSOPHY

In the Graduate College
UNIVERSITY OF ARIZONA

2022

THE UNIVERSITY OF ARIZONA
GRADUATE COLLEGE

As members of the Dissertation Committee, we certify that we have read the dissertation prepared by: Trevor T. McKellar
titled: DROUGHT MONITORING IN THE SOUTHWESTERN UNITED STATES: ANALYSIS OF SEASONAL PRECIPITATION, MULTISCALAR INDICES, AND SOIL WATER

and recommend that it be accepted as fulfilling the dissertation requirement for the Degree of Doctor of Philosophy.

Michael A Crimmins
Michael Crimmins — Date: Jul 26, 2022

Marcel Schaap
Marcel Schaap — Date: Jul 27, 2022

Craig Rasmussen — Date: Jul 26, 2022

Paul Ferre — Date: Jul 29, 2022

Final approval and acceptance of this dissertation is contingent upon the candidate's submission of the final copies of the dissertation to the Graduate College.

I hereby certify that I have read this dissertation prepared under my direction and recommend that it be accepted as fulfilling the dissertation requirement.

Michael A Crimmins
Michael Crimmins — Date: Jul 26, 2022
Department of Environmental Science

ACKNOWLEDGEMENTS

I would like to thank my advisor and friend, Mike Crimmins, for his support and guidance throughout my graduate academic career. His advice and direction during the development of this dissertation have been instrumental, especially during model development, R-coding, data analysis and interpretation, literature review, and the writing process. I would also like to thank Marcel Schaap, whose expertise with HYDRUS was greatly valued during model development and data interpretation. I would also like to thank Craig Rasmussen and Ty Ferré, whose contributions were greatly beneficial for model development and dissertation framing.

I would like to thank the funding sources for this dissertation: the Climate Assessment for the Southwest (CLIMAS), the UA/NASA Space Grant Graduate Fellowship, and the Department of Environment Science. I would also like to thank local partners of this dissertation: The Nature Conservancy in Tucson, specifically Gita Bodner and Marcos Robles, rangeland managers, ranchers, and environmentalists involved with the Las Cienegas National Conservation Area, and faculty and fellow students of the Environmental Science Department (formerly the Department of Soil, Water, and Environmental Science). Thank you for your support.

Lastly, I would like to thank my family and friends for their support and encouragement throughout this process – I could not have done it without you. Most importantly, I am overwhelmingly grateful for the love and support I received from my girlfriend, Kaitlyn, and dog, Odo. Thanks for your endless love, friendship, and strength.

DEDICATION

For Doug and Mark

TABLE OF CONTENTS

LIST OF FIGURES

ABSTRACT

Drought is a complex, natural hazard that can cause widespread socioeconomic and environmental impacts. Drought can be defined as a water deficit that arises compared to normal conditions and lasts long enough to cause a lasting hydrological imbalance; however, what constitutes normal conditions varies based on the local climate regime and water source being studied. It is therefore that drought can be subjective to the observer and accounting for the correct environmental drivers is important to accurately assess drought impacts. In water-limited ecosystems like the Southwestern United States, hereby referred to as the Southwest, monitoring drought conditions presents unique challenges as annual potential evapotranspiration is significantly greater than precipitation. Primary production of Southwestern vegetation is adapted to the timing and magnitude of soil water recharge from seasonal precipitation. Variations in precipitation timing and magnitude can thus lead to lasting drought impacts and therefore tracking soil water at different depths is key for understanding overall ecosystem health.

Studies have monitored soil water availability by placing Time Domain Reflectometry (TDR) probes at different depths within a soil profile. However, varying measurements between TDR probes due to differences in soil properties, calibration complications, and maintenance issues have led to the lack of long-term, reliable soil water datasets. This has restricted drought analysis using soil water data to a more local scale. As an alternative approach, land managers and decisions makers use meteorological drought indices as proxies for soil water availability. Meteorological drought indices are numerical timeseries that convey the frequency and magnitude of meteorological indicators, such as precipitation and temperature. Examples of meteorological drought indices are the Standardized Precipitation Index (SPI) and Standardized

Precipitation-Evapotranspiration Index (SPEI), which use monthly total precipitation and water balance values, respectively, to communicate drought conditions. A key feature of the SPI and SPEI is the ability to be calculated at any monthly timescale length ('multiscalar'), allowing for drought conditions of different water sources, such as shallow soil water, to be evaluated. Furthermore, the SPI and SPEI require minimal data inputs and are simple to calculate. It is therefore that the SPI and SPEI are commonly used by land managers for drought monitoring and decision making.

Using SPI and SPEI timescales to estimate soil water in the semi-arid Southwest can be complicated as not all falling precipitation can be assumed to infiltrate into a soil profile. This is due to low intensity precipitation events being captured by tree canopy interception or evaporation and increased runoff during high intensity events. These issues complicate objectively identifying the index and timescale length that best represents soil water availability at different depths, leaving a significant gap between applying meteorological drought index information to land management action for the Southwest. Furthermore, the lack on in-situ soil water datasets prevents characterizing the full relationship between index timescale and soil water. Moreover, the lack of soil water datasets limit the study of links between Southwestern climate, intra-annual soil water variability, and soil drought dynamics on a regional scale. This dissertation address these gaps by creating a regional soil water dataset for the Southwestern United States for the purpose of improving drought monitoring and our understanding of drought development in soils.

By coupling sophisticated computer modeling, site-specific soils information, and spatially continuous, high resolution meteorological datasets, this dissertation simulated daily matric potential values from 0-200cm at 240 locations across the Southwest. Through a series of

investigative studies central to the Southwest, this dissertation quantified historical drought events in soils (appendix A), defined the relationship between meteorological drought index timescale and soil water depth (Appendix B), and developed a time-varying approach designed to improve multiscalar index approximation of soil water in climates with seasonal precipitation distributions (Appendix C).

The first study (Appendix A) quantified how changes in the timing or magnitude of seasonal precipitation translated to soil drought onset and cessation patterns. Results showed that annual matric potential values followed a location's seasonal precipitation distribution. Short-term droughts (60 – 270 days) were frequent, and typically resulted from delayed or slowed starts to a locations major rainy season. Long-term droughts (>270 days) were infrequent and occurred only during specific years, requiring anomalous below average precipitation in one or more consecutive rainy seasons to develop. Long-term droughts were more likely to occur in locations with unimodal precipitation distributions (a majority of rain occurring once annually), due to soil water anomalies likely remaining unresolved until the following rainy season. Locations with bimodal precipitation distributions (rainy seasons occurring twice annually) made long-term drought development difficult as consecutive below average rainy seasons were needed.

The second study (Appendix B) defined the relationship between multiscalar index timescale and soil water availability for the Southwest. For all 240 locations, a new matric potential index (MPI) was created at 5cm intervals between 0-200cm and correlated with timescales from 1-24 months for the SPI and SPEI. Results showed the relationship between the highest correlating index timescale at each MPI depth operates roughly on a 1:1 step progression at shallow depths. Further analysis showed that soil type impacts the timescale-depth

relationship, with clay loam soils correlating at longer timescales than sandy soils when correlating with the same depth MPI. Additionally, the SPI produced higher correlations and with the MPI compared to the SPEI. Therefore, this studied recommended SPI usage for shallow (<80cm) soil water monitoring on Southwestern drylands, with a general rule that the relationship between timescale and depth scales linearly in a 1:1 progression. However, if land managers have access to local soils information, it should be consulted given the impacts of soil type on the timescale-depth relationship.

Given the importance of seasonal precipitation timing and magnitude for vegetation productivity, the use of a single multiscalar index timescale is unlikely to fully represent intra-annual variability of soil water. The third study (Appendix C) used a novel approach that created a time-varying multiscalar composite index for the SPI and SPEI ('composites indices') designed to better approximate seasonal soil water variability in the Southwest. The composite indices were compared with the SPI and SPEI using a traditional single timescale to evaluate improvement in soil water approximation at different depths. Results showed that the timescale-varying approach significantly improved the ability of the SPI and SPEI to approximate soil water over the use of a single timescale. Improvements varied by multiscalar index, depth, and soil type. Land managers can benefit from this approach by understanding general seasonal relationships between timescale length and soil water availability.

Together, this dissertation links Southwestern climatology, intra-annual soil water availability, and drought development in soils by creating a regional soil water dataset with high spatial and temporal resolution. This dissertation's findings will aid further research efforts into soil drought dynamics and improve drought monitoring in the semi-arid Southwest. As climate change exacerbates stress on water limited ecosystems, fully utilizing available drought

monitoring strategies is key for forming strong mitigation and adaptation plans. The author of this dissertation hopes these results will benefit land managers and policymakers during the decision-making process and increase usage of multiscalar meteorological indices, such as the SPI and SPEI, as a viable drought monitoring tool of soil water availability in the Southwestern United States.

INTRODUCTION

Drought is a complex, natural hazard that can cause widespread socioeconomic impacts such as decreased agricultural yields, food shortages, reduced hydroelectric power, water quality issues, and human health difficulties (Wilhite and Glantz 1985; Van Loon 2015; Svoboda and Fuchs 2016; Sugg et al. 2020). Droughts naturally occurs in any climate regime, including deserts and rainforests (Svoboda and Fuchs 2016), which can lead to environmental impacts such as transitions from native to non-native grass species (Bodner and Robles 2017), increased wildfire risk (Littell et al. 2016), or, in extreme cases, widescale vegetation die off, such as mortality of pinon pine and juniper trees (Neilson et al. 1992; Breshears et al. 2008; Restaino et al. 2016). With population growth, urban expansion, water security issues, and climate change expected to exacerbate drought impacts over the coming decades (Sugg et al. 2020; Romero-Lankao et al. 2014), it is important to form strong mitigation and adaptation plans by actively monitoring drought conditions.

In general, drought is as a water deficit that arises compared to normal conditions and lasts long enough to cause a lasting hydrological imbalance (Dracup et al. 1980; Wilhite and Glantz 1985; Van Lanen and Peters 2000; Mishra and Singh 2010). However, what constitutes *normal conditions* varies based on the local climate regime and water source being studied (Wilhite and Glantz 1985). Thus, defining drought can be subjective to the observer and it is important to account for different types of droughts to fully understand drought impacts. Traditionally, four major drought types exist – meteorological, hydrological, agricultural, and socioeconomic (Wilhite and Glantz 1985) – each having its own dedicated fields of literature examining drought drivers and impacts. Over recent decades, there has been increased attention to the interplay between fields, specifically meteorological and hydrological, and the role of soil

moisture on climate-soil-vegetation dynamics (Rodriguez-Iturbe 2000). This is particularly important in water-limited dryland ecosystems like the Southwestern United States, hereby referred to as the 'Southwest', where soil water recharge is the primary control of vegetation dynamics (Noy-Meir 1973; Hadley and Szarek 1981; Neilson et al. 1992; Wilcox et al. 2003).

Dryland ecosystems comprise about 40% of the Earth's land area and contain about 38% of global population (Reynolds et al. 2007; Prăvălie 2016). Monitoring drought in dryland environments poses unique challenges, as distinguishing water deficits from background aridity can be problematic due to potential evapotranspiration being significantly greater than precipitation (Wilcox et al. 2003). In the Southwest, semi-arid climatic variability can influence drought development, as higher summer temperatures can increase atmospheric evapotranspirational demand (Weiss et al. 2009), delayed timing in seasonal precipitation can lead to drought onset (Hadley and Szarek 1981; St. George et al. 2010), and below or above average seasonal precipitation can strongly influence future soil water availability (Koehn et al. 2021). Seasonal precipitation timing and magnitude are important for soil water recharge, which is the primary control on vegetation dynamics in dryland ecosystems (Noy-Meir 1973; Hadley and Szarek 1981; Neilson et al. 1992; Wilcox et al. 2003). Tracking soil water availability at different depths is thus key for understanding overall ecosystem health (Lauenroth and Bradford, 2006; Schlaepfer et al. 2012; Biederman et al. 2018; Barnard et al. 2021). Climate change is projected to increase temperatures and change precipitation patterns for the Southwest over the coming decades, leaving southwestern vegetation vulnerable to increased heatwave frequency and drought duration (Romero-Lankao et al. 2014; Bunting et al. 2016). Thus, monitoring soil water availability at different depths is a key area of drought research for the Southwest over the coming decades.

Attempts to characterize soil water impacts on drought development have been ongoing since the mid to late 20th century (Karl and Koscielny 1982; Oglesby and Erickson 1989). Many studies have utilized Time Domain Reflectometry (TDR) probes, which use wave propagation through a soil medium to indirectly measure soil water content (Topp et al. 1980; Emus et al. 2006). Placing TDR probes at different depths within a soil profile can be critical for evaluating plant water availability of different rooting zones. However, many issues exist that limit TDR probe usefulness for analyzing drought on a regional scale. For example, measurements can vary widely (on the order of meters) due to differences in soil bulk density, compaction, hydraulic conductivity, and vegetation (Bradford 1986; Ayers and Bowen 1987; Vaz and Hopmans 2001; Vaz et al. 2001). Additionally, maintaining TDR probes can be expensive and labor intensive (Dobriyal et al., 2012). Furthermore, the lack of long-term, reliable soil moisture datasets continues to be an obstacle, with the need for an online global database being well documented (Robock et al. 2000; Robock et al. 2005; Dorigo et al. 2011; Dorigo et al. 2012).

While using TDR probes would prove to be an ideal drought monitoring approach, the aforementioned issues have restricted drought analysis using *in-situ* soil moisture to a local scale. As an alternative approach, recent studies have utilized remote sensing products to conduct widescale drought analyses (Prigent et al. 2005; Entekhabi et al. 2010; Chan et al. 2016). Advancements in remote sensing technologies have offered the promise of soil moisture estimation from satellite platforms over large areas, however the microwave instrumentation used for soil moisture measurements is limited to the top few centimeters of soil (Dorigo et al. 2011; Reichle et al. 2016; Berg and Sheffield 2018). This has restricted studies utilizing remote sensing technologies to short temporal analysis, low spatial resolution, and shallow depths

(Sheffield et al. 2004; Mo 2008; Notaro et al. 2010; AghaKouchak 2014; Otkin et al. 2016; Martínez-Fernández et al. 2016).

Land managers have thus turned to using drought indices as proxies for soil water availability to conduct regional drought analysis. Drought indices are numerical timeseries that convey the severity of drought indicators, which are variables used to describe drought conditions (Svoboda and Fuchs, 2016). Examples of drought indicators are precipitation, temperature, groundwater, streamflow, snowpack, and soil moisture. Drought indices vary based on ease of use, amount of required input data, and calculation complexity (Svoboda and Fuchs, 2016). Over 70 different drought indices exist and are subdivided into five main categories – meteorology, soil moisture, hydrology, remote sensing, and composite (Svoboda and Fuchs, 2016). No single index measures conditions for every type of drought, and thus dryland managers use a suite of drought indices to evaluate drought conditions.

The Standardized Precipitation Index (SPI) and Standardized Precipitation-Evapotranspiration Index (SPEI) are meteorological drought indices that communicate drought conditions using monthly total precipitation and water balance values, respectively (McKee et al. 1993, Vicente-Serrano et al. 2010). These indices are commonly used by dryland managers for drought monitoring due to minimal input requirements, ease of data availability, and simple calculations (Svoboda and Fuchs 2016). By standardizing index values, the SPI and SPEI communicate statistical severity, frequency, and duration of drought events (McKee et al. 1993, Vicente-Serrano et al. 2010). This is important for dryland managers, as anticipating, preparing, and comparing drought events between locations can aid in fully realizing regional drought impacts (Slette et al. 2019).

A key feature of the SPI and SPEI is that they are multiscalar, meaning they can be calculated at any monthly timescale length (McKee et al. 1993; Vicente-Serrano et al. 2010). This allows for drought conditions of different water sources to be evaluated depending on timescale length (McKee et al. 1993; Vicente-Serrano et al. 2010). However, using multiscalar meteorological drought indices to estimate soil water availability in a semi-arid dryland environment presents complex challenges as not all falling precipitation can be assumed to infiltrate into a soil profile. For example, low intensity precipitation events can be captured by tree canopy interception (Owens et al. 2006); soil burn from fire can result in large scale runoff events, especially during high intensity precipitation from the North American Monsoon (Moody and Martin 2001; Adams and Comrie 1997; Grover 2021); soil infiltration and evaporation rates can be limited by texture and compaction (Wythers et al. 1999; Newman et al. 1997); ground litter can reduce infiltration rates (Madsen et al. 2008); and high temperatures can increase evapotranspiration, limiting infiltration of low intensity precipitation events (Weiss et al. 2009). These issues complicate objectively identifying the index and timescale length that best represents soil water availability at different depths, leaving a significant gap between applying meteorological drought index information to land management action for the Southwest.

Studies examining the relationship between the multiscalar indices and soil moisture on a global scale have used satellite derived soil moisture, which is limited to shallow depths and low spatial resolution (Scaini et al. 2015; Pablos et al. 2017; Kwon et al. 2019; Afshar et al. 2022). However, these studies have established that short multiscalar index timescales closely align with shallow soil moisture, and the SPI and SPEI align with shallow soil moisture differently based on climate region (Scaini et al. 2015; Afshar et al. 2022). Studies using in-situ soil moisture measurements have established that the multiscalar aspect of the SPI and SPEI can be

good indicators of soil water availability at deeper depths (<10cm); however, these studies have been restricted to examining discrete depths, specific soil types, and locations outside the Southwest (Sims et al. 2002; Wang et al. 2015; Wang et al. 2016).

Recent advancements in computer modeling have allowed for sophisticated simulation of water movement through a soil profile (Simunek et al. 1998). Studies have begun to couple these hydrological models with satellite-based spatially continuous, high resolution meteorological datasets to drive daily model outputs of soil water availability, allowing for a more complete regional drought analysis of soil water (Abatzoglou 2013; Bradford et al. 2019; Bradford et al. 2020). Studies utilizing this framework have begun to explore the relationship between meteorological drought index timescale and soil water availability at different depths (McKellar 2017; Halwatura et al 2017; Barnard et al. 2021). Thus far, these studies have demonstrated promise in fully characterizing the soil water depth – multiscalar index timescale continuum; however, these studies have been limited in scale, examined discrete depths, or have been conducted outside the Southwest (McKellar 2017; Halwatura et al 2017; Barnard et al. 2021). Furthermore, the impacts of soil type and annual precipitation variability on the relationship between timescale and soil water depth have yet to be characterized, which are important for drought monitoring in dryland environments (Shepard et al. 2015; Hadley and Szarek 1981). Thus, characterizing the relationship between index timescale and soil water availability warrants further investigation for the Southwest.

This dissertation focuses on quantifying drought events in soils and improving drought monitoring techniques for the semi-arid Southwestern United States. The research presented here explores the links between Southwestern precipitation seasonality and drought onset and cessation patterns of different soil types. It further investigates the relationship between water

availability at different depths throughout a soil profile and the multiscalar aspect of meteorological drought indices. The impacts of soil type and annual precipitation variability on the relationship between soil water and timescale are also investigated given their importance on dryland vegetation productivity. The research presented here aims to advance the usage of meteorological drought indices, specifically the SPI and SPEI, as a drought monitoring technique of soil water availability in semi-arid dryland environments. By understanding drought propagation in soils and fully utilizing multiscalar drought indices, Southwestern land and resource managers can form better drought mitigation and adaptation plans for the future.

REVIEW OF DROUGHT INDICES

The purpose of this section is to provide an overview of the history, methodology, strengths, and weakness of drought indices referred to throughout this dissertation. Specifically, the Palmer Indices, Standardized Precipitation Index (SPI), Standardized Precipitation Evapotranspiration Index (SPEI) are covered. While the Palmer indices are not used for research purposes during this dissertation, their historical significance toward the development of the SPI and SPEI make them a topic worth discussing. Examples of soil moisture, hydrological, and composite indices are not covered in this review. Additional details about these indices can be found in the World Meteorological Organization handbook on drought indices (Svoboda and Fuchs 2016).

Palmer Drought Severity Index (PDSI)

The Palmer Drought Severity Index (PDSI) was developed to measure drought severity beyond using just monthly precipitation totals for agricultural lands of the interior United States (Palmer 1965). The PDSI calculates monthly water balance values by accounting for precipitation, temperature, and soil water holding capacity information, allowing for drought intensity, onset, and cessation to be investigated (Palmer 1965). Importantly, the inclusion of a two-layer soil model allows the PDSI to approximate soil moisture storage, which is important for Southwestern vegetation primary production (Palmer 1965; Noy-Meir 1973). Being one of the first indices produced to measure drought severity, the PDSI has become popular tool used by the drought monitoring community to evaluate drought conditions (Heddinghaus and Sabol 1991; Svoboda and Fuchs 2016). However, a complex methodology and arbitrary ruleset for defining dry and wet periods complicates useability for regional drought analysis (Alley 1984). Furthermore, several issues limit interpretation of PDSI values in a semi-arid environment (Alley

1984; Heddinghaus and Sabol 1991; Guttman 1998; Heim Jr 2002; Hayes 2006; Liu et al. 2017). For example:

- Simplification of the soil component limits usage for monitoring drought conditions to longer timescales (Alley 1984; Guttman 1998; Liu et al. 2017). Numerous studies have demonstrated that the PDSI is a good indicator of soil water variability, but is limited by its inherent timescale to observing long-term drought (Sims et al. 2002; Mika et al. 2005; Szép et al. 2005).
- The use of the Thornthwaite method to estimate evapotranspiration can cause errors in regions with energy extremes (Hobbins et al. 2008; Dai 2011).
- Reliability of PDSI values to evaluate current drought conditions is limited due to a retrospective 'backstepping' approach used to determine the end of dry and wet periods (Karl 1986; Guttman 1999).
- Data from Central Iowa and Western Kansas used to during PDSI development leads to classification of severe and extreme drought to vary between locations, requiring expertise judgment when using PDSI values for decision making (Guttman et al. 1992; Guttman 1998; Alley 1984; Hayes 2006).
- The PDSI was developed for US agricultural regions, limiting its usability in mountains regions, areas with extreme climate regimes, and international locations (Hayes 2006; Keyantash and Dracup 2002).
- The PDSI deals poorly with snow, treating all precipitation as rain and potentially creating inaccurate values for snow dominated climates (Keyantash and Dracup 2002; Hayes 2006).

- No runoff is allowed until the surface soil layer is filled to capacity, causing underestimation of runoff (Alley 1984).

Multiple PDSI variants have been developed that correct for these issues. During the PDSI calculation, a moisture anomaly value, Z, is obtained, which portrays the weather deviation of a particular month from average (Palmer 1965; Karl 1986; Heim Jr 2002). These values have become known as the Palmer Z Index, which can be used to evaluate drought on shorter timescales (Karl 1985). The most widely used variant is the self-calibrated PDSI (sc-PDSI), which adjusts empirical constants in the PDSI calculation to allow for more direct comparisons between locations (Wells et al. 2004). However, as the Palmer Z Index and the sc-PDSI are derivatives of the PDSI, both contain many of the same weaknesses, such as issues with identifying rapid drought development or ignoring frozen precipitation (Svoboda and Fuchs, 2016). The PDSI, and its variations, are commonly referred to as the 'Palmer Drought Indices' or 'Palmer Indices' given that much of the original derivation for the indices are the same. Despite issues, the Palmer Indices remain widely used today for drought monitoring due to their inclusion of a soil component and historical significance.

Standardized Precipitation Index (SPI)

Issues with the Palmer Indices have led the development of other drought indices (Svoboda and Fuchs 2016). The Standardized Precipitation Index (SPI) uses monthly precipitation totals to convey the frequency of wet and dry periods as a timeseries of z-score values, where positive values represent water surplus and negative values represent water deficits (McKee et al. 1993). Looking to find a more functional definition of drought, McKee et al. proposed using standardized precipitation to evaluate water storage of five major sources – soil moisture, ground water, snowpack, streamflow, and reservoir storage. Water storage in these

sources moves at different rates, requiring the SPI to be flexible enough to evaluate water movement at a variety of temporal resolutions. This 'multiscalar' aspect allows the SPI to be calculated at timescales from 1-48 months (Figure 1). Shorter SPI timescales represent faster rates of water movement (i.e. shallow soil moisture), while longer timescales represent slower rates of water movement (i.e. ground water). Thus, selecting the appropriate timescale length allows for drought conditions of different water sources to be evaluated (McKee et al. 1993; Svoboda and Fuchs 2016).

Southwestern climate is characterized by short pulses of moisture followed by extended periods of dryness, leading to monthly precipitation totals often not being normally distributed (Sheppard et al. 2002; Gudmundsson and Stagge 2016). Thus, data must undergo a transformation process to better approximate a standard normal distribution before an index timeseries is produced. This dissertation uses the 'fitSCI' R-package for data standardization, which forces timeseries of environmental data to take the shape of a standard normal distribution by estimating fit parameters of different probability distributions (Gudmundsson and Stagge 2016). Numerous studies have examined the impacts of different probability distributions on SPI values (Guttman 1999; Kumar et al. 2009; Alam et al. 2012; Stagge et al. 2015; Blain and Meschiatti 2015; Shiau 2020). These studies have noted that drought intensity can be misinterpreted depending on distribution choice and thus different probability distributions should be evaluated before SPI calculation (Kumar et al. 2009; Stagge et al. 2015; Angelidis et al. 2012). Shapiro-Wilk normality tests were conducted on different probability distributions available through the 'fitSCI' R package (Gudmundsson and Stagge 2016) (Figure 2). For this dissertation, it was determined that transforming precipitation data using a gamma distribution resulted in the best normal fit.

The SPI standardization process results in a z-score timeseries that communicates the number of standard deviation units an occurrence of precipitation falls from the historical mean. SPI users can interpret monthly z-score values of various timescales to assess drought conditions of different water sources. Larger negative SPI values represent increasingly dry conditions and larger positive values represent increasingly wet conditions. Unlike the PDSI, standardizing precipitation data allows for direct comparison of SPI values from different locations (Guttman 1999). This is important for land managers and decisions makers, as SPI values from two locations indicate the same information about drought frequency, duration, and magnitude (McKee et al. 1993).

The use of monthly data and simple calculation makes the SPI an attractive option for land managers looking to approximate drought conditions but are limited by data availability (Svoboda and Fuchs 2016). Furthermore, the standardization process and multiscalar aspect provide the flexibility for SPI users to evaluate drought conditions of different water sources on a regional scale (McKee et al. 1993). However, the SPI does have some notable weaknesses. For example, as previously mentioned, the choice of probability distribution can impact interpretation of drought magnitude (Kumar et al. 2009). The exclusion of temperature, which is important for PET and monthly water balance, can limit comparison between SPI values from separate locations that occurred under different temperature scenarios (Svoboda and Fuchs, 2016). Uncertainty when estimating transformation parameters during the standardization process can occur when a high number of no-rain months are included in the SPI timescale, resulting in an unrealistic SPI value being portrayed (Gudmundsson and Stagge 2016; Stagg et al. 2015; Wu et al. 2006). While these issues should be noted, the SPI is a powerful tool that is

easy to use and has the multiscalar flexibility to evaluate drought of different hydrological sources.

The Standardized Precipitation Evapotranspiration Index (SPEI)

The Standardized Precipitation Evapotranspiration Index (SPEI) adds a temperature component to the index calculation, allowing for the impacts of PET on drought conditions to be evaluated (Vicente-Serrano et al. 2010). By subtracting PET from precipitation, the SPEI uses a monthly water balance as the basis for the index input (Vicente-Serrano et al. 2010). The SPEI is multiscalar, allowing for drought conditions of different water sources to be evaluated (Vicente-Serrano et al. 2010). Furthermore, the SPEI is standardized, communicating information about drought duration, frequency, and magnitude to index users.

The SPEI is calculated using a similar methodology as the SPI. Monthly water balance values are often not normally distributed and must undergo a standardization process (Vicente-Serrano et al. 2010). This dissertation uses the 'fitSCI' R-package to transform climate data to fit a normal distribution (Gudmundsson and Stagge 2016). It is important choose the correct probability distribution when transforming monthly data, as different distributions can lead to discrepancies in SPEI values (Beguería et al. 2014; Stagge et al. 2015). There has been some debate over which probability distribution to use when transforming monthly water balance values, with log-logistic, gamma, and generalized extreme value (gev) being noted (Stagge et al. 2015; Vicente-Serrano and Beguería 2016; Stagge et al. 2016). Shapiro-Wilk normality tests were conducted for different probability distributions available through the 'fitSCI' R package on monthly water balance values (Gudmundsson and Stagge 2016). For this dissertation, it was determined that the 'gev' distribution transformed the data to best fit a normal distribution.

The inclusion of PET in the SPEI is a key strength compared to the SPI, allowing for impacts of temperature on drought conditions to be evaluated (Vicente-Serrano et al. 2010). However this comes at the expense of needing additional data and the choice of method used to estimate PET. The original SPEI derivation used the Thornthwaite method to estimate potential evapotranspiration (Vicente-Serrano et al. 2010), which only accounts for monthly mean temperature (Thornthwaite 1948). However, studies have noted inconsistencies between SPEI values calculated using different PET estimation methods (Stagge et al. 2014, Beguería et al. 2014). This study uses the Penman-Monteith method to estimate PET, which is more accurate than the Thornthwaite method due to its incorporation of wind, relative humidity, temperature, and solar radiation (Allen 1998; Majumder and Kumar 2019). Additionally, the choice of probability distribution during the standardizing process is an important consideration, as discrepancies between SPEI values have been noted (Beguería et al. 2014; Stagge et al. 2015). Despite these issues, increased SPEI popularity has been observed since its introduction, with many studies still categorizing differences between SPI values in semi-arid environments (McClaran and Wei 2014; Hernandez and Uddameri 2014; Wable et al. 2018; Afshar et al. 2022). Thus, both the SPI and SPEI are used for the basis this dissertation research.

Indices Comparison

The Palmer Indices, SPI, and SPEI were developed during different times of scientific understanding about how drought operates. Issues with the Palmer indices led to development of the SPI, which sought to better represent abnormal wet and dry periods, be more comparable between locations, and allow for evaluation of drought at different time scales (McKee et al. 1993). The SPI's exclusion of temperature led to the development of the SPEI, which included PET through a simple water balance calculation and allowed the impacts of temperature to be

evaluated on drought conditions (Vicente-Serrano et al. 2010). Each index is commonly used by land managers and decision makers for drought mitigation and adaptation planning and therefore it is important to understand operational differences between these indices.

Comparison between the PDSI, sc-PDSI, SPI, and SPEI are shown in figure 3. Both the PDSI and sc-PDSI respond slower to changes in precipitation due to the built in 9-month time scale of the PDSI derivation (Alley 1984). This causes longer durations of wet and dry phases and reiterates the PDSI's usage for long-term drought evaluation. Due to the SPI and SPEI being multiscalar, any desired timescale can be chosen to represent drought conditions of different water sources (McKee et al. 1993; Vicente-Serrano et al. 2010) (example of 3-month SPI and SPEI, respectively, shown in figure 3). When compared to the Palmer indices, both the SPI and SPEI frequently move above and below zero, demonstrating their faster response to changes in precipitation and usability to evaluate short-term drought. Plotting the SPI and SPEI at larger time scales would show longer durations of wet and dry phases, allowing for long-term drought monitoring (Figure 1).

The SPI and SPEI are used for research purposes throughout this dissertation due to their multiscalar ability. Conceptually, the multiscalar aspect of the SPI and SPEI timescales will align with different depths of soil water availability. However, as previously mentioned, numerous Southwestern climatological and soil physical aspects limit direct translation of precipitation into plant available water in the root zone. Furthermore, the lack of in-situ soil water datasets has prevented the timescale-depth continuum from being fully explored. This dissertation investigates this topic by creating a high resolution spatial and temporal dataset of soil water estimates for the Southwest. Important aspects of this approach are discussed in the next two sections.

HYDRAULIC PROPERTIES OF UNSATURATED SOILS

This section provides a review of hydraulic properties of unsaturated soils important to this dissertation. This dissertation focuses on water movement in the vadose zone, which is the variably saturated subsurface soil that extends from the surface to the groundwater table (figure 4). Soil water availability in this zone is commonly measured by using volumetric water content or matric potential. Volumetric water content (VWC) is the percentage of water in a soil medium compared to soil and air. However, VWC does not directly indicate the amount of water available for root water uptake, which is important for dryland vegetation dynamics (Noy-Meir 1973).

Potential energy is needed to transfer a unit volume of water from one elevation in the soil to another. Darcy's law dictates that water flows from areas of high potential energy to low potential energy (Darcy 1856). Within a soil matrix, capillary, adsorptive, and gravitational forces act on a unit volume of water. Capillary and adsorptive forces tightly hold water to the surface of soil particles, creating a negative pressure, or suction. The measure of this pressure is referred to as matric potential (commonly referred to as pressure head when defined per unit weight of water) (Bonan 2019). Matric potential is always negative in the vadose zone and values vary depending on soil type. Plant roots are a main mechanism applying suction in a soil medium, and thus matric potential can be conceptually thought of as how much pressure plant roots must apply to extract water molecules from a soil matrix. In the semi-arid southwest, plants want to remove more water from the soil than is supplied by precipitation, with soils acting as a buffer during times of dryness. Studying the amount of plant available water via matric potential is thus critical for monitoring ecosystem health. This dissertation uses matric potential values rather than VWC for research purposes due to this reasoning.

The relationship between matric potential and VWC is defined by the water retention curve (WRC) (Brooks and Corey 1966; van Genuchten 1980; Russo 1988) (Figure 5). When a soil is near saturation, water is mainly held in a soil matrix by capillary forces. As the soil dries, plant roots extract water from large pores first before extracting water from smaller pores. As a soil becomes drier, strong adsorption forces hold water molecules to the surface of soil particles. Thus, plants must exert increasing amounts of force to extract water molecules from a soil matrix during the drying phase. This relates to increasingly negative matric potential values as soil dries, and values approach zero when a soil nears saturation. Additionally, the relationship between matric potential and VWC varies by soil type. Figure 5 shows the WRC for different textured soils (*figure adapted from van Genuchten and Pachepsky 2011)*. Larger pore size distribution of coarse textured soils causes water to be held more loosely, leading to less suction (i.e. small matric potentials) needed to extract water molecules and thus faster drying rates. The opposite is true in fine textured soils, were increased connections between pores results in more suction needed to extract water molecules and slower drying rates (van Genuchten and Pachepsky 2011).

Another important soil property is hydraulic conductivity, which describes the ease of flow that water can move through a soil matrix. Hydraulic conductivity is a product of a materials porosity characteristics, pore distribution, and saturation level. The relationship between hydraulic conductivity and VWC or matric potential is given by the hydraulic conductivity function (HCF). Figure 6 shows the HCF for coarse, medium, and fine textured soils (*figure adapted from van Genuchten and Pachepsky 2011*). Near saturation, larger pores within coarse textured soils allow for higher hydraulic conductivity rates compared to fine textured soils (figure 6). Hydraulic conductivity decreases nonlinearly as a soil dries due to flow paths between pores becoming disconnected. Large pores within coarse textured soils become

more easily disconnected during the drying process than fine textured soils, contributing to more dramatic decreases in hydraulic conductivity rates (van Genuchten and Pachepsky 2011). Thus, hydraulic conductivity can be higher in fine textured soils at moderate to low matric potential values (figure 6).

This dissertation evaluates the impacts of soil type on the relationship between simulated matric potential and multiscalar index timescales. Previous research has found that the major soil types throughout the Southwest are sand, loamy sand, sandy loam, loam, sandy clay loam, and clay loam (Shepard et al. 2015). The principles outlined by the WRC and HCF dictate that infiltration and drying rates will vary between these soil types. Furthermore, plant roots will need to apply different amounts of matric potential to extract available water from the soil. Relating this concept back to multiscalar index timescales, it can be theorized that timescale length will vary with modeled matric potential based on soil type. This would translate to sandy soils aligning with shorter index timescales and clay soils aligning with longer timescales.

HYDRUS-1D MODELING

This dissertation is a first attempt at understanding the relationship between seasonal precipitation, multiscalar drought indices, and soil water availability at different profile depths for the Southwestern United States. As such, some decisions were made that simplified the modeling process to allow for more straightforward interpretation of model output. Therefore, it should be noted that this dissertation does not attempt to exactly model daily matric potential at each study location. Rather, this dissertation seeks to use location-based climate and soils information to help quantify general relationships between soil drought index timescales and matric potential on a regional scale.

This section covers the HYDRUS-1D model, important input files, and decisions made during the modeling process. Using the HYDRUS-1D model, this dissertation created a dataset of matric potential values at 5cm intervals from 0-200cm for 240 study locations throughout the Southwest. For a detailed review on how each study uses this dataset, see appendices 1-3.

HYDRSUD-1D OVERVIEW

HYDRUS-1D is a deterministic computer modeling software designed for simulating water movement through a one-dimensional variably-saturated porous media (Simunek et al. 2005). HYDRUS-1D, hereby referred to as 'HYDRUS', solves a modified version of the Richards equation (Richards 1931) for water movement through unsaturated soils through time by including a sink term that accounts for root water uptake (Simunek et al. 2005). The modified Richards equation is described as:

$$\frac{\partial \theta}{\partial t} = \frac{\partial}{\partial x}\left[K\left(\frac{\partial h}{\partial x} + \cos\alpha\right)\right] - S$$

where θ is the volumetric water content, t is time, x is the spatial coordinate, K is hydraulic conductivity, h is the water pressure head (matric potential), α is angle between flow direction

and the vertical axis, and S is the sink term. HYDRUS solves the modified Richards equation at a defined timestep. This dissertation uses daily timesteps to drive model simulations.

Feddes et al. 1978 defined the sink term, S, as the volume of water removed from the soil during each timestep due to root water uptake. The sink term, S, is defined as:

$$S(h) = \alpha(h)S_p$$

where S_p is the potential root water uptake rate and $\alpha(h)$ is a dimensionless parameter. Feddes et al. 1978 purposed a root water uptake function with four prescribed pressure heads that varied root water uptake linearly between pressure values depending on soil saturation. This model allowed for water uptake to be zero near saturation and below a prescribed wilting point (Feddes et al. 1978; Simunek et al. 2005). A simpler S-shaped function was purposed by van Genuchten 1987, given by:

$$\alpha(h) = \frac{1}{1 + \left(\frac{h}{h_{50}}\right)^p}$$

where p is a dimensionless coefficient and h_{50} is the pressure head at which root water uptake is reduced by 50% (Feddes et al. 1978; van Genuchten 1987; Simunek et al. 2005). This model ignores reductions in uptake near saturation and uses a non-linear S-shaped function to describe root water uptake (van Genuchten 1987). This dissertation uses the van Genuchten S-shaped model due to its simplification and less data requirements (van Genuchten 1987).

HYDRUS offers the use of different analytical models to govern water movement through unsaturated soils via the water retention curve (Simunek et al. 2005). This dissertation uses the van Genuchten model for describing the relationship between hydraulic conductivity and water content in unsaturated soils (van Genuchten 1980). In unsaturated soils, the soil water retention, $\theta(h)$, is defined by:

$$\theta(h) = \theta_r + \frac{\theta_s - \theta_r}{[1 + |\alpha h|^n]^m}$$

where θ_r is the residual water content, θ_s is the saturated water content, α is the inverse of the air-entry value, and n is the pore size distribution. The parameter, m, is defined as:

$$m = 1 - \frac{1}{n}, \qquad n > 1$$

The unsaturated hydraulic conductivity, $K(h)$, is defined as:

$$K(h) = K_s S_e^l \left[1 - \left(1 - S_e^{1/m}\right)^m\right]^2$$

Where K_s is the saturated hydraulic conductivity and l is the pore connectivity parameter. The effective saturation, S_e, is given by:

$$S_e = \frac{\theta - \theta_s}{\theta_s - \theta_r}$$

Together, these equations govern water movement in unsaturated soils. The parameters θ_r, θ_s, α, n, K_s, and l are soil-specific, and therefore change the relationship between soil water retention and hydraulic conductivity depending on soil type. During the modeling process, values for these parameters were acquired to improve the accuracy of matric potential estimation. For more detailed information about the derivation of these equations, further definitions of terms, or generalized units, see the *HYDRUS-1D Version 4.17* manual (Simunek et al. 2005).

Modeling Process

Five main input files are needed to compile HYDRUS during each modeling simulation – ATMOSPH.IN, METEO.IN, SELECTOR.IN, PROFILE.DAT, and HYDRUS1D.DAT. Daily records of meteorological information are contained in the ATMOSPH.IN and METEO.IN input files. Model basic, water flow, timestep, root water uptake, and soil physical parameter information are contained in the SELECTOR.IN file. The PROFILE.DAT file contains nodal

and root distribution information of the soil profile. Lastly, HYDRUS1D.DAT is an information file that communicates between different modules of the HYDRUS executable code (Simunek et al. 2005). Notable variable descriptions and values for each file are summarized in tables 1-5.

For this dissertation, three HYDRUS files - ATMOSPH.IN, METEO.IN, and SELECTOR.IN – change during each modeling simulation due to varying meteorological and soil information specific to each study location. Each of these files were populated with the necessary information for each unique model simulation. Soils information – including percent sand, silt, and clay, soil physical parameters, and latitude and longitude coordinates – were downloaded from the 'soilDB' R-package, which extracts information from publicly available online soil databases (Beaudette et al. 2021). Daily meteorological records – including solar radiation, minimum and maximum temperature, relative humidity, and wind – were acquired from gridMET (Abatzoglou 2013) using the latitude and longitude coordinates for each location obtained from 'soilDB'. Notably, gridMET contains all the necessary information to estimate PET using the Penman-Monteith method (Allen 1998). A total of 15539 daily meteorological records were acquired from 1-1-1979 through 7-17-2020.

While HYDRUS offers an interactive graphics-based user interface for the Microsoft Windows environment, data entry is limited to 9999 rows of input. Thus, HYDRUS source code was compiled outside the user interface to accommodate for the increased amount of data. A series of R-scripts were developed that populated the ATMOSPH.IN, METEO.IN, and SELECTOR.IN files with the necessary information and executed the source code. As previously mentioned, some decisions made during the modeling process were designed for more straightforward interpretation of model output. These decisions did not vary between model simulations. Notable decisions made during the modeling process were:

- Each modeling simulation consisted of a single, homogeneous soil material extending from 0-200cm.
- Model soil type was based on the subsurface 'B-horizon' due to its regulation of vegetation production in dryland soils (Shepard et al. 2015).
- Jackson et al. defined cumulative root profiles for different biomes in their landmark 1996 global study of root distributions (Jackson et al. 1996). A cumulative root distribution profile based on the 'desert' biome to simulate transpiration from 0-200cm, with root concentration declining in an exponential pattern with depth (*see Fig.1 in Jackson et al. 1996*).
- Root profiles between model simulations are static, and therefore the PROFILE.DAT file does not change. Furthermore, crop height, albedo, LAI, and maximum root depth does not vary between model simulations.
- No root growth was considered.
- Potential evapotranspiration was estimated using the Penman-Monteith method due to its higher accuracy with pan evaporation (Allen 1998; Majumder and Kumar 2019).
- To account for impacts of initial conditions on model output, a 10 year 'spin up' period was added to the beginning of the model simulation using meteorological data from 1/1/1979 through 12/31/1988. This made the total length of simulation 19,191 days, or approximately 52.5 years. The 'spin up' years were removed post simulation.
- Snow melt was not considered. However, most sites included in this dissertation are low elevation, with snow events being rare to non-existent in each sites respective period of record.
- Precipitation was allowed to accumulate at the surface with no runoff.

- Free drainage was allowed at the bottom of the soil profile.
- The S-shaped van Genuchten model was used for root water uptake (van Genuchten 1987). The h_{50} value, at which root water uptake is reduced by 50%, was set to -1500, and the P_3 coefficient was set to 2. These values were based on findings from Skaggs et al. 2006, and cross validated with in-situ soil moisture from the Climate Reference Network (CRN).

A generalized conceptual diagram of a model simulation is shown in figure 7. Daily inputs consist of precipitation at the top boundary. Daily outputs consist of PET (evaporation and transpiration) and water leaving the profile via free drainage at the bottom boundary. Root water uptake is restricted to the top 200cm of the profile. Timeseries of daily matric potential values were printed into the OBS_NODE.OUT output file. An R script compiled these values into a single dataset. This dataset contained daily matric potential values at 5cm intervals from 0-200cm for all 240 study locations. This dataset is the basis for studies conducted in appendices 1-3.

This dissertation seeks to link Southwestern climatology, intra-annual soil water availability, and drought development in soils by creating a regional soil water dataset with high spatial and temporal resolution. Southwestern climatology presents unique challenges when studying drought development and monitoring techniques due to complex interactions between seasonal precipitation timing, event size, soil properties, and soil water recharge. By simulating daily matric potential values at 5cm intervals from 0-200cm at 240 locations throughout the Southwestern United States, this dissertation investigates drought dynamics in soils and the usefulness of current drought metrics as viable options for soil water approximation.

Update on Standalone Version of HYDRUS-1D

Recently, the standalone version of HYDRUS-1D used throughout this dissertation, version 4.17, was discontinued by the publisher. HYDRUS-1D is now available in the new 'HYDRUS 5' release, which combines standalone versions of HYDRUS-1D, HYDRUS-2D, and HYDRUS-3D into a single package (Šimůnek et al. 2022). However, the version of HYDRUS-1D included in HYDRUS 5 is version 4.17 (as of June 2022).

DISSERTATION FORMAT AND COLLABORATIVE CONTRIBUTIONS

Major findings of this dissertation are summarized in the following 'Present Study' chapter. Research completed during this dissertation is organized into appendices following the 'Present Study' chapter, titled Appendices A, B, and C, respectively. Each appended manuscript is designed for publication to a scientific journal, listed on appendix title page. Detailed methods, results, and conclusions can be found the respective appendix. The author, Trevor T. McKellar, completed all modeling, script development, data processing and analysis, and writing for this dissertation. Significant contributions to model design, script development, statistical analysis, and text edits were contributed by Dr. Michael A. Crimmins. Further contributions of model development were contributed by Dr. Marcel G. Schaap, Dr. Craig Rasmussen, and Dr. Paul Ferré.

PRESENT STUDY

Major findings of this dissertation are presented here. For more detailed information on methods, results, discussion, and conclusions of each study, see appendix A, B, and C.

The complex interactions between seasonal climatology, soil hydraulic properties, and soil water recharge presents unique challenges for drought monitoring in the Southwestern United States. Variations in the seasonal timing and magnitude of precipitation can result in lasting drought impacts on vegetation productivity. Studying soil water availability is thus crucial for drought monitoring in the Southwest; however, the lack of long-term, reliable *in-situ* soil water datasets has restricted studies of regional drought dynamics in soils. This dissertation seeks to bridge the gap between drought monitoring, variations in seasonal climate, and soil water availability by coupling sophisticated soil modeling, site-specific soils information, and spatially continuous, high resolution meteorological datasets to simulate daily matric potential values at 5cm intervals from 0-200cm at 240 sites across the Southwest. Through a series of investigative studies, this dissertation quantified historical drought events in soils and improved methods for monitoring soil water availability using popular drought metrics. The first study (Appendix A) quantified drought onset and cessation seasons using a unique approach that defined drought events using daily matric potential values. The second study (Appendix B) evaluated the relationship between multiscalar drought index timescales and different depths of soil water availability. The third study (Appendix C) developed an innovative approach for multiscalar indices that varied timescale length monthly to better approximate precipitation seasonality in the Southwest.

Due to the lack of in-situ soil water measurements, the first study (Appendix A) sought to quantify drought events in soils across the Southwest. Historical matric potential anomaly time

series from 1979-2020 were created at 10cm and 30cm for 240 study sites. Anomaly time series were percent ranked from 0-100%, with a unique approach used that define 'drought events' as consecutive days below the 15th percentile. Drought events were categorized by duration and analyzed by onset and cessation seasons. Results show that short-term droughts (60 – 270 days) were frequent, and typically resulted from delayed or slowed starts to the locations major rainy season. Long-term droughts (>270 days) were infrequent and occurred only during specific years, requiring below average anomalies in one or more consecutive rainy seasons to develop. Long-term droughts are more likely to occur in locations with unimodal precipitation distributions (a majority of rain occurring once annually), due to soil water anomalies likely remaining unresolved until the following rainy season. Locations with bimodal precipitation distributions (rainy seasons occurring twice annually) make long-term drought development difficult as consecutive below average rainy seasons are needed.

Further consequences of the lack of *in-situ* soil water datasets have led land managers toward using multiscalar meteorological drought indices as proxies for soil water availability. However, objectively identifying the index and timescale that best represents soil water availability in semi-arid environments remains a significant gap for fully applying index information to land management action. The second study (Appendix B) defined the regional relationship between multiscalar index timescale and soil water availability of different depths. A new matric potential index (MPI) was created from 0-200cm and correlated with timescales from 1-24 months for the Standardized Precipitation Index (SPI) and Standardized Precipitation-Evapotranspiration Index (SPEI). This process was repeated at 240 study sites for the purpose of defining the timescale-depth continuum regionally and by soil type. Results indicate the regional relationship between the highest correlating index timescale and MPI depth operates roughly on

a 1:1 step progression from 0-80cm. Below 80cm, the timescale-depth relationship becomes less linear with a shallower slope. Further analysis showed that soil type impacts the timescale-depth relationship, with clay loam soils correlating at longer timescales than sandy soils when comparing the same depth MPI. Additionally, the SPI produced higher correlations and lower RMSE values with the MPI compared to the SPEI. Therefore, this studied recommended SPI usage for shallow (<80cm) soil water monitoring on Southwestern drylands, with a general rule that the relationship between timescale and depth scales linearly in a 1:1 progression. However, if land managers have access to local soils information, it should be consulted given the impacts of soil type on the timescale-depth relationship.

Given the importance of seasonal precipitation timing and magnitude for vegetation productivity, the use of a single multiscalar index timescale is unlikely to fully represent intra-annual variability of soil water. The third study (Appendix C) used a novel approach that created a time-varying multiscalar index designed to better approximate seasonal soil water variability in the Southwest. Similar to the second study, the MPI at 5cm, 30cm, and 60cm was correlated with SPI and SPEI timescales from 1-24 months. A time-varying composite index for the SPI and SPEI ('composite indices') was created that varied index timescale length during each calendar month based on the highest correlating timescale with the MPI during that same month. Correlation values between the composite indices and MPI were compared with correlation values between the SPI and SPEI using a traditional single timescale and MPI (i.e. like the second study). Results were analyzed regionally, by depth, and by soil type. Results showed that both the composite-SPI and composite-SPEI significantly ($p<0.05$) improved correlation values with the MPI compared to when using a single timescale for all depths and soil types. Higher correlation values were observed between the MPI and composite-SPI compared to the

composite-SPEI. Significant differences ($p<0.05$) were observed between soil types for shallow and deep depths, with greater improvement observed for clay loam composite indices at shallow depths and greater improvement for sand composite indices at deeper depths.

Together, the three studies of this dissertation link Southwestern climatology with intra-annual soil water availability, increasing our understanding of drought development in Southwestern soils and improving drought monitoring in semi-arid environments. As climate change exacerbates stress on water limited ecosystems, fully utilizing available drought monitoring strategies is key for forming strong mitigation and adaptation plans. The author of this dissertation hopes these results will benefit land managers and policymakers during the decision-making process and increase usage of multiscalar meteorological indices as a viable drought monitoring tool of soil water availability in the Southwestern United States.

FIGURES AND TABLES

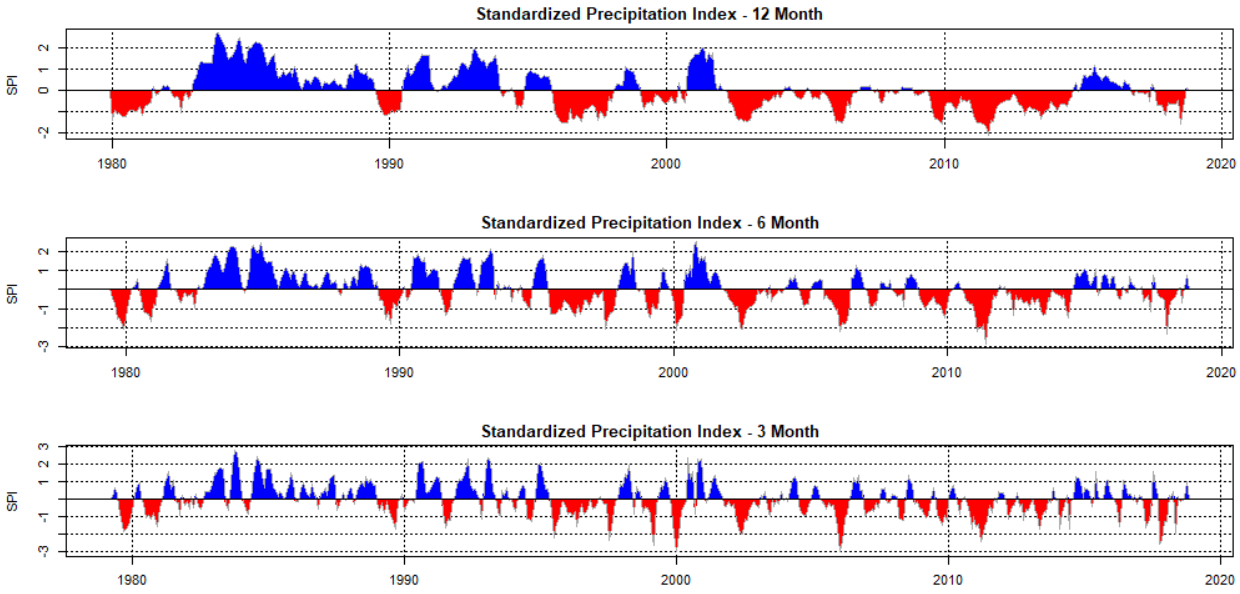

Figure 1: The Standardized Precipitation Index (SPI) at 3, 6 and 12 months.

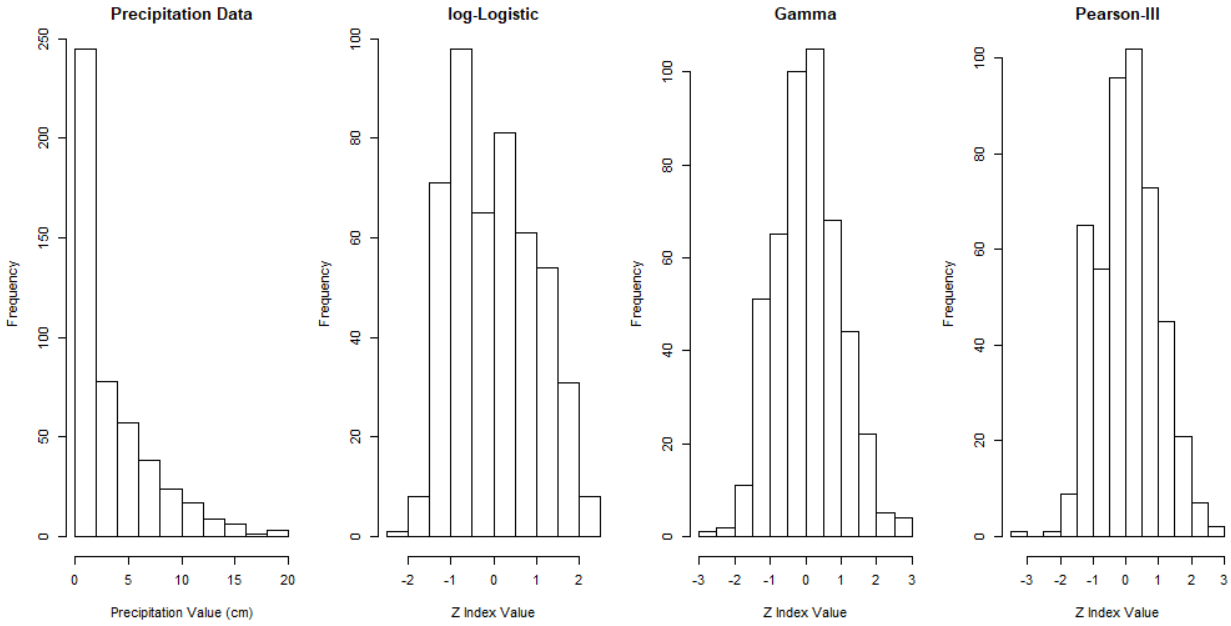

Figure 2: Histograms of monthly precipitation data transformed using different distributions available in the fitSCI R-package: log-Logistic, Gamma and Pearson-III. The far-left plot shows untransformed precipitation data.

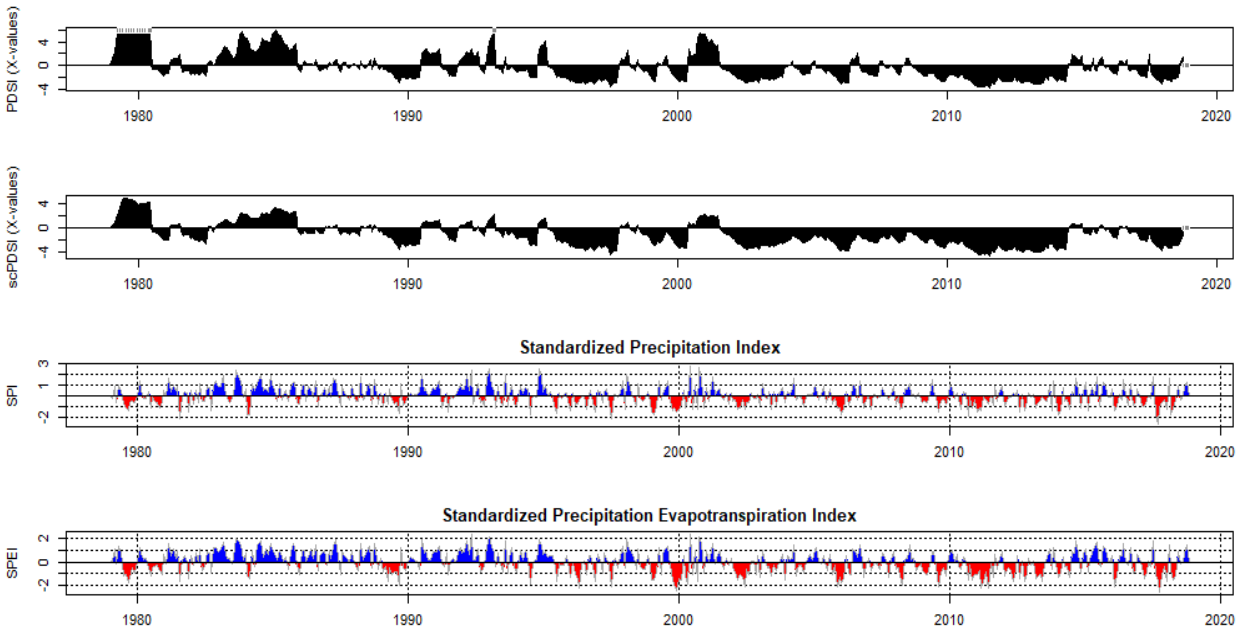

Figure 3: (From top to bottom) comparison of the PDSI, sc-PDSI, 3-month SPI, and 3-month SPEI.

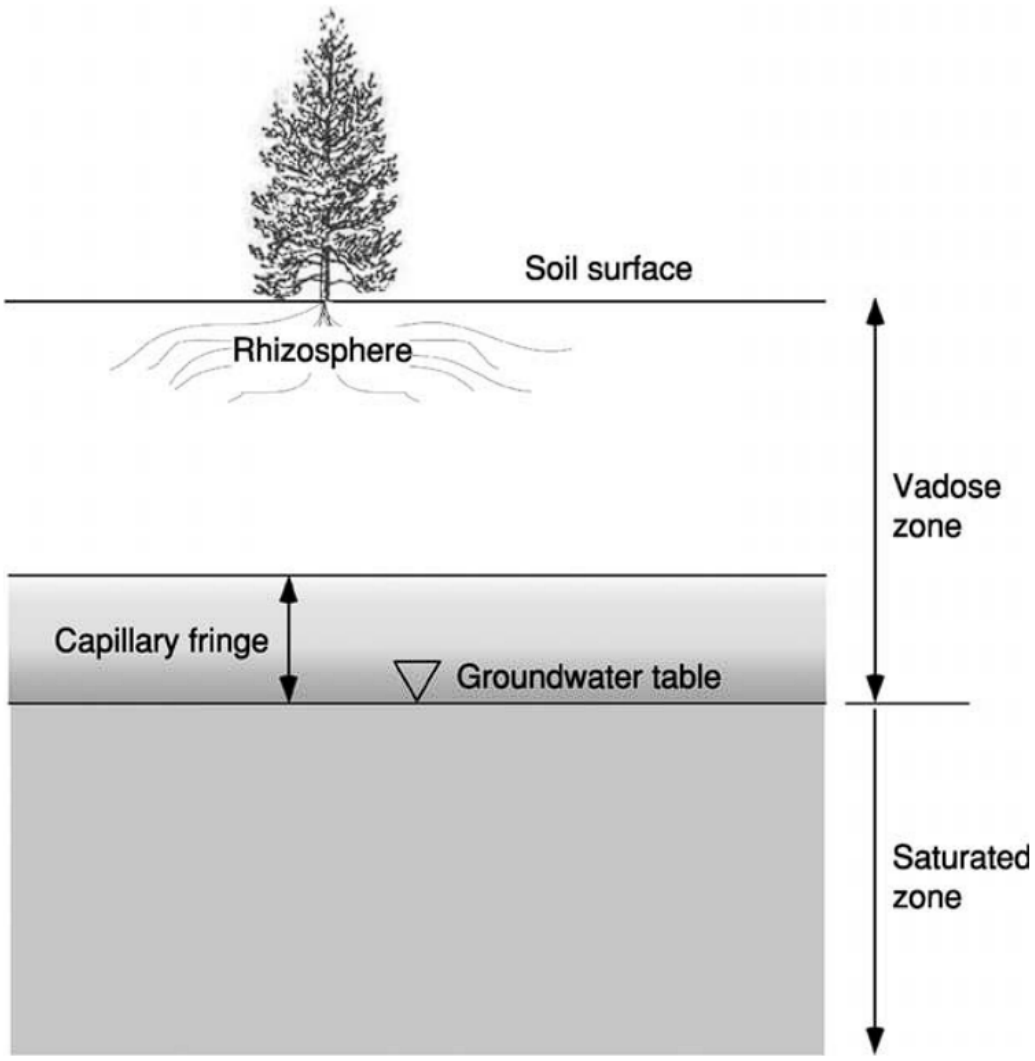

Figure 4: The vadose zone *from Holden and Fierer 2005*

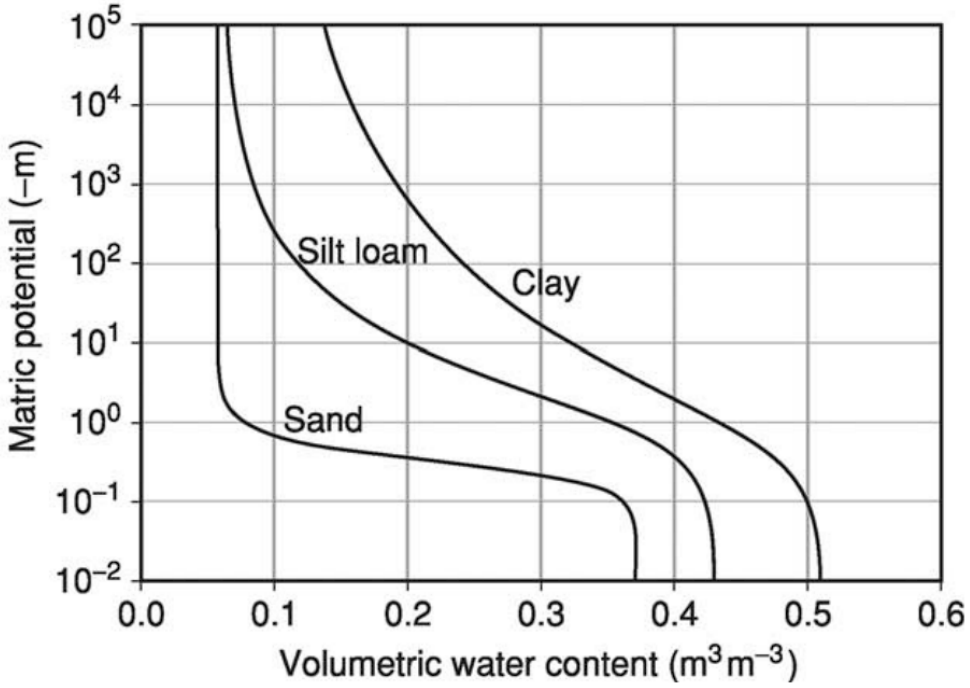

Figure 5: Water Retention Curve (WRC) for sand, silt loam, and clay soil types. *From Tuller and Or 2004*

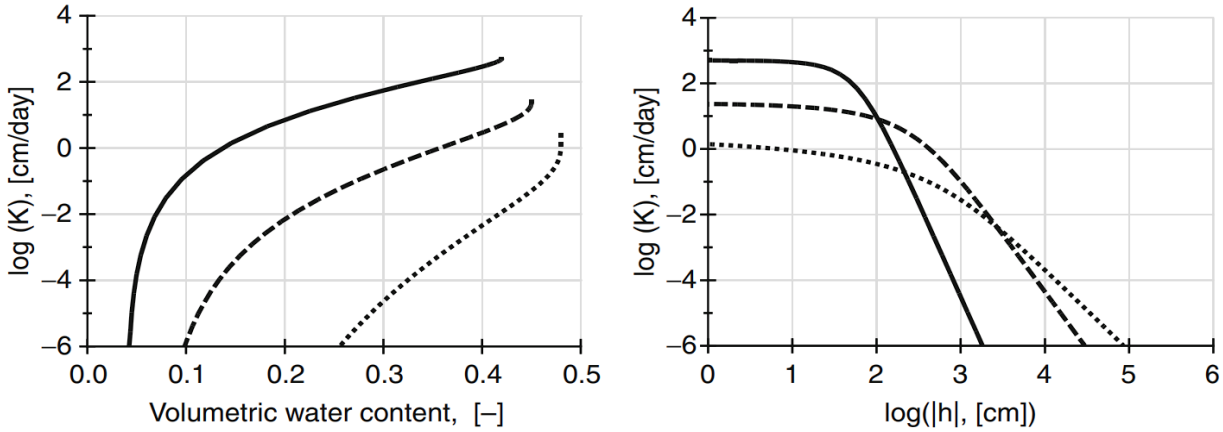

Figure 6: Hydraulic conductivity curves as a function of VWC (left) or matric potential (right) for coarse (solid), medium (dashed), and fine (dotted) textured soil types. *Figure from van Genuchten and Pachepsky 2011*

Table 1: ATMOSPH.IN		
Variable	*Description/Unit*	*Value*
MaxAL	Number of atmospheric data-records [day]	19191
hCritS	Max allowed pressure head at the soil surface [cm]	0
tAtm	Timestep [day]	1
Prec[cm/d]	Daily Precipitation [cm]	-
hCritA	Absolute value of the minimum allowed pressure head at the soil surface [cm]	100000

Table 2: HYDRUS1D.DAT			
Group	*Variable*	*Description/Unit*	*Information*
Main	HYDRUS_Version	HYDRUS-1D Version	4.17
	WaterFlow	Specifies whether or not transient water flow is calculated	Yes
	HeatTransport	Specifies whether or not heat transport is calculated	No
	RootWaterUptake	Specifies whether or not root water uptake is calculated	Yes
	RootGrowth	Specifies whether or not root growth is calculated	No
	MaterialNumebers	Number of materials considered	1
	SpaceUnit	Space unites	cm
	TimeUNit	Time unites	day
Profile	NumberofNodes	Number of nodes used to discretize the soil profile	101
	ProfileDepth	Depth of soil profile	200
	ObservationNodes	Number of observation nodes	41

Table 3: METEO.IN		
Variable	*Description*	*Information/Value*
Penman-Hargreaves	False if PET is to be estimated using the Penman-Monteith method; True if PET is to be estimated using the Hargreaves method	False
iCrop	Value specifying if crop height, albedo, LAI, and root depth are to be 0) not considered, 1) constant with time, 2) provided by a table, 3) specified daily	1
iLAI	Should leaf area index be 0) specified, 1) calculated from grass, 2) calculated from alfalfa, 3) calculated from surface fraction	0
Interception	Should interception be considered	No
CropHeight	Crop Height [cm]	30
Albedo	Albedo	0.15
LAI	Leaf Area Index value	1.0
rRoot	Rooting Depth [cm]	200

Table 4: PROFILE.DAT		
Variable	*Description*	*Information/Value*
NFix	Number of fixed nodes	41
MatNum(n)	Number of materials	1
LayNum(n)	Number of layers	1
x(n)	x-coordinate of node	x(1) = 0cm x(41) = -200cm
hNew(n)	Initial pressure head value at node	hNew(1) = -200cm hNew(41) = 0cm
Beta(n)	Value of water uptake distribution in the root zone	Beta(1) = 59.7 Beta(41) = 1

Table 5: SELECTOR.IN		
Variable	*Description*	*Information/Value*
LUnit	Length Unit	cm
TUnit	Time Unit	days
lWat	Ture if transient flow occurs	True
lChem	True if solute transport occurs	False
lTemp	True if heat transport occurs	False
lSink	True if water extraction in the root zone occurs	True
lRoot	True if root growth occurs	False
lWDep	True if hydraulic properties are temperature dependent	False
lVariableBC	True if variable boundary conditions are supplied via the ATMOSPH.IN file	True
lSnow	True if snow accumulation of the soil surface is allowed	False
lMeteo	True if meteorological information is supplied via the METEO.IN file	True
lVapor	True if vapor transport occurs	False
NMat	Number of soil profile materials	1
Nlay	Number of subregions in the soil profile	1
CosAlfa	Angle between flow direction and vertical axis (α=1 for vertical flow, α=0 for horizontal flow)	1
TopInf	True if time dependent boundary condition is imposed at the at the top of the profile. Data are supplied by the ATMOSPH.IN file	True
WLayer	True if water can accumulate at the surface with zero runoff	True
KodTop	Code specifying type of boundary condition at the surface. In the case of 'Atmospheric BC' set KodTop=-1	-1
lUnitW	True if initial condition is given in water content. False if initial condition given in pressure head	False
BotInf	True if time dependent boundary condition is imposed at the bottom of the profile. False if time independent boundary condition	False
FreeD	True if free drainage is considered as the bottom boundary condition	True
KodBot	Code specifying type of boundary condition for water flow at the bottom of the profile. In case of free drainage, set KodBot=-1	-1
iModel	Soil hydraulic properties model	van Genuchten (code 0)
iHyst	Hysteresis in the soil properties	No
Θ_r	Residual water content of the soil	Model Dependent
Θ_s	Saturated water content of the soil	Model Dependent
Alfa	α parameter in soil retention function	Model Dependent
n	n parameter in the soil water retention function	Model Dependent
Ks	Saturated hydraulic conductivity of soil material	Model Dependent

l	Tortuosity parameter in the conductivity function (also referred to as the pore connectivity parameter)	Model Dependent
Model	Root water uptake model	S Shape (code 1)
h50	Value of the pressure head at which the root water uptake is reduced by 50%. For more information about value selection see Skaggs et al. 2006	-1500
P3	Exponent, p, in the S-shaped root water uptake stress response function. For more information about value selection see Skaggs et al. 2006	2

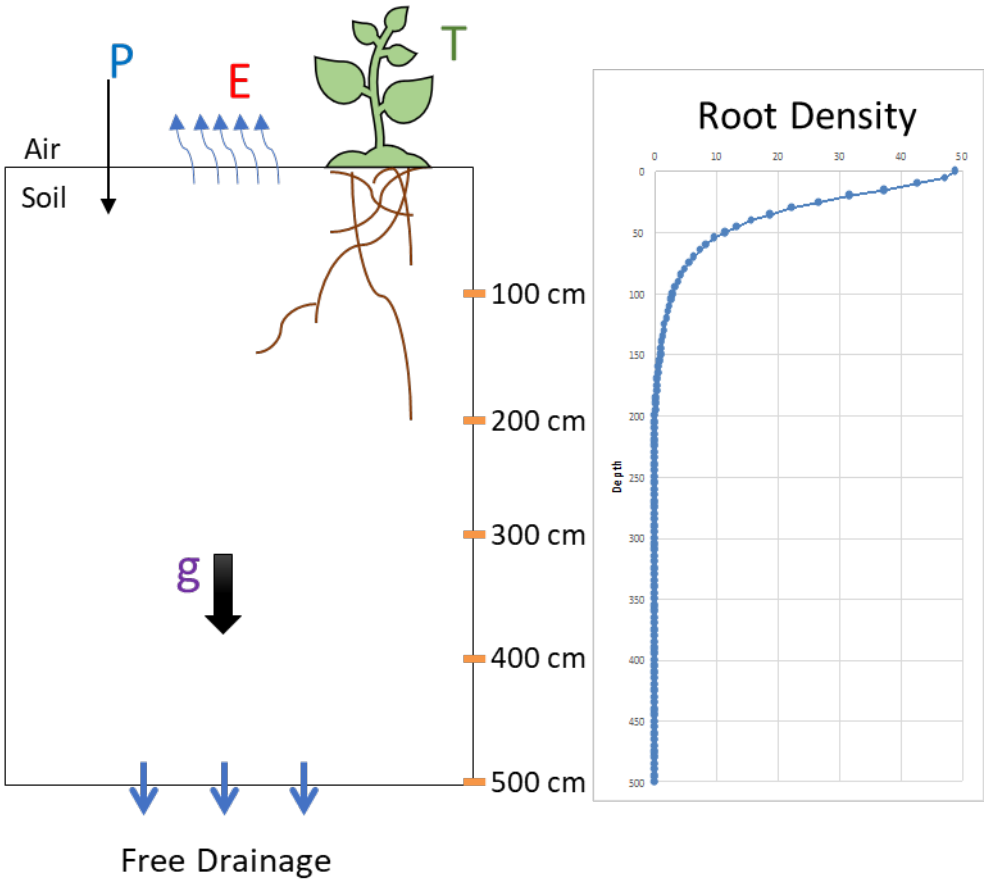

Figure 7: Conceptual diagram of HYDRUS-1D model profile showing major inputs (precipitation) and outputs (evaporation, transpiration, bottom drainage). The generalized root density profile based on Jackson et al. 1996 is shown (right).

REFERENCES

Abatzoglou, J. T. (2013). Development of gridded surface meteorological data for ecological applications and modelling. International Journal of Climatology, 33(1), 121-131.

Adams, D. K., & Comrie, A. C. (1997). The north American monsoon. Bulletin of the American Meteorological Society, 78(10), 2197-2214.

Afshar, M. H., Bulut, B., Duzenli, E., Amjad, M., & Yilmaz, M. T. (2022). Global spatiotemporal consistency between meteorological and soil moisture drought indices. Agricultural and Forest Meteorology, 316, 108848.

AghaKouchak, A. (2014). A baseline probabilistic drought forecasting framework using standardized soil moisture index: application to the 2012 United States drought. Hydrology and Earth System Sciences, 18(7), 2485-2492.

Alam, A. T. M. J., Rahman, M. S., Saadat, A. H. M., & Huq, M. M. (2012). Gamma distribution and its application of spatially monitoring meteorological drought in Barind, Bangladesh. Journal of Environmental Science and Natural Resources, 5(2), 287-293.

Allen, R. G., Pereira, L. S., Raes, D., & Smith, M. (1998). Crop evapotranspiration-Guidelines for computing crop water requirements-FAO Irrigation and drainage paper 56. Fao, Rome, 300(9), D05109.

Alley, W. M. (1984). The Palmer drought severity index: limitations and assumptions. Journal of Applied Meteorology and Climatology, 23(7), 1100-1109.

Angelidis, P., Maris, F., Kotsovinos, N., & Hrissanthou, V. (2012). Computation of drought index SPI with alternative distribution functions. Water resources management, 26(9), 2453-2473.

Ayers, P. D., & Bowen, H. D. (1987). Predicting soil density using cone penetration resistance and moisture profiles. Transactions of the ASAE, 30(5), 1331-1336.

Barnard, D. M., Germino, M. J., Bradford, J. B., O'Connor, R. C., Andrews, C. M., & Shriver, R. K. (2021). Are drought indices and climate data good indicators of ecologically relevant soil moisture dynamics in drylands?. Ecological Indicators, 133, 108379.

Beguería, S., Vicente-Serrano, S. M., Reig, F., & Latorre, B. (2014). Standardized precipitation evapotranspiration index (SPEI) revisited: parameter fitting, evapotranspiration models, tools, datasets and drought monitoring. International journal of climatology, 34(10), 3001-3023.

Berg, A., & Sheffield, J. (2018). Climate change and drought: the soil moisture perspective. Current Climate Change Reports, 4(2), 180-191.

Biederman, J. A., Scott, R. L., Arnone III, J. A., Jasoni, R. L., Litvak, M. E., Moreo, M. T., ... & Vivoni, E. R. (2018). Shrubland carbon sink depends upon winter water availability

in the warm deserts of North America. Agricultural and Forest Meteorology, 249, 407-419.

Blain, G. C., & Meschiatti, M. C. (2015). Inadequacy of the gamma distribution to calculate the Standardized Precipitation Index. Revista Brasileira de Engenharia Agrícola e Ambiental, 19, 1129-1135.

Bodner, G. S., & Robles, M. D. (2017). Enduring a decade of drought: Patterns and drivers of vegetation change in a semi-arid grassland. Journal of Arid Environments, 136, 1-14.

Bonan, G. (2019). Soil Moisture. In Climate Change and Terrestrial Ecosystem Modeling (pp. 115-133). Cambridge: Cambridge University Press. doi:10.1017/9781107339217.009

Bradford, J. B., Schlaepfer, D. R., Lauenroth, W. K., & Palmquist, K. A. (2020). Robust ecological drought projections for drylands in the 21st century. Global Change Biology, 26(7), 3906-3919.

Bradford, J. B., Schlaepfer, D. R., Lauenroth, W. K., Palmquist, K. A., Chambers, J. C., Maestas, J. D., & Campbell, S. B. (2019). Climate-driven shifts in soil temperature and moisture regimes suggest opportunities to enhance assessments of dryland resilience and resistance. Frontiers in Ecology and Evolution, 358.

Bradford, J. M. (1986). Penetrability. Methods of Soil Analysis: Part 1 Physical and Mineralogical Methods, 5, 463-478.

Breshears, D. D., Myers, O. B., Meyer, C. W., Barnes, F. J., Zou, C. B., Allen, C. D., ... & Pockman, W. T. (2009). Tree die-off in response to global change-type drought: mortality insights from a decade of plant water potential measurements. Frontiers in Ecology and the Environment, 7(4), 185-189.

Brooks, R. H., & Corey, A. T. (1966). Properties of porous media affecting fluid flow. Journal of the irrigation and drainage division, 92(2), 61-88.

Bunting, E. L., Munson, S. M., & Villarreal, M. L. (2017). Climate legacy and lag effects on dryland plant communities in the southwestern US. Ecological Indicators, 74, 216-229.

Chan, S. K., Bindlish, R., O'Neill, P. E., Njoku, E., Jackson, T., Colliander, A., ... & Kerr, Y. (2016). Assessment of the SMAP passive soil moisture product. IEEE Transactions on Geoscience and Remote Sensing, 54(8), 4994-5007.

Dai, A. (2011). Drought under global warming: a review. Wiley Interdisciplinary Reviews: Climate Change, 2(1), 45-65.

Darcy, H. (1856). Les fontaines publiques de la ville de Dijon: exposition et application... Victor Dalmont.

Dobriyal, P., Qureshi, A., Badola, R., & Hussain, S. A. (2012). A review of the methods available for estimating soil moisture and its implications for water resource management. Journal of Hydrology, 458, 110-117.

Dorigo, W. A., Wagner, W., Hohensinn, R., Hahn, S., Paulik, C., Xaver, A., ... & Jackson, T. (2011). The International Soil Moisture Network: a data hosting facility for global in situ soil moisture measurements. Hydrology and Earth System Sciences, 15(5), 1675-1698.

Dorigo, W., de Jeu, R., Chung, D., Parinussa, R., Liu, Y., Wagner, W., & Fernández-Prieto, D. (2012). Evaluating global trends (1988–2010) in harmonized multi-satellite surface soil moisture. Geophysical Research Letters, 39(18).

Dracup, J. A., Lee, K. S., & Paulson Jr, E. G. (1980). On the definition of droughts. Water resources research, 16(2), 297-302.

Eamus, D., Hatton, T., Cook, P., & Colvin, C. (2006). Ecohydrology: vegetation function, water and resource management. Csiro Publishing.

Entekhabi, D., Njoku, E. G., O'Neill, P. E., Kellogg, K. H., Crow, W. T., Edelstein, W. N., ... & Van Zyl, J. (2010). The soil moisture active passive (SMAP) mission. Proceedings of the IEEE, 98(5), 704-716.

Feddes, R. A., Kowalik, P. J., & Zaradny, H. (1978). Simulation of field water use and crop yield. Simulation monographs. Pudoc, Wageningen, 9-30.

Grover, H. 2021. Mitigating Postfire Runoff and Erosion in the Southwest using Hillslope and Channel Treatments. ERI Working Paper No. 44. Ecological Restoration Institute, Northern Arizona University. 11 pp

Gudmundsson, L., & Stagge, J. H. (2016). Package "SCI": Standardized Climate Indices Such as SPI, SRI or SPEI, v1. 0-2, CRAN [code].

Guttman, N. B. (1998). Comparing the palmer drought index and the standardized precipitation index 1. JAWRA Journal of the American Water Resources Association, 34(1), 113-121.

Guttman, N. B. (1999). Accepting the standardized precipitation index: a calculation algorithm 1. JAWRA Journal of the American Water Resources Association, 35(2), 311-322.

Guttman, N. B., Wallis, J. R., & Hosking, J. R. M. (1992). SPATIAL COMPARABILITY OF THE PALMER DROUGHT SEVERITY INDEX 1. JAWRA Journal of the American Water Resources Association, 28(6), 1111-1119.

Hadley, N. F., & Szarek, S. R. (1981). Productivity of desert ecosystems. BioScience, 31(10), 747-753.

Halwatura, D., McIntyre, N., Lechner, A. M., & Arnold, S. (2017). Capability of meteorological drought indices for detecting soil moisture droughts. Journal of Hydrology: Regional Studies, 12, 396-412.

Hayes, M. J. (2006). Drought Indices, What is Drought. Climate Impacts Specialist, National Drought Mitigation Center us.

Heddinghaus, T. R., & Sabol, P. (1991, September). A review of the Palmer Drought Severity Index and where do we go from here. In Proc. 7th Conf. on Applied Climatology (pp. 242-246). Boston, MA: American Meteorological Society.

Heim Jr, R. R. (2002). A review of twentieth-century drought indices used in the United States. Bulletin of the American Meteorological Society, 83(8), 1149-1166.

Hernandez, E. A., & Uddameri, V. (2014). Standardized precipitation evaporation index (SPEI)-based drought assessment in semi-arid south Texas. Environmental Earth Sciences, 71(6), 2491-2501.

Hobbins, M. T., Dai, A., Roderick, M. L., & Farquhar, G. D. (2008). Revisiting potential evapotranspiration parameterizations as drivers of long-term water balance trends. Geophys. Res. Lett, 35, L12403.

Holden, P. A., & Fierer, N. (2005). VADOSE ZONE| Microbial Ecology. Encyclopedia of Soils in the Environment, 216-224.

Jackson, R. B., Canadell, J., Ehleringer, J. R., Mooney, H. A., Sala, O. E., & Schulze, E. D. (1996). A global analysis of root distributions for terrestrial biomes. Oecologia, 108(3), 389-411.

Karl, T. R. (1986). The sensitivity of the Palmer Drought Severity Index and Palmer's Z-index to their calibration coefficients including potential evapotranspiration. Journal of Climate and Applied Meteorology, 77-86.

Karl, T. R., & Koscielny, A. J. (1982). Drought in the united states: 1895–1981. Journal of Climatology, 2(4), 313-329.

Keyantash, J., & Dracup, J. A. (2002). The quantification of drought: an evaluation of drought indices. Bulletin of the American Meteorological Society, 83(8), 1167-1180.

Kwon, M., Kwon, H. H., & Han, D. (2019). Spatio-temporal drought patterns of multiple drought indices based on precipitation and soil moisture: A case study in South Korea. International Journal of Climatology, 39(12), 4669-4687.

Lauenroth, W. K., & Bradford, J. B. (2006). Ecohydrology and the partitioning AET between transpiration and evaporation in a semiarid steppe. Ecosystems, 9(5), 756-767.

Littell, J. S., Peterson, D. L., Riley, K. L., Liu, Y., & Luce, C. H. (2016). A review of the relationships between drought and forest fire in the United States. Global change biology, 22(7), 2353-2369.

Liu, Y., Zhu, Y., Ren, L., Singh, V. P., Yang, X., & Yuan, F. (2017). A multiscalar Palmer drought severity index. Geophysical Research Letters, 44(13), 6850-6858.

Loik, M. E., Breshears, D. D., Lauenroth, W. K., & Belnap, J. (2004). A multi-scale perspective of water pulses in dryland ecosystems: climatology and ecohydrology of the western USA. Oecologia, 141(2), 269-281.

Madsen, M. D., Chandler, D. G., & Belnap, J. (2008). Spatial gradients in ecohydrologic properties within a pinyon-juniper ecosystem. Ecohydrology: Ecosystems, Land and Water Process Interactions, Ecohydrogeomorphology, 1(4), 349-360.

Majumder, D., & Kumar, B. (2019). Estimation of monthly average pet by various methods and its relationship with pan evaporation at Bhagalpur, Bihar. Journal of Pharmacognosy and Phytochemistry, 8(1), 2481-2484.

Martínez-Fernández, J., González-Zamora, A., Sánchez, N., Gumuzzio, A., & Herrero-Jiménez, C. M. (2016). Satellite soil moisture for agricultural drought monitoring: Assessment of the SMOS derived Soil Water Deficit Index. Remote Sensing of Environment, 177, 277-286.

McClaran, M. P., & Wei, H. (2014). Recent drought phase in a 73-year record at two spatial scales: implications for livestock production on rangelands in the Southwestern United States. Agricultural and Forest Meteorology, 197, 40-51.

McKee, T. B., Doesken, N. J., & Kleist, J. (1993, January). The relationship of drought frequency and duration to time scales. In Proceedings of the 8th Conference on Applied Climatology (Vol. 17, No. 22, pp. 179-183).

Mika, J., Horvath, S. Z., Makra, L., & Dunkel, Z. (2005). The Palmer Drought Severity Index (PDSI) as an indicator of soil moisture. Physics and Chemistry of the Earth, Parts A/B/C, 30(1-3), 223-230.

Mo, K. C. (2008). Model-based drought indices over the United States. Journal of Hydrometeorology, 9(6), 1212-1230.

Moody, J. A., & Martin, D. A. (2001). Post-fire, rainfall intensity–peak discharge relations for three mountainous watersheds in the western USA. Hydrological processes, 15(15), 2981-2993.

Naresh Kumar, M., Murthy, C. S., Sesha Sai, M. V. R., & Roy, P. S. (2009). On the use of Standardized Precipitation Index (SPI) for drought intensity assessment. Meteorological Applications: A journal of forecasting, practical applications, training techniques and modelling, 16(3), 381-389.

Naresh Kumar, M., Murthy, C. S., Sesha Sai, M. V. R., & Roy, P. S. (2009). On the use of Standardized Precipitation Index (SPI) for drought intensity assessment. Meteorological Applications: A journal of forecasting, practical applications, training techniques and modelling, 16(3), 381-389.

Neilson, R. P., King, G. A., & Koerper, G. (1992). Toward a rule-based biome model. Landscape Ecology, 7(1), 27-43.

Newman, B. D., Campbell, A. R., & Wilcox, B. P. (1997). Tracer-based studies of soil water movement in semi-arid forests of New Mexico. Journal of Hydrology, 196(1-4), 251-270.

Notaro, M., Liu, Z., Gallimore, R. G., Williams, J. W., Gutzler, D. S., & Collins, S. (2010). Complex seasonal cycle of ecohydrology in the Southwest United States. Journal of Geophysical Research: Biogeosciences, 115(G4).

Noy-Meir, I. (1973). Desert ecosystems: environment and producers. Annual review of ecology and systematics, 4(1), 25-51.

Oglesby, R. J., & Erickson, D. J. (1989). Soil moisture and the persistence of North American drought. Journal of Climate, 2(11), 1362-1380.

Otkin, J. A., Anderson, M. C., Hain, C., Svoboda, M., Johnson, D., Mueller, R., ... & Brown, J. (2016). Assessing the evolution of soil moisture and vegetation conditions during the 2012 United States flash drought. Agricultural and forest meteorology, 218, 230-242.

Owens, M. K., Lyons, R. K., & Alejandro, C. L. (2006). Rainfall partitioning within semiarid juniper communities: effects of event size and canopy cover. Hydrological Processes: An International Journal, 20(15), 3179-3189.

Pablos, M., Martínez-Fernández, J., Sánchez, N., & González-Zamora, Á. (2017). Temporal and spatial comparison of agricultural drought indices from moderate resolution satellite soil moisture data over Northwest Spain. Remote sensing, 9(11), 1168.

Palmer, W. C. (1965). Meteorological drought (Vol. 30). US Department of Commerce, Weather Bureau.

Prăvălie, R. (2016). Drylands extent and environmental issues. A global approach. Earth-Science Reviews, 161, 259-278.

Prigent, C., Aires, F., Rossow, W. B., & Robock, A. (2005). Sensitivity of satellite microwave and infrared observations to soil moisture at a global scale: Relationship of satellite observations to in situ soil moisture measurements. Journal of Geophysical Research: Atmospheres, 110(D7).

Reichle, R. H., De Lannoy, G. J., Liu, Q., Ardizzone, J. V., Chen, F., Colliander, A., ... & Smith, E. B. (2016). Soil Moisture Active Passive Mission L4_SM data product assessment (version 2 validated release) (No. GSFC-E-DAA-TN31807).

Restaino, C. M., Peterson, D. L., & Littell, J. (2016). Increased water deficit decreases Douglas fir growth throughout western US forests. Proceedings of the National academy of Sciences, 113(34), 9557-9562.

Reynolds, J. F., Smith, D. M. S., Lambin, E. F., Turner, B. L., Mortimore, M., Batterbury, S. P., ... & Walker, B. (2007). Global desertification: building a science for dryland development. science, 316(5826), 847-851.

Richards, L. A. (1931). Capillary conduction of liquids through porous mediums. Physics, 1(5), 318-333.

Robock, A., Mu, M., Vinnikov, K., Trofimova, I. V., & Adamenko, T. I. (2005). Forty-five years of observed soil moisture in the Ukraine: No summer desiccation (yet). Geophysical Research Letters, 32(3).

Robock, A., Vinnikov, K. Y., Srinivasan, G., Entin, J. K., Hollinger, S. E., Speranskaya, N. A., ... & Namkhai, A. (2000). The global soil moisture data bank. Bulletin of the American Meteorological Society, 81(6), 1281-1300.

Rodriguez-Iturbe, I. (2000). Ecohydrology: A hydrologic perspective of climate-soil-vegetation dynamies. Water Resources Research, 36(1), 3-9.

Romero-Lankao, P., Smith, J. B., Davidson, D. J., Diffenbaugh, N. S., Kinney, P. L., Kirshen, P., ... & Villers Ruiz, L. (2014). North America. Climate Change 2014: impacts, adaptation, and vulnerability part B: regional aspects contribution of working group II to the Fifth Assessment Report of the Intergovernmental Panel of Climate Change.

Russo, D. (1988). Determining soil hydraulic properties by parameter estimation: On the selection of a model for the hydraulic properties. Water resources research, 24(3), 453-459.

Scaini, A., Sánchez, N., Vicente-Serrano, S. M., & Martínez-Fernández, J. (2015). SMOS-derived soil moisture anomalies and drought indices: A comparative analysis using in situ measurements. Hydrological Processes, 29(3), 373-383.

Schlaepfer, D. R., Lauenroth, W. K., & Bradford, J. B. (2012). Ecohydrological niche of sagebrush ecosystems. Ecohydrology, 5(4), 453-466.

Sheffield, J., Goteti, G., Wen, F., & Wood, E. F. (2004). A simulated soil moisture based drought analysis for the United States. Journal of Geophysical Research: Atmospheres, 109(D24).

Shepard, C., Schaap, M. G., Crimmins, M. A., Van Leeuwen, W. J., & Rasmussen, C. (2015). Subsurface soil textural control of aboveground productivity in the US Desert Southwest. Geoderma Regional, 4, 44-54.

Sheppard, P. R., Comrie, A. C., Packin, G. D., Angersbach, K., & Hughes, M. K. (2002). The climate of the US Southwest. Climate Research, 21(3), 219-238.

Shiau, J. T. (2020). Effects of gamma-distribution variations on SPI-based stationary and nonstationary drought analyses. Water Resources Management, 34(6), 2081-2095.

Sims, A. P., Niyogi, D. D. S., & Raman, S. (2002). Adopting drought indices for estimating soil moisture: A North Carolina case study. Geophysical Research Letters, 29(8), 24-1.

Šimůnek, J., M. Šejna, G. Brunetti, and M. Th. van Genuchten (2022). The HYDRUS Software Package for Simulating the One-, Two, and Three-Dimensional Movement of Water, Heat, and Multiple Solutes in Variably Saturated Media, Technical Manual I, Hydrus 1D, Version 5.0, PC Progress, Prague, Czech Republic, 334p.

Simunek, J., Sejna, M., Van Genuchten, M. T., Šimůnek, J., Šejna, M., Jacques, D., & Sakai, M. (1998). HYDRUS-1D. Simulating the one-dimensional movement of water, heat, and multiple solutes in variably-saturated media, version, 2.

Simunek, J., Van Genuchten, M. T., & Sejna, M. (2005). The HYDRUS-1D software package for simulating the one-dimensional movement of water, heat, and multiple solutes in variably-saturated media. University of California-Riverside Research Reports, 3, 1-240.

Skaggs, T. H., Shouse, P. J., & Poss, J. A. (2006). Irrigating forage crops with saline waters: 2. Modeling root uptake and drainage. Vadose Zone Journal, 5(3), 824-837.

Slette, I. J., Smith, M. D., Knapp, A. K., Vicente Serrano, S. M., Camarero, J. J., & Beguería, S. (2020). Standardized metrics are key for assessing drought severity.

St. George, S., Meko, D. M., & Cook, E. R. (2010). The seasonality of precipitation signals embedded within the North American Drought Atlas. The Holocene, 20(6), 983-988.

Stagge, J. H., Tallaksen, L. M., Gudmundsson, L., Van Loon, A. F., & Stahl, K. (2015). Candidate distributions for climatological drought indices (SPI and SPEI). International Journal of Climatology, 35(13), 4027-4040.

Stagge, J. H., Tallaksen, L. M., Gudmundsson, L., Van Loon, A. F., & Stahl, K. (2016). Response to comment on ‘candidate distributions for climatological drought indices (SPI and SPEI)’. International Journal of Climatology, 36(4), 2132-2138.

Stagge, J. H., Tallaksen, L. M., Xu, C. Y., & Van Lanen, H. A. (2014). Standardized precipitation-evapotranspiration index (SPEI): Sensitivity to potential evapotranspiration model and parameters. In Hydrology in a changing world (Vol. 363, pp. 367-373).

Sugg, M., Runkle, J., Leeper, R., Bagli, H., Golden, A., Handwerger, L. H., ... & Woolard, S. (2020). A scoping review of drought impacts on health and society in North America. Climatic Change, 162(3), 1177-1195.

Svoboda, M. D., & Fuchs, B. A. (2016). Handbook of drought indicators and indices (pp. 1-44). Geneva, Switzerland: World Meteorological Organization.

Szép, I. J., Mika, J., & Dunkel, Z. (2005). Palmer drought severity index as soil moisture indicator: physical interpretation, statistical behaviour and relation to global climate. Physics and Chemistry of the Earth, Parts a/B/C, 30(1-3), 231-243.

Thornthwaite, C. W. (1948). An approach toward a rational classification of climate. Geographical review, 38(1), 55-94.

Topp, G. C., Davis, J. L., & Annan, A. P. (1980). Electromagnetic determination of soil water content: Measurements in coaxial transmission lines. Water resources research, 16(3), 574-582.

Tuller, M., Or, D., & Hillel, D. (2004). Retention of water in soil and the soil water characteristic curve. Encyclopedia of Soils in the Environment, 4, 278-289.

Van Genuchten, M. T. (1980). A closed-form equation for predicting the hydraulic conductivity of unsaturated soils. Soil science society of America journal, 44(5), 892-898.

Van Genuchten, M. T. (1987). A Numerical Model for Water and Solute Movernent.

Van Genuchten, M. T., & Pachepsky, Y. A. (2011). Hydraulic properties of unsaturated soils. Encyclopedia of agrophysics, 368-376.

Van Lanen, H. A. J., & Peters, E. (2000). Definition, effects and assessment of groundwater droughts. In Drought and drought mitigation in Europe (pp. 49-61). Springer, Dordrecht.

Van Loon, A. F. (2015). Hydrological drought explained. Wiley Interdisciplinary Reviews: Water, 2(4), 359-392.

Vaz, C. M. P., & Hopmans, J. W. (2001). Simultaneous measurement of soil penetration resistance and water content with a combined penetrometer–TDR moisture probe. Soil Science Society of America Journal, 65(1), 4-12.

Vaz, C. M., Bassoi, L. H., & Hopmans, J. W. (2001). Contribution of water content and bulk density to field soil penetration resistance as measured by a combined cone penetrometer–TDR probe. Soil and Tillage Research, 60(1-2), 35-42.

Vicente-Serrano, S. M., & Beguería, S. (2016). Comment on ‘Candidate distributions for climatological drought indices (SPI and SPEI)’by James H. Stagge et al. International Journal of Climatology, 36(4), 2120-2131.

Vicente-Serrano, S. M., Beguería, S., & López-Moreno, J. I. (2010). A multiscalar drought index sensitive to global warming: the standardized precipitation evapotranspiration index. Journal of climate, 23(7), 1696-1718.

Wable, P. S., Jha, M. K., & Shekhar, A. (2019). Comparison of drought indices in a semi-arid river basin of India. Water resources management, 33(1), 75-102.

Wang, H., Rogers, J. C., & Munroe, D. K. (2015). Commonly used drought indices as indicators of soil moisture in China. Journal of Hydrometeorology, 16(3), 1397-1408.

Wang, H., Vicente-Serrano, S. M., Tao, F., Zhang, X., Wang, P., Zhang, C., ... & El Kenawy, A. (2016). Monitoring winter wheat drought threat in Northern China using multiple climate-based drought indices and soil moisture during 2000–2013. Agricultural and Forest Meteorology, 228, 1-12.

Weiss, J. L., Castro, C. L., & Overpeck, J. T. (2009). Distinguishing pronounced droughts in the southwestern United States: Seasonality and effects of warmer temperatures. Journal of Climate, 22(22), 5918-5932.

Wells, N., Goddard, S., & Hayes, M. J. (2004). A self-calibrating Palmer drought severity index. Journal of climate, 17(12), 2335-2351.

Wilcox, B. P., Seyfried, M. S., Breshears, D. D., Stewart, B., & Howell, T. (2003). The water balance on rangelands. Encyclopedia of water science, 791(4).

Wilhite, D. A., & Glantz, M. H. (1985). Understanding: the drought phenomenon: the role of definitions. Water international, 10(3), 111-120.

Wu, H., Svoboda, M. D., Hayes, M. J., Wilhite, D. A., & Wen, F. (2007). Appropriate application of the standardized precipitation index in arid locations and dry seasons. International Journal of Climatology: A Journal of the Royal Meteorological Society, 27(1), 65-79.

Wythers, K. R., Lauenroth, W. K., & Paruelo, J. M. (1999). Bare-soil evaporation under semiarid field conditions. Soil Science Society of America Journal, 63(5), 1341-1349.

APPENDIX A

RELATIONSHIPS BETWEEN SEASONAL PRECIPITATION AND DROUGHT DEVELOPMENT IN SOILS OF THE SOUTHWESTERN UNITED STATES

Trevor T. McKellar[*1]

[*]Corresponding Author

[1]Department of Environmental Science

1177 E. 4th St.

Tucson, AZ 85721, USA

Phone: +1 (520) 621-1646

Email: envs-dept@arizona.edu

Targeted for Publication in Agricultural and Forest Meteorology

ABSTRACT

The semi-arid climate of the Southwestern United States ('Southwest') presents unique challenges for quantifying drought conditions due to annual potential evapotranspiration being significantly greater than annual precipitation. Southwestern vegetation is dependent on seasonal soil water recharge for primary productivity, with recharge delays potentially resulting in drought impacts. Understanding how delays in seasonal precipitation timing and magnitude can create soil water anomalies is thus key for characterizing drought dynamics in Southwestern soils; however, the lack of long-term, reliable soil water datasets have restricted this effort to a local scale. Here, we couple sophisticated soil modeling, site-specific soils information, and spatially continuous, high resolution meteorological data to create a soil water dataset for the purpose of characterizing drought onset and cessation patterns for the Southwest. Daily matric potential at 10cm and 30cm was simulated from 1979-2020 at 240 locations throughout 4 Major Land Resource Areas (MLRA). Historical matric potential anomaly time series were percent ranked from 0-100%, with consecutive days below the 15th percentile quantified as drought events. Drought events were categorized by duration and analyzed by onset and cessation season. Results showed that short-term droughts (60 – 270 days) were frequent, and typically resulted from delayed or slowed starts to the MLRAs major modal precipitation season. Long-term droughts (>270 days) were infrequent and occurred only during specific years, requiring below average anomalies in one or more consecutive rainy seasons. Long-term droughts were more likely to occur in MLRAs with unimodal precipitation distributions, due to soil water anomalies likely remaining unresolved until the following rainy season. MLRAs with bimodal precipitation distributions made long-term drought development difficult as consecutive below average rainy seasons were needed. Climate change is expected to impact precipitation patterns across the

Southwest over the coming decades. Understanding how changes in precipitation patterns will impact drought development is key for future drought impact assessment and mitigation.

INTRODUCTION

Drought is a complex phenomenon that can cause widespread socioeconomic and environmental impacts that vary both spatially and temporally (Wilhite and Glantz 1985; Van Loon 2015). In general, drought can be defined as a water deficit that arises when compared to normal conditions and lasts long enough to cause a lasting hydrological imbalance (Dracup et al. 1980; Wilhite and Glantz 1985; Van Lanen and Peters 2000; Mishra and Singh 2010). However, what constitutes *normal conditions* varies based on the local climate regime and water source being studied (Wilhite and Glantz 1985). In the arid and semi-arid Southwestern United States ('Southwest'), defining drought is challenging due to potential evapotranspiration being significantly greater than precipitation (Wilcox et al. 2003). Alterations in seasonal precipitation timing and magnitude can delay soil water recharge, which is the primary control on vegetation dynamics in dryland ecosystems (Noy-Meir 1973; Hadley and Szarek 1981; Neilson et al. 1992; Wilcox et al. 2003). However, the lack of long-term, reliable soil water datasets (Dorigo et al. 2011) limits the understanding of how seasonal climate variations link to drought development in soils on a regional scale. This study investigates this link by coupling sophisticated soil modeling, site-specific soils information, and high-resolution meteorological datasets to create a soil water dataset for the Southwestern United States. Climate change is expected to exacerbate drought impacts on dryland ecosystems over the coming decades (Sugg et al. 2020; Romero-Lankao et al. 2014) and thus understanding the relationship between seasonal precipitation, soil water recharge, and drought development is key for informing future impact analysis (Garfin et al. 2013; Bradford et al. 2020).

Southwestern climatology is characterized by high evapotranspiration, limited annual rainfall, and long durations between precipitation seasons (Shepard et al. 2002; Wilcox et al.

2003; Loik et al. 2004). Precipitation is the main source of moisture in the Southwest and primary control on vegetation dynamics in dryland ecosystems (Noy-Meir 1973; Hadley and Szarek 1981; Neilson et al. 1992; Wilcox et al. 2003). Southwestern vegetation is dependent on stored precipitation in the soil profile for aboveground productivity (Janerette et al. 2010; Williamson et al. 2012; Shepard et al. 2015; Koehn et al. 2021). However, precipitation timing and amount vary seasonally, impacting water availability (Shepard et al. 2002; Loik et al. 2004). Drought conditions alter the timing and magnitude of seasonal soil water recharge and lead to landscape vegetation changes, such as transitions from native to non-native grass species (Bodner and Robles 2017), shifts in species composition (Báez et al. 2013), or, in extreme cases, widescale vegetation die off, such as mortality of pinon pine and juniper trees (Neilson et al. 1992; Breshears et al. 2008; Restaino et al. 2016). Additionally, these changes can lead to increased risk of wildfire (Littell et al. 2016). Therefore, quantifying variability in the timing and magnitude of seasonal precipitation, and how that influences soil water recharge, is important for understanding regional drought onset and cessation patterns.

The relationship between seasonal precipitation and soil water recharge in the Southwest is complex, as not all surface precipitation infiltrates into the soil profile. Most precipitation events at Southwestern locations are small (<5mm) and occur within short intervals of one another (<10 days) (Loik et al. 2004). Small precipitation events can be captured by tree canopy interception (Reynolds et al. 2000; Wilcox et al. 2003; Owens et al. 2006) or lost to soil evaporation (Wythers et al. 1999; Newman et al. 1997). It is therefore larger precipitation events that will impact soil water recharge (Cable 1980). However, soil infiltration rates can be limited by texture and compaction (Wythers et al. 1999; Newman et al. 1997); ground litter can reduce infiltration rates (Madsen et al. 2008); and soil burn from fire can result in large scale runoff

events, especially during high intensity precipitation from the North American Monsoon (Moody and Martin 2001; Adams and Comrie 1997; Grover 2021). Only studying precipitation totals thus offers an incomplete view of water that will become available for root water uptake.

While using in-situ soil moisture measurements would be ideal to directly gauge soil water availability, the lack of long-term reliable datasets and the need for an online global database is well documented (Robock et al. 2000; Robock et al. 2005; Dorigo et al. 2011; Dorigo et al. 2012). Recent advances in remote sensing technology have offered the promise of soil moisture estimation from satellite platforms over large areas, however the microwave instrumentation used for soil moisture measurements is limited to the top few centimeters of soil (Dorigo et al. 2011; Reichle et al. 2016; Berg and Sheffield 2018). Additionally, studies utilizing remote sensing products to investigate soil moisture drought impacts on drylands have been limited to macro-scale resolution, short temporal analysis, and low spatial resolution (Karl and Koscielny 1982; Oglesby and Erikson III 1989; Sheffield et al. 2004; Mo 2008; Notaro et al. 2010; AghaKouchak 2014; Otkin et al. 2016).

A recent study using the U.S. Drought Monitor (USDM) to examine seasonal drought onset and cessation patterns found that seasonal drought onset was highly variable across the Southwest, while seasonal drought cessation had lower variability (Leeper et al. 2022). The USDM combines drought indicators, indices, and information from local experts to portray drought conditions (Svoboda et al. 2002). These inputs are limited to surface analysis and therefore its interpolation with soil water recharge remains unknown. Other studies have used multiscalar drought indices as proxies for soil water availability; however, these studies are only beginning to establish the links between multiscalar index timescale and soil water availability at

different depths (McKellar 2016; Barnard et al. 2021; McKellar et al. 2022b; McKellar et al. 2022c).

Issues with the lack of in-situ soil moisture measurements and other proxies have led studies in recent decades to use sophisticated computer models to simulate water movement through a soil profile (Simunek et al. 2005). Additionally, advancements in estimating spatially continuous climate variables have led to the creation of high-resolution meteorological time series at site-specific locations (Abatzaglou 2013). Coupling soil modeling with high-resolution climate datasets has established a framework enabling largescale analysis of soil water availability across the Southwest – including the exploration of ecological responses to soil moisture changes, the relationships between seasonal precipitation and soil moisture, and future soil moisture regimes shifts related to climate change (Gremer et al. 2015; Koehn et al. 2021; Bradford et al. 2019). However, propagation of drought in soils has yet to quantified on a regional scale for the Southwest.

Here, we conduct a regional analysis of seasonal drought onset and cessation patterns in soils for the Southwestern United States. We hypothesize that seasonal variability of Southwestern climate drives unique drought onset and cessation patterns in soil water availability. By coupling sophisticated computer modeling with spatially continuous meteorological datasets, daily matric potential values are simulated at two depths (10cm and 30cm) for 240 locations across the Southwest from 1979 through 2020. Utilizing methods often employed in climatological analyses with long-term datasets, we establish baseline conditions and develop time series of daily matric potential anomalies for all study sites. Fine-scale assessment of daily matric potential anomalies allows for the quantification of consecutive days of below average soil water to be categorized as “drought events”. Drought events are analyzed

by duration for spatial and temporal patterns based on location and depth. Finally, we evaluate prominent drought years amongst our study sites for causes of drought onset and cessation with relation to daily precipitation and PET anomalies.

MATERIAL AND METHODS

Study Region Background

This study defines the semi-arid lower elevation Southwestern United States, hereby referred to as the 'Southwest' or 'study region', as areas comprised of the Mojave, Sonoran, and Chihuahuan Deserts. The United States Department of Agriculture (USDA) classifies land area into a hierarchical system for the purpose of land management, agricultural planning, drought monitoring, conservation of natural resources, and environmental preservation (Salley et al. 2016). This hierarchy allows planning and management strategies to be specified across board landscapes or down to the local ecosystems. The primary organization unit is the Major Land Resource Area (MLRA), which are geographically associated areas that share similar physiography, geology, climatology, hydrology, soils, biology, and land usage (Austin 1965; Salley et al. 2016). In total, the United States is divided into 278 MLRAs – four of which are within the study region. This study focuses on MLRA 30 (Mojave Desert), MLRA 40 (Western Sonoran Desert), MLRA 41 (Eastern Sonoran Desert), and MLRA 42 (Chihuahuan Desert) (Figure 1).

The study region has a gradient of major modal precipitation season from west to east, with MLRAs in the west receiving unimodal precipitation during the fall-winter months and MLRAs in the east receiving unimodal precipitation during the summer months (Figure 1). This study defines the fall-winter months as the 'cool' season and the spring-summer months as the 'warm' season. MLRAs in the middle of the study region receive precipitation during both the

cool and warm seasons, producing a bimodal precipitation distribution (figure 2). Study locations in western MLRAs receive approximately 70% of precipitation during the cool season during low intensity, long duration events when evapotranspiration is low. In contrast, study locations in eastern MLRAs receive 50-70% of precipitation during the warm season from the North American Monsoon (NAM), which is a series of high intensity, short duration thunderstorms occurring when evapotranspiration is high (Carleton et al. 1990; Douglas et al. 1993; Mitchell et al. 2002). Onset of the NAM is highly consistent, typically starting in early July (Ellis et al. 2004, Higgins et al. 1997).

Data and Site Selection

Study sites were selected using publicly available soil sampling data from sites across the Southwest. Soils information was downloaded for all available profiles in the study region using the R package 'soilDB', which extracts information from PedonPC and AK Site databases, local NASIS databases, and the SDA web service (Beaudette et al. 2022). Previous research has found that six main subsurface soil types are common throughout the study region – sand, loamy sand, sandy loam, loam, sandy clay loam, and clay loam (Shepard et al. 2015). In each MLRA, 10 sites were selected from each of the main soil types, for a total of 60 sites in each MLRA. Across the 4 MLRAs, 240 sites were selected in total. A spatial algorithm was used to maximize the distance between selected sites to increase coverage of the study region. Soil hydraulic parameters, lab texture percentages of sand-silt-clay, soil horizon depths, altitude, and latitude and longitude coordinates were downloaded for these study sites.

Latitude and longitude coordinates of each study site obtained through 'soilDB' were used to download 4km gridded surface meteorological (gridMET) data from January 1st, 1979, through October 31st, 2020 (Abatzaglou 2013). Daily meteorological data from GridMET

consisted of precipitation [mm], minimum and maximum temperature [K], minimum and maximum relative humidity [%], wind [km/day], and mean shortwave radiation at surface [W/m^2] (Abatzaglou 2013).

Modeling

Daily matric potential was simulated at each study site using HYDRUS-1D, a deterministic modeling software designed for simulating water movement in a one-dimensional variably saturated porous media (Simunek et al. 2005). Each study site had a unique modeling simulation parameterized by the acquired soils information and driven by the daily meteorological time series extracted for that site. Profile simplifications were made to allow for more straightforward interpretation of model output. A single, homogeneous, 200cm soil layer consisting of study sites subsurface 'B horizon' was used due to its regulation on aboveground vegetation productivity (Shepard et al. 2015). A generalized root profile typical of dryland vegetation was used to simulate root water uptake in the top 200cm of the soil profile, with root concentration decreasing exponentially from top to bottom (Jackson et al. 1996). The majority of roots in this profile are concentration in the top 50cm. Potential evapotranspiration was estimated using the Penman-Monteith equation and required gridMET data (Allen 1998). To account for initial conditions influencing model output, a 'spin-up' was included at the beginning of each model simulation that consisted of the first 10 years of gridMET data specific to each site (i.e. 1-1-1979 through 12-31-1988). These 10 years were removed from model output post simulation. For this study, model output at 10cm and 30cm was analyzed to focus on relatively shallow soil water status variability and high frequency drought events that impact shallow rooted vegetation.

Analyzing output and drought definitions

At each study site, a daily anomaly was calculated using the output time series of matric potential values at 10cm and 30cm. The long-term median matric potential value was calculated for each day of year (DOY) and subtracted from the daily time series [Daily MP value – long-term median DOY MP value]. This created a historical anomaly time series for each study site. Each anomaly time series was percent ranked from 0-100%. Consecutive days below the 15th percentile, which is a common threshold due to its approximation of moderate drought using other drought metrics (Kam et al. 2013; Herrera-Estrada et al. 2017; Ukkola et al. 2020), were quantified as 'drought events'. Drought events were categorized by duration into short-term (lasting longer than 60 days but less than 270 days) and long-term (lasting longer than 270 days). Drought events were analyzed by seasonal onset and cessation period using the cool and warm season classification.

RESULTS AND DISCUSSION

Climatology and Soil Water Regimes

The unimodal and bimodal distributions of seasonal precipitation across the study area control soil water regimes and, ultimately, the emergence of unique drought patterns (Figure 2). In general, monthly mean matric potential (MMP) values in each MLRA (n=60) follow seasonal precipitation distributions specific to that MLRA (Figure 2a-d and 2e-h, respectively). Across all MLRAs, MMP values are lower (more negative) at 10cm compared to 30cm. The study region observes more dry than wet days, with most precipitation events being small (Loik et al. 2004; Lauenroth and Bradford 2006). Small precipitation events are likely captured by interception (Reynolds et al. 2000; Wilcox et al. 2003; Owens et al. 2006) or soil evaporation (Wythers et al. 1999; Newman et al. 1997), leading to fast wetting and drying of the upper soil profile layers.

Water loss to plant interception and evaporation for large precipitation events is much lower, allowing for increased infiltration into the root zone. Thus, MMP values at 10cm will be dryer, on average, then 30cm. A seasonal lag is observed in peak MMP values between 10cm and 30cm, which can be attributed to the time delay in water movement to deeper soil depths associated with soil hydraulic parameters.

Unimodal MLRAs

Mean annual precipitation (MAP) in MLRA 30 is 19.8 cm (n=60), with 70% of precipitation occurring during the cool season and 30% occurring during the warm season (Figure 1a). MMP values in MLRA 30 are highest in the late winter and lowest in the summer, corresponding with PET seasonality (Figure 1e). Precipitation during the warm season has minimal effect on MMP values due to 1) the low frequency and inconsistency of NAM storms reaching MLRA 30 and 2) small events being lost to interception and soil evaporation. At 10cm, the percentage of study sites registering drought during each DOY increases gradually with monthly precipitation during the early cool season; however, at the 30cm, this increase is more abrupt (figure 2i). These patterns indicate that the greatest risk for low matric potential anomalies and drought onset emerges during the cool season, which corresponds with the major precipitation season in MLRA 30.

MAP in MLRA 42 is 28.8 cm (n=60), with 32% of precipitation occurring during the cool season and 68% occurring during the warm season (Figure 1d). MMP values are highest after the NAM and lowest in the late spring before the start of the following NAM when PET is seasonally increasing (Figure 1h). The percentage of study sites registering drought during each DOY increases during the start of the NAM (Figure 2l). NAM onset is highly consistent (Ellis et

al. 2004, Higgins et al. 1997) and deviations in expected soil water can lead to negative matric potential anomalies and greater risk of drought onset.

Annual precipitation distributions in both MLRA 30 and MLRA 42 are unimodal, with most precipitation occurring during either the cool or warm seasons, respectively. This explains the distribution of MMP values peaking near the major precipitation season and declining until the occurrence of next year's major precipitation season. Drought onset patterns indicate that the greatest risk of low matric potential also corresponds with the unimodal distribution of each MLRA.

Bimodal MLRAs

The unimodal seasonal precipitation of MLRA 30 and MLRA 42 contrasts with that of MLRA 40 and MLRA 41, which receive bimodal precipitation during both cool and warm seasons. MLRA 41 is the wettest MLRA in the study region, with a MAP of 37 cm, 58% of which occurs during the warm season (Figure 1c). High MMP values are observed during the cool (February) and warm (August) seasons, corresponding with the bimodal precipitation distribution of the MLRA (Figure 1g). Lowest MMP values are observed before that start of the NAM, when precipitation is lowest and seasonal PET rates are rising. Increases in the percentage of study sites registering drought during each DOY are observed during the cool and warm seasons, indicating that the risk of low matric potential values and drought onset in MLRA 41 is also bimodal (figure 2k).

The MAP of MLRA 40 is 20.8 cm, with 55% of precipitation occurring during the cool season (Figure 1b). While MLRA 40 receives bimodal precipitation, both seasons are notably muted compared to other MLRAs. Additionally, MLRA 40 has the highest PET values of the study region. These factors result in MMP values at 10cm drying to a study region minimum

during June (Figure 2f). Highest MMP values are observed during the cool season. The percentage of study sites registering drought during each DOY increases during the early cool season. Notably, no increase is observed during the warm season, which is associated with inconsistency of the NAM reaching this MLRA (Figure 2j). Thus, despite MPP values being lowest during the warm season, the risk of drought onset is associated with delayed or missed precipitation during the cool season.

Drought Seasonal Occurrence

Drought events were categorized by duration into short-term (lasting longer than 60 days but less than 270 days) and long-term (lasting longer than 270 days). These events were further subdivided by 1) MLRA, 2) depth, and 3) start and end season (cool and warm) (Figure 3). This study designates the fall and winter months (October – March) as the 'cool' season and spring and summer months (April – September) as the 'warm' season.

Short-term

In MLRA 30, a total of 532 short-term drought events occurred across all study sites (n=240) at 10cm between 1979 and 2020, with 46% starting and ending during the 'cool-cool' seasons (figure 3a). A total of 516 events occurred across all study sites at 30cm, with 45% starting and ending during the 'cool-warm' seasons (figure 3a). MLRA 30 has a unimodal precipitation distribution, with a majority of precipitation occurring during the cool season (figure 2a). Below average precipitation during the early cool season will lead to matric potential anomalies and drought onset. Further into the cool season, the likelihood of precipitation increases, leading to drought cessation. The difference in drought end season between 10cm and 30cm is due to 1) the time lag in water movement to deeper depths causing these droughts to end in the early warm season (i.e. Spring) or 2) NAM precipitation.

In MLRA 40, a total of 594 short-term drought events occurred at 10cm with 40% starting and ending during the ‘cool-cool’ months, 28% during the ‘cool-warm’ months, and 30% during the ‘warm-cool’ months (figure 3b). At 30cm, a total of 631 events occurred with 38% occurring during both the ‘cool-cool’ and ‘cool-warm’ months (figure 3b). The more evenly distributed occurrences of short-term drought events reflect the bimodal precipitation distribution of MLRA 40. Like MLRA 30, below average precipitation during the more reliable cool season increases the chance of matric potential anomalies developing at both 10cm and 30cm. While some of these anomalies will recover later in the cool season, others will be solved by NAM storms during warm months, explaining the high occurrence of ‘cool-cool’ and ‘cool-warm’ drought events, respectively. Increased frequency of drought occurrence during the ‘warm-cool’ months can be attributed to years when less NAM storms reach MLRA 40, creating soil water anomalies that are not ameliorated until the following cool season. The minimal occurrence of ‘warm-warm’ droughts reflects low frequency of NAM precipitation in this MLRA.

In MLRA 41, a total of 391 short-term drought events occurred at 10cm with 49% starting and ending during the ‘cool-warm’ months (figure 3c). At 30cm, a total of 634 events occurred with 48% occurring during to ‘cool-warm’ months (figure 3c). Although MLRA 41 has a bimodal precipitation distribution, these results indicate that below average precipitation during the cool season is the primary cause of short-term drought onset at both 10cm and 30cm. The resulting soil water anomalies are ended by NAM storms during the warm season. High frequency (~25%) of ‘cool-cool’ and ‘cool-warm’ categories at 10cm and 30cm, respectively, follow the same explanations as MLRA 30 and MLRA 40. More dependable NAM precipitation during warm months causes reduced occurrences of ‘warm-warm’ droughts.

In MLRA 42, a total of 460 short-term drought events occurred at 10cm with 37% starting and ending during the ‘cool-warm’ seasons (figure 3d). At 30cm, a total of 529 events occurred with 40% starting and ending during the ‘warm-cool’ seasons (figure 3d). The unimodal precipitation of MLRA 42 occurs mainly during the warm season from the NAM. Below average NAM precipitation can result in soil water anomalies at 10cm that develop during the following cool season (see cool season, figure 2h). These 10cm anomalies will recover during the following NAM season, explaining the high frequency of the ‘cool-warm’ start and end season category. Given the consistency of NAM onset, delayed starts can result in fast developing soil water anomalies. This, combined with the beforementioned time lag of soil water to deeper depths, can result in matric potential anomalies at 30cm. These anomalies will not be ameliorated until the early cool months (i.e. Fall), explaining the high percentage of ‘warm-cool’ short-term drought events at this depth.

Across the study region, start and end seasons of short-term drought events are the result of complex interactions between modal precipitation timing, infiltration time lags, and NAM variability. A west to east gradient in start and end season of short-term drought events is observed from ‘cool’ to ‘warm’. Short-term droughts in western MLRAs often begin with below average precipitation during the early cool season and end later into the same cool season when the chance of precipitation climatologically increases. In eastern MLRAs, short-term drought events typically begin due to delayed onset or below average NAM precipitation and end further into the NAM season. Overall, more short-term droughts occur at 30cm compared to 10cm – except in MLRA 30 where precipitation occurs more regularly during the cool season when ET is low, allowing for more infiltration. More rapid drought development can occur at 30cm in

eastern MLRAs where some or most precipitation occurs during warm months when ET is high, especially if NAM events are small or infrequent.

Long-term Drought Seasonal Occurrence

Long-term drought events lasting longer than 270 days are shown in Figure 3e-h. A total of 45 and 221 long-term drought events occurred at 10cm and 30cm, respectively, across all MLRAs and all study sites (n=240) between 1979 and 2020. It is important to note that when reporting start and end season occurrence percentages that those percentages are made up of only one or a few years (figure 3).

In MLRA 30, a total of 28 long-term drought events occurred at 10cm, with 79% starting and ending during the 'cool-cool' months. A total of 91 events occurred at 30cm, with 91% starting and ending during the 'cool-cool' months. Most of these events occurred during the early 2000s. Given the unimodal precipitation distribution of MLRA 30, these long-term drought events were predominantly caused by large below average cool season precipitation anomalies resulting in longer than average dry spells that are unlikely to be resolved until the following rainy season.

In MLRA 40, a total of 11 long-term drought events occurred at 10cm, with 82% starting and ending during the 'cool-cool' months. A total of 58 events occurred at 30cm, with 52% starting and ending during 'cool-cool' months and 45% during 'cool-warm' months. Like in MLRA 30, most of these events occurred in the early 2000s. Although MLRA 30 has a bimodal precipitation distribution, its lower elevation results in higher interannual precipitation variability, especially during the warm season. This can lead to increased risk of a below average rainy season and thus higher potential for long-term drought.

In MLRA 41, no long-term drought events occurred at 10cm based on our definition. At 30cm, a total of 7 long-term drought events occurred, with 6 occurring in the early 2000s. The bimodal precipitation distribution and more consistent nature of cool and NAM rains in MLRA 41 make it difficult for long-term droughts to occur at 10cm, given that these two seasons are within 270 days of each other. Long-term droughts that do occur require unusually long dry spells that emerge and span through the two wetter times of the year in the cool and warm seasons.

In MLRA 42, a total of 6 long-term drought events occurred at 10cm, with 2 (33%) starting and ending during the 'cool-cool' months and 2 (33%) during the 'cool-warm' months. A total of 65 events occurred at 30cm, with 48% starting and ending during the 'warm-warm' months. Most events occurred between 2011 and 2013. Given the unimodal precipitation distribution of MLRA 42, it is likely that most long-term drought events are the result of below average NAM precipitation that produce soil water anomalies which typically not resolved until the following NAM.

The climatological reliability of seasonal precipitation totals in bimodal MLRAs needs to be considered when analyzing long-term drought development. Average cool and warm season precipitation totals in MLRA 41 are larger and more consistent over time than those in MLRA 40 due to more reliable warm season precipitation from the NAM. This leads to long-term drought events being more common in MLRA 40, albeit not as common as unimodal MLRAs, despite having a bimodal precipitation distribution. In years when monsoon precipitation fails to reach MLRA 40, long-term drought development can operate more like an MLRA with unimodal precipitation. This explains the difference in frequency of long-term droughts between MLRA 40 and 41.

Based on our definition, long-term matric potential drought events across the study region are infrequent and occur only during specific years due to unusual deviations from seasonal precipitation patterns (Figure 3e-h). Long-term drought events that do occur are more frequent in MLRAs with unimodal precipitation distributions, likely caused by below average rainy seasons resulting in especially long dry spells. Long-term drought events in MLRAs with bimodal precipitation distributions require multiple below average rainy seasons to occur, which is abnormal of these MLRAs climatology. Across all MLRAs, it is difficult to get long-term drought events at 10cm due to matric potential values being closely coupled with small precipitation events. Long-term drought events that do occur at 10cm are often linked with deeper drought events at 30cm, such as the prominent early 2000s drought (yellow-colored years, Figure 3e-h).

Longest 30cm Drought at Each Location

The maximum 30cm long-term drought (>270 days) that occurred at each study site between 1979 and 2020 is shown in Figure 4. The event year is represented by color and the event duration is represented by symbol size. Most long-term droughts occurred during a few specific years, were similar in duration, and are specific to each MLRA. In MLRA 30, the 2002 drought was most prominent, especially in the northeastern portion of the MLRA. Study sites in MLRA 40 experienced long-term drought events during 1997, 2002, 2010, and 2018. As previously discussed, although MLRA 40 has a bimodal precipitation distribution, the MLRAs lower elevation and generally more arid climate leads to high variability in season-to-season precipitation during the cool and warm months. This leads to increased risk of long-term drought. In contrast, the bimodal precipitation distribution and lower interannual variability of MLRA 41 make long-term drought development difficult, explaining why the MLRA

experienced only one localized long-term drought in 2003. Major long-term droughts in MLRA 42 are specific to 1993-1994 and 2011-2013. Case studies of the 2002 drought in MLRA 30, 2003 drought in MLRA 41, and 2011-2013 drought in MLRA 42 are conducted given their prominence throughout their respective MLRAs to analyze drought development.

Analysis of 2001-2003 Drought in MLRA 30

Causes and mechanisms behind the 2002 drought in the Southwest are well-studied, with above average warm season temperatures and anomalous atmospheric ridging being associated with drought development (Quiring and Goodrich 2008; Weiss et al. 2009). Our results offer a matric potential perspective to these findings. Daily precipitation, PET, and matric potential values were analyzed to evaluate soil water anomaly development during the 2002 drought in MLRA 30 (Figure 5). Percent rank values of daily matric potential anomalies (henceforth referred to as MPAs) at 10cm and 30cm dropped below 15% in late fall 2001 and early winter 2001, respectively, indicating drought onset (Figure 5c). MPAs climbed above 15% at 10cm and 30cm in fall of 2002 and winter of 2003, respectively, indicating drought cessation. Drought duration totaled 368 days at 10cm and 420 days at 30cm.

MLRA 30 has a unimodal precipitation distribution, with 70% of precipitation occurring during the cool season (Figure 2a). Matric potential values in MLRA 30 rely on cool season precipitation for recharge, and normally decline through the remainder of the water year (Figure 2e). Above average PET and below average precipitation during the 2001 warm months lead to the emergence of rapid developing matric potential anomalies and drought onset during early 2002. These anomalies would have been typically resolved by average levels of precipitation during the following cool season. However, anomalous atmospheric ridging (Quiring and Goodrich 2008) caused well below average 2002 cool season precipitation, ultimately changing a

would-be short-term drought into a long-term drought. Drought cessation would not occur until the following 2003 cool season. Therefore, the 2002 long-term drought in MLRA 30 was caused above average PET during the 2001 warm season, exacerbated by below average precipitation during the 2002 cool seasons, and ended by above average precipitation during the 2003 cool season.

Analysis of 2002-2003 Drought in MLRA 41

In MLRA 41, a long-term drought occurred at 30cm from 2002-2003 with a duration of 411 days (Figure 6). Drought onset occurred in October of 2002 and cessation occurred in November 2003. Below average precipitation during the 2002 cool season and 2002 monsoon (blue, figure 6b), coupled with above average PET (green, figure 6b), created compounding anomalies which led to drought onset at 30cm in August 2002 (green, figure 6c). Drought conditions continued through the following year due to below average precipitation and above average PET during the 2003 winter and 2003 monsoon seasons. It is worth noting that 10cm MPAs did not experience long-term drought during this period, and multiple precipitation events led to substantial increases in MPAs (orange, figure 6c). Precipitation during the 2004 winter and early spring months would eventually cause drought cessation at 30cm.

MLRA 41 receives precipitation during the winter and summer (monsoon) months. When compared to other MLRAs which are dominated by a single precipitation season, long droughts in MLRA 41 require the combination of multiple consecutive underperforming precipitation seasons. The 2003 drought is an example of this scenario, as interactions between La Nina from the Pacific Decadal Oscillation, warm phase of the Atlantic Multidecadal Oscillation, and positive phase of the Eastern Pacific Oscillation caused below average cool and warm season precipitation during 2002 and 2003 (Quiring and Goodrich 2008). These conditions were

exacerbated by above average PET during period. Seasonal precipitation during the 2004 cool season would eventually cause drought cessation at 30cm.

Analysis of 2010-2011 and 2012-2013 Droughts in MLRA 42

In MLRA 42, two consecutive long-term droughts occurred at 30cm from 2010-2011 and 2012-2013 following below average monsoon precipitation during the previous season (Figure 7). Onset of the 2010-2011 drought occurred in December of 2010 and cessation occurred during December of 2011, lasting 366 days. Onset of the 2013 drought occurred in October of 2012 and cessation occurred in July of 2013, lasting 280 days.

Onset of the 2010-2011 and 2012-2013 droughts occurred due to below average precipitation coupled with above average PET during the previous monsoon seasons. Pulses of precipitation were able to increase 10cm matric potential during both the 2010-2011 and 2012-2013 droughts (orange, figure 7c), but were not able to propagate to deeper depths like 30cm (green, figure 7c) due to the combination of precipitation event size and high levels of PET. Cessation of the 2010-2011 drought at 30cm would occur following the anomalous above average precipitation during the 2012 winter season. Cessation of the 2012-2013 drought at 30cm would occur during the following 2013 monsoon season.

In MLRA 42, monsoon precipitation is the dominate control on matric potential values (figure 2d). Underperforming monsoon seasons can lead to drought onset by the late fall or early winter months. While small precipitation events in average or even below average winter seasons can lead to drought cessation at 10cm, drought is likely to continue at 30cm. The importance of the 2012 winter rainy season should be noted. Without the above average precipitation and below average PET, it is likely that the 2011 and 2013 droughts would have become connected.

CONCLUSION

The arid and semi-arid climate of the Southwestern United States presents unique challenges for quantifying drought conditions as limited annual precipitation availability and high potential evapotranspiration make distinguishing dry conditions from background aridity difficult (Wilcox et al. 2003). Due to the tight coupling between Southwestern vegetation productivity and soil water availability (Neilson et al. 1992), understanding how delays in the seasonal timing and magnitude of precipitation can lead to drought onset required further investigation. We conducted a widescale drought event analysis of the Southwestern United States to better understand the relationship between drought occurrence and seasonal precipitation timing and magnitude. By coupling soil modeling, site-specific soils information, and high resolution, spatially continuous datasets, we simulated daily matric potential values at 10cm and 30cm from 1979-2020 for 240 study sites across the Southwest. A historical anomaly time series was created at each study site and percent ranked from 0-100%. Consecutive days below the 15th percentile were quantified as drought events. Drought events were categorized by duration (short-term vs long-term) and analyzed by seasonal onset and cessation period using cool and warm season classifications.

The study region's precipitation gradient from west to east creates unique matric potential patterns within each MLRA. In general, annual matric potential values follow the modal precipitation distribution of their respective MLRA. Annual matric potential values in unimodal MLRAs peak once pre year during rainy months and decline until the following years rainy season. Annual matric potential values in bimodal MLRAs peak twice per year and decline through the next rainy season. Analysis of drought emergence patterns indicated delayed or

slowed starts to modal precipitation seasons can bring on rapidly developing soil water anomalies.

Evaluation of drought event occurrence intervals showed that short-term droughts across the study region are frequent. At 10cm, short-term drought events typically start and end during a MLRAs major modal precipitation season. At 30cm, short-term drought events typically start during a MLRAs major modal precipitation season, but end in the following season. This shift is attributed to delayed infiltration to deeper depths.

Long-term droughts are infrequent and occur only during specific years. Long-term droughts are more common at 30cm compared to 10cm, typically starting and ending during a MLRAs major modal precipitation season. Long-term droughts are more frequent in MLRAs with unimodal precipitation distributions compared to MLRAs with bimodal precipitation distributions.

Analysis of the most common drought years in each MLRA showed that tight coupling between surface precipitation inputs and 10cm matric potential make long-term drought development difficult compared to 30cm. While above average PET can lead to rapidly developing matric potential anomalies, it is ultimately below average rainy seasons that lead to long-term drought development at 30cm. In unimodal MLRAs, soil water anomalies at 30cm produced by below average rainy seasons will likely go unresolved until the following rainy season. In MLRAs with bimodal precipitation distributions, long-term drought development is difficult due to consecutive below average rainy seasons being needed.

Comparing our results with Leeper et al. 2022 reveals that the variability they noted in seasonal drought onset and cessation can be linked with the modal precipitation distribution of each MLRA. In western MLRAs, drought onset mostly occurs due to delayed or slowed starts to

cool season precipitation, which can lead to drought onset in the winter or spring at 10cm and 30cm, respectively. However, our results differ in eastern MLRAs, where drought onset is mainly the product of delayed starts to the NAM. Most droughts end during each MLRAs respective rainy season, which is confirmatory with Leeper et al. 2022.

As climate change is expected to increase heat wave frequency and duration over the coming decades (Romero-Lankao et al. 2014), the timing and magnitude of seasonal soil water recharge will become more important for vegetation productivity. Understanding how delays in precipitation can lead to soil water anomalies is thus key for evaluating future drought impacts. This study illustrated the importance of seasonal precipitation and how that translates to short- and long-term drought development. By categorizing these relationships, this study hopes to advance discussions on drought propagation in Southwestern soils, which is key for future drought impact assessment and mitigation plans.

FIGURES

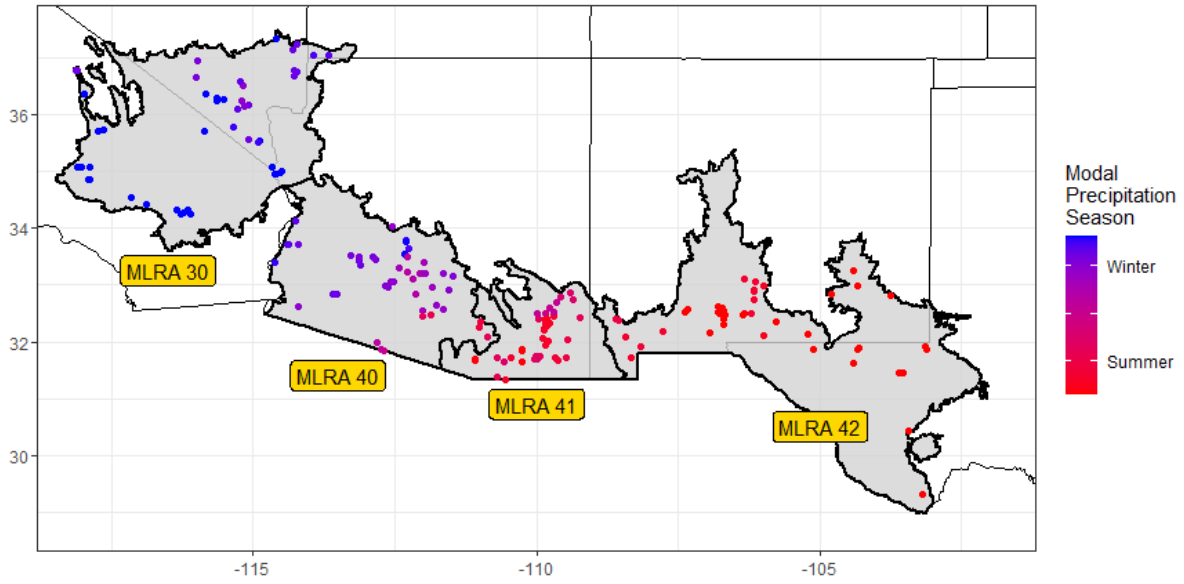

Figure 1: Map of study region with outlines of MLRAs 30 (Mojave Desert), 40 (Western Sonoran Desert), 41 (Eastern Sonoran Desert), 42 (Chihuahuan Desert). Color of each study location (n=240) represents the location's major modal precipitation season.

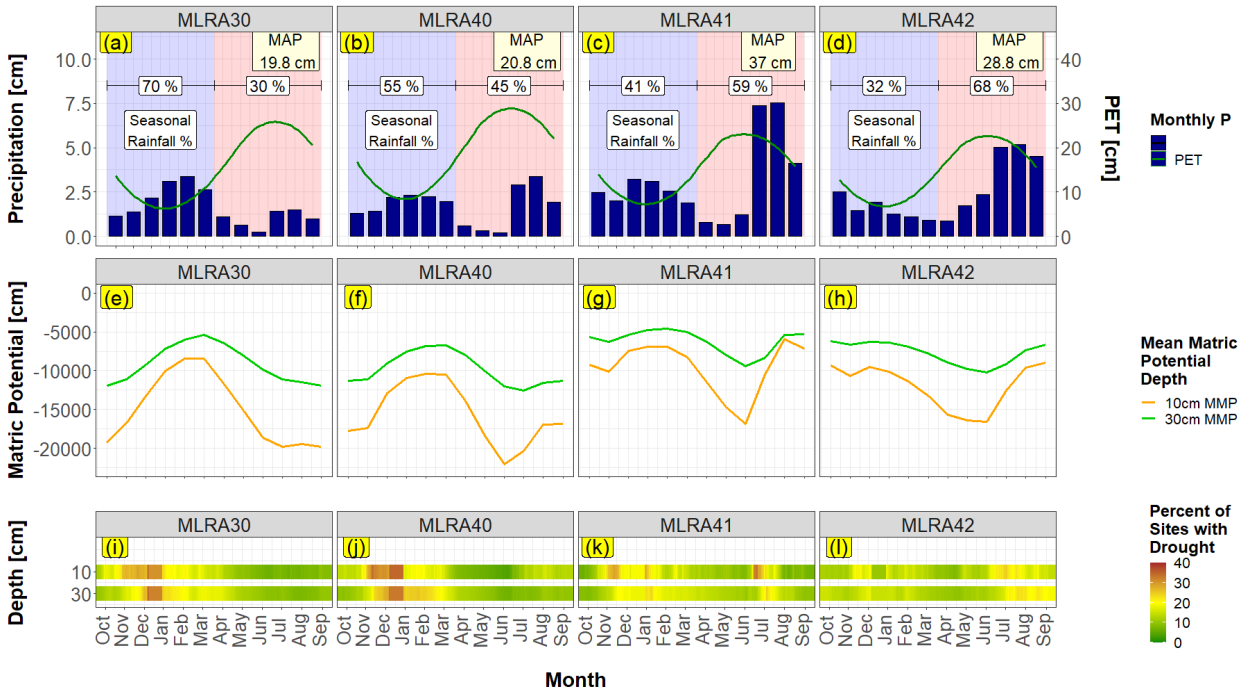

Figure 2: Climatology of each MLRA, including seasonal rainfall percentages (a-d). Monthly mean matric potential values at 10cm and 30cm of each MLRA (e-h). Percentage of study sites within each MLRA (n=60) that register drought conditions during each DOY (i-l).

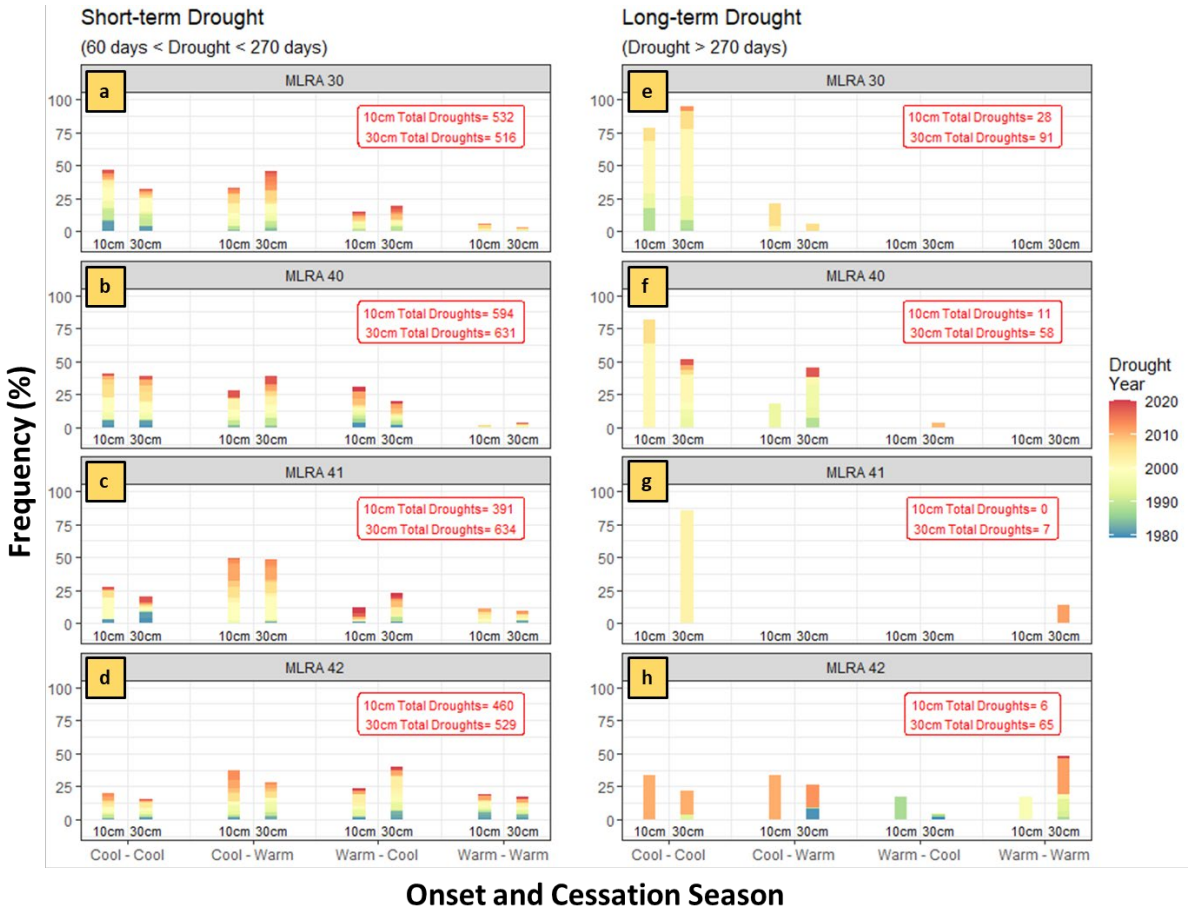

Figure 3: Percent frequency of onset and cessation season for short-term (a-d) and long-term (e-h) droughts at 10cm and 30cm. Drought onset year is color coded.

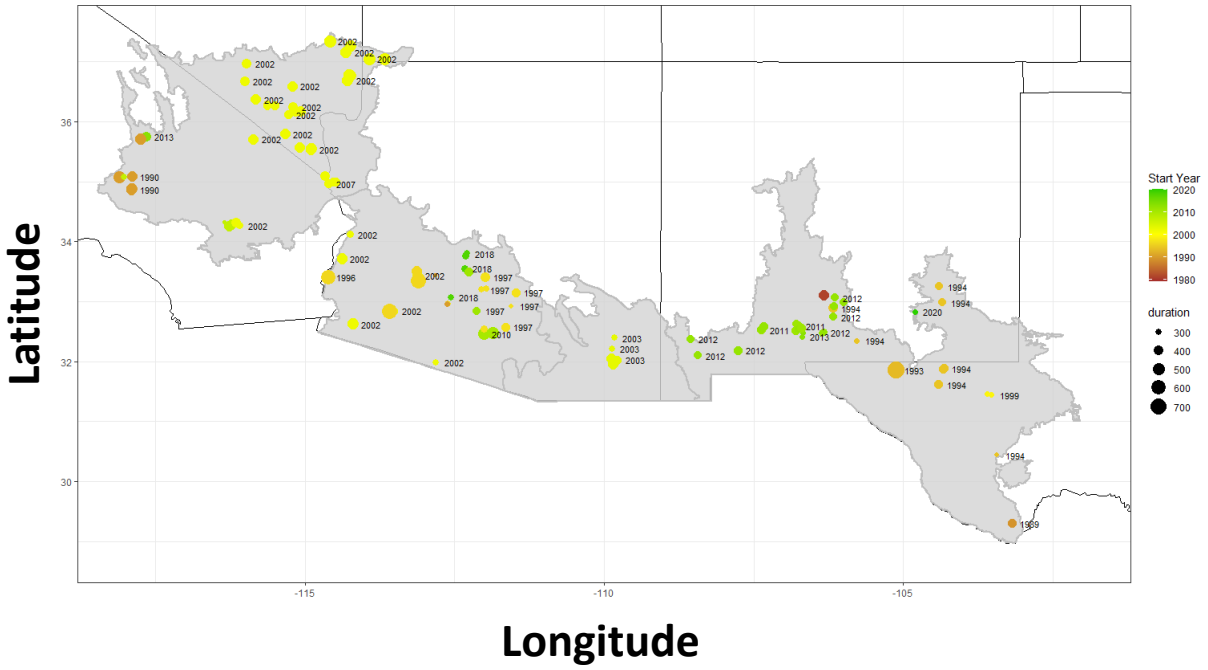

Figure 4: Longest long-term (>270 days) drought at each study location between 1979 - 2020. Dot color represents drought onset year and dot size represents drought duration.

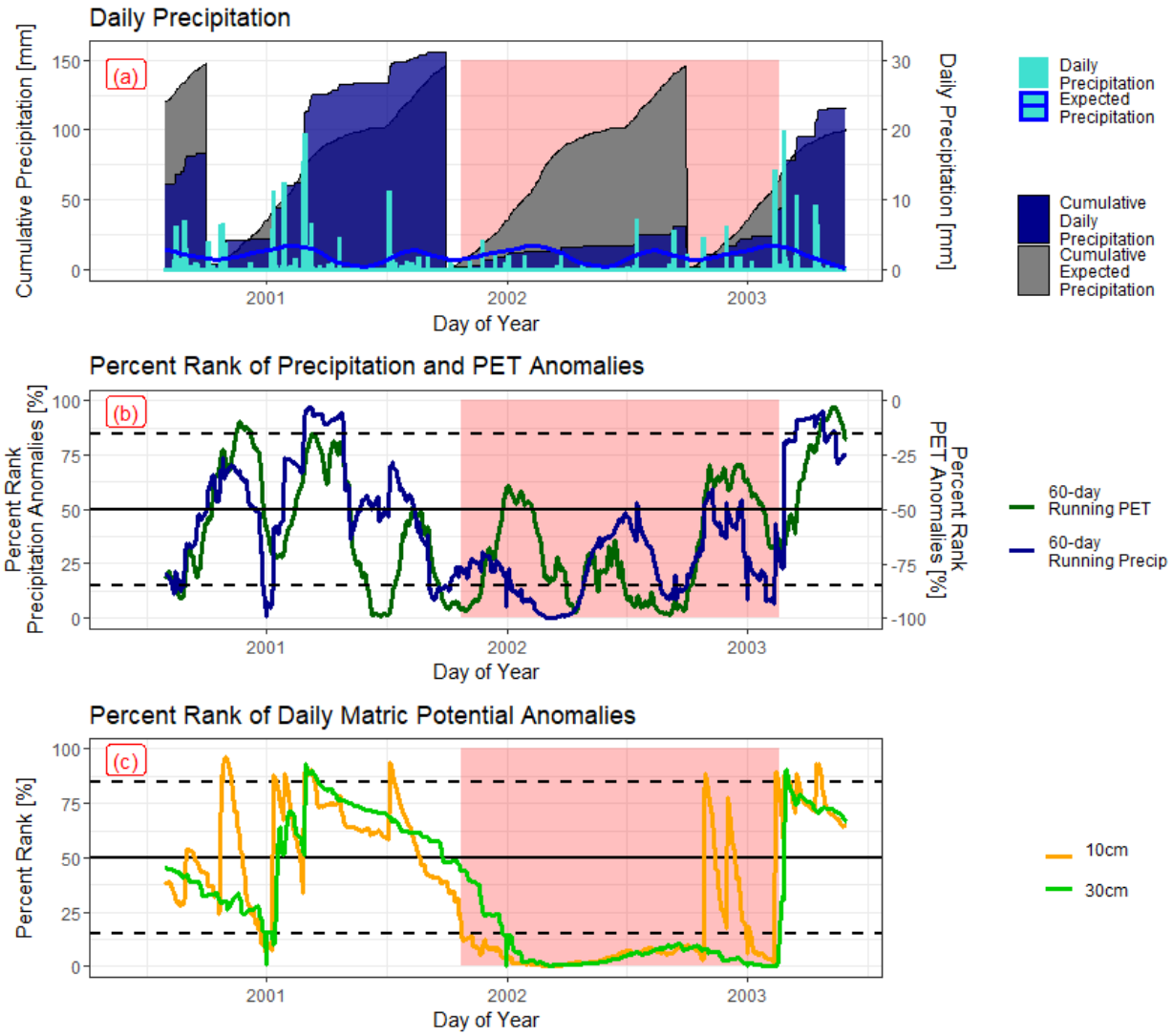

Figure 5: Case study of the 2001-2003 drought in MLRA 30 (model #129). Daily precipitation (a), the percent rank of daily precipitation and PET anomalies (b), and the percent rank of daily matric potential anomalies at 10cm and 30cm (c) are shown from 2001 through 2003. Drought onset at 10cm and cessation at 30cm is highlighted in red.

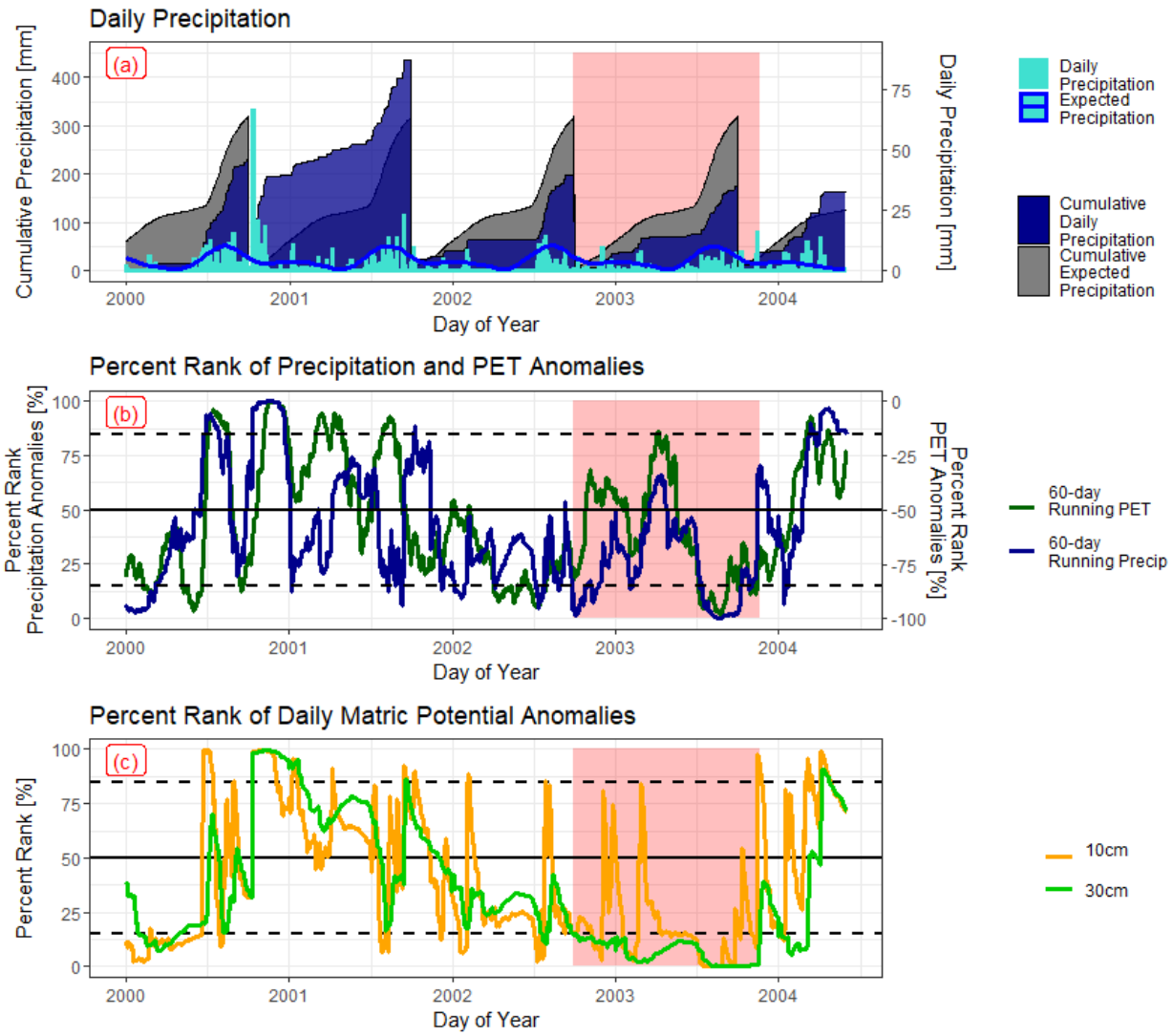

Figure 6: Case study of the 2002-2003 drought in MLRA 41 (model #228). Daily precipitation (a), the percent rank of daily precipitation and PET anomalies (b), and the percent rank of daily matric potential anomalies at 10cm and 30cm (c) are shown from 2000 through 2004. Drought onset at 10cm and cessation at 30cm is highlighted in red.

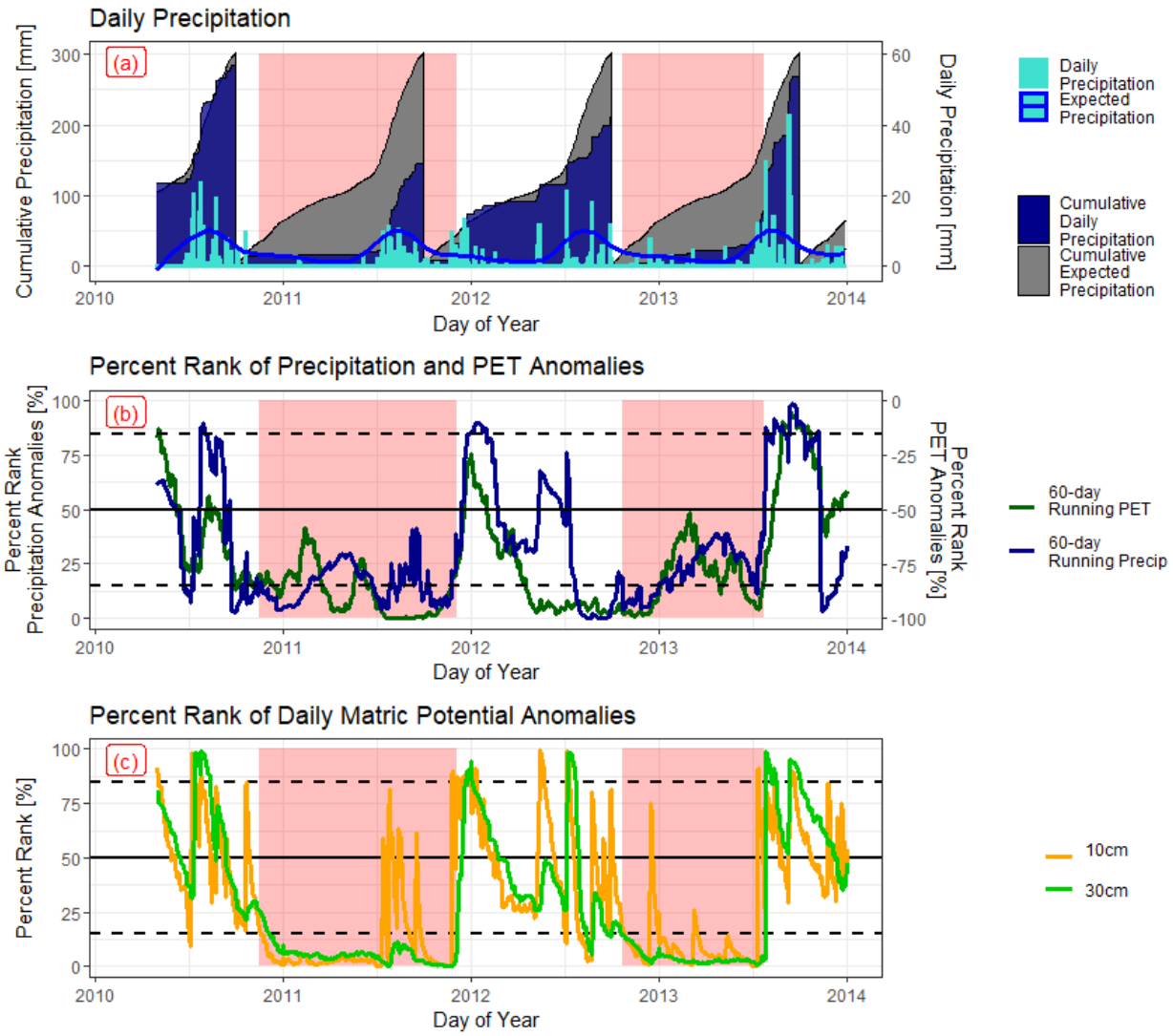

Figure 7: Case study of the 2010-2011 and 2012-2013 drought in MLRA 42 (model #77). Daily precipitation (a), the percent rank of daily precipitation and PET anomalies (b), and the percent rank of daily matric potential anomalies at 10cm and 30cm (c) are shown from 2010 through 2013. Drought onset at 10cm and cessation at 30cm is highlighted in red.

REFERENCES

Abatzoglou, J. T. (2013). Development of gridded surface meteorological data for ecological applications and modelling. International Journal of Climatology, 33(1), 121-131.

Adams, D. K., & Comrie, A. C. (1997). The north American monsoon. Bulletin of the American Meteorological Society, 78(10), 2197-2214.

AghaKouchak, A. (2014). A baseline probabilistic drought forecasting framework using standardized soil moisture index: application to the 2012 United States drought. Hydrology and Earth System Sciences, 18(7), 2485-2492.

Allen, R. G., Pereira, L. S., Raes, D., & Smith, M. (1998). Crop evapotranspiration-Guidelines for computing crop water requirements-FAO Irrigation and drainage paper 56. Fao, Rome, 300(9), D05109.

Austin, M. E. (1965). *Land resource regions and major land resource areas of the United States (exclusive of Alaska and Hawaii)* (No. 296-301). Soil Conservation Service, US Department of Agriculture.

Báez, S., Collins, S. L., Pockman, W. T., Johnson, J. E., & Small, E. E. (2013). Effects of experimental rainfall manipulations on Chihuahuan Desert grassland and shrubland plant communities. Oecologia, 172(4), 1117-1127.

Barnard, D. M., Germino, M. J., Bradford, J. B., O'Connor, R. C., Andrews, C. M., & Shriver, R. K. (2021). Are drought indices and climate data good indicators of ecologically relevant soil moisture dynamics in drylands?. Ecological Indicators, 133, 108379.

Beaudette, D. E., Skovlin, J., Roecker, S., & Beaudette, M. D. (2022). Package 'soilDB'.

Berg, A., & Sheffield, J. (2018). Climate change and drought: the soil moisture perspective. Current Climate Change Reports, 4(2), 180-191.

Bodner, G. S., & Robles, M. D. (2017). Enduring a decade of drought: Patterns and drivers of vegetation change in a semi-arid grassland. Journal of Arid Environments, 136, 1-14.

Bradford, J. B., Schlaepfer, D. R., Lauenroth, W. K., & Palmquist, K. A. (2020). Robust ecological drought projections for drylands in the 21st century. Global Change Biology, 26(7), 3906-3919.

Bradford, J. B., Schlaepfer, D. R., Lauenroth, W. K., Palmquist, K. A., Chambers, J. C., Maestas, J. D., & Campbell, S. B. (2019). Climate-driven shifts in soil temperature and moisture regimes suggest opportunities to enhance assessments of dryland resilience and resistance. Frontiers in Ecology and Evolution, 358.

Breshears, D. D., Myers, O. B., Meyer, C. W., Barnes, F. J., Zou, C. B., Allen, C. D., ... & Pockman, W. T. (2009). Tree die-off in response to global change-type drought: mortality

insights from a decade of plant water potential measurements. Frontiers in Ecology and the Environment, 7(4), 185-189.

Carleton, A. M., Carpenter, D. A., & Weser, P. J. (1990). Mechanisms of interannual variability of the southwest United States summer rainfall maximum. Journal of Climate, 3(9), 999-1015.

Dorigo, W. A., Wagner, W., Hohensinn, R., Hahn, S., Paulik, C., Xaver, A., ... & Jackson, T. (2011). The International Soil Moisture Network: a data hosting facility for global in situ soil moisture measurements. Hydrology and Earth System Sciences, 15(5), 1675-1698.

Dorigo, W., de Jeu, R., Chung, D., Parinussa, R., Liu, Y., Wagner, W., & Fernández-Prieto, D. (2012). Evaluating global trends (1988–2010) in harmonized multi-satellite surface soil moisture. Geophysical Research Letters, 39(18).

Douglas, M. W., Maddox, R. A., Howard, K., & Reyes, S. (1993). The mexican monsoon. Journal of Climate, 6(8), 1665-1677.

Dracup, J. A., Lee, K. S., & Paulson Jr, E. G. (1980). On the definition of droughts. Water resources research, 16(2), 297-302.

Ellis, A. W., Saffell, E. M., & Hawkins, T. W. (2004). A method for defining monsoon onset and demise in the southwestern USA. International Journal of Climatology: A Journal of the Royal Meteorological Society, 24(2), 247-265.

Garfin, G., Jardine, A., Merideth, R., Black, M., & LeRoy, S. (Eds.). (2013). Assessment of climate change in the southwest United States: a report prepared for the National Climate Assessment. Washington, DC, USA: Island Press/Center for Resource Economics.

Gremer, J. R., Bradford, J. B., Munson, S. M., & Duniway, M. C. (2015). Desert grassland responses to climate and soil moisture suggest divergent vulnerabilities across the southwestern United States. Global Change Biology, 21(11), 4049-4062.

Grover, H. 2021. Mitigating Postfire Runoff and Erosion in the Southwest using Hillslope and Channel Treatments. ERI Working Paper No. 44. Ecological Restoration Institute, Northern Arizona University. 11 pp

Hadley, N. F., & Szarek, S. R. (1981). Productivity of desert ecosystems. BioScience, 31(10), 747-753.

Herrera-Estrada, J. E., Satoh, Y., & Sheffield, J. (2017). Spatiotemporal dynamics of global drought. Geophysical Research Letters, 44(5), 2254-2263.

Higgins, R. W., Yao, Y., & Wang, X. L. (1997). Influence of the North American monsoon system on the US summer precipitation regime. Journal of Climate, 10(10), 2600-2622.

Jackson, R. B., Canadell, J., Ehleringer, J. R., Mooney, H. A., Sala, O. E., & Schulze, E. D. (1996). A global analysis of root distributions for terrestrial biomes. Oecologia, 108(3), 389-411.

Jenerette, G. D., Scott, R. L., & Huete, A. R. (2010). Functional differences between summer and winter season rain assessed with MODIS-derived phenology in a semi-arid region. Journal of Vegetation Science, 21(1), 16-30.

Kam, J., Sheffield, J., Yuan, X., & Wood, E. F. (2013). The influence of Atlantic tropical cyclones on drought over the eastern United States (1980–2007). Journal of Climate, 26(10), 3067-3086.

Karl, T. R., & Koscielny, A. J. (1982). Drought in the united states: 1895–1981. Journal of Climatology, 2(4), 313-329.

Koehn, C. R., Petrie, M. D., Bradford, J. B., Litvak, M. E., & Strachan, S. (2021). Seasonal precipitation and soil moisture relationships across forests and woodlands in the southwestern united states. Journal of Geophysical Research: Biogeosciences, 126(4), e2020JG005986.

Lauenroth, W. K., & Bradford, J. B. (2006). Ecohydrology and the partitioning AET between transpiration and evaporation in a semiarid steppe. Ecosystems, 9(5), 756-767.

Leeper, R. D., Bilotta, R., Petersen, B., Stiles, C. J., Heim, R., Fuchs, B., ... & Ansari, S. Characterizing US Drought over the Past Twenty Years using the US Drought Monitor. International Journal of Climatology.

Littell, J. S., Peterson, D. L., Riley, K. L., Liu, Y., & Luce, C. H. (2016). A review of the relationships between drought and forest fire in the United States. Global change biology, 22(7), 2353-2369.

Loik, M. E., Breshears, D. D., Lauenroth, W. K., & Belnap, J. (2004). A multi-scale perspective of water pulses in dryland ecosystems: climatology and ecohydrology of the western USA. Oecologia, 141(2), 269-281.

Madsen, M. D., Chandler, D. G., & Belnap, J. (2008). Spatial gradients in ecohydrologic properties within a pinyon-juniper ecosystem. Ecohydrology: Ecosystems, Land and Water Process Interactions, Ecohydrogeomorphology, 1(4), 349-360.

Mitchell, D. L., Ivanova, D., Rabin, R., Brown, T. J., & Redmond, K. (2002). Gulf of California sea surface temperatures and the North American monsoon: Mechanistic implications from observations. Journal of Climate, 15(17), 2261-2281.

Mo, K. C. (2008). Model-based drought indices over the United States. Journal of Hydrometeorology, 9(6), 1212-1230.

Moody, J. A., & Martin, D. A. (2001). Post-fire, rainfall intensity–peak discharge relations for three mountainous watersheds in the western USA. Hydrological processes, 15(15), 2981-2993.

Neilson, R. P., King, G. A., & Koerper, G. (1992). Toward a rule-based biome model. Landscape Ecology, 7(1), 27-43.

Newman, B. D., Campbell, A. R., & Wilcox, B. P. (1997). Tracer-based studies of soil water movement in semi-arid forests of New Mexico. Journal of Hydrology, 196(1-4), 251-270.

Notaro, M., Liu, Z., Gallimore, R. G., Williams, J. W., Gutzler, D. S., & Collins, S. (2010). Complex seasonal cycle of ecohydrology in the Southwest United States. Journal of Geophysical Research: Biogeosciences, 115(G4).

Noy-Meir, I. (1973). Desert ecosystems: environment and producers. Annual review of ecology and systematics, 4(1), 25-51.

Oglesby, R. J., & Erickson, D. J. (1989). Soil moisture and the persistence of North American drought. Journal of Climate, 2(11), 1362-1380.

Otkin, J. A., Anderson, M. C., Hain, C., Svoboda, M., Johnson, D., Mueller, R., ... & Brown, J. (2016). Assessing the evolution of soil moisture and vegetation conditions during the 2012 United States flash drought. Agricultural and forest meteorology, 218, 230-242.

Owens, M. K., Lyons, R. K., & Alejandro, C. L. (2006). Rainfall partitioning within semiarid juniper communities: effects of event size and canopy cover. Hydrological Processes: An International Journal, 20(15), 3179-3189.

Quiring, S. M., & Goodrich, G. B. (2008). Nature and causes of the 2002 to 2004 drought in the southwestern United States compared with the historic 1953 to 1957 drought. Climate Research, 36(1), 41-52.

Reichle, R. H., De Lannoy, G. J., Liu, Q., Ardizzone, J. V., Chen, F., Colliander, A., ... & Smith, E. B. (2016). Soil Moisture Active Passive Mission L4_SM data product assessment (version 2 validated release) (No. GSFC-E-DAA-TN31807).

Restaino, C. M., Peterson, D. L., & Littell, J. (2016). Increased water deficit decreases Douglas fir growth throughout western US forests. Proceedings of the National academy of Sciences, 113(34), 9557-9562.

Reynolds, J. F., Kemp, P. R., & Tenhunen, J. D. (2000). Effects of long-term rainfall variability on evapotranspiration and soil water distribution in the Chihuahuan Desert: a modeling analysis. Plant Ecology, 150(1), 145-159.

Robock, A., Mu, M., Vinnikov, K., Trofimova, I. V., & Adamenko, T. I. (2005). Forty-five years of observed soil moisture in the Ukraine: No summer desiccation (yet). Geophysical Research Letters, 32(3).

Robock, A., Vinnikov, K. Y., Srinivasan, G., Entin, J. K., Hollinger, S. E., Speranskaya, N. A., ... & Namkhai, A. (2000). The global soil moisture data bank. Bulletin of the American Meteorological Society, 81(6), 1281-1300.

Romero-Lankao, P., Smith, J. B., Davidson, D. J., Diffenbaugh, N. S., Kinney, P. L., Kirshen, P., ... & Villers Ruiz, L. (2014). North America. Climate Change 2014: impacts, adaptation, and vulnerability part B: regional aspects contribution of working group II to the Fifth Assessment Report of the Intergovernmental Panel of Climate Change.

Salley, S. W., Talbot, C. J., & Brown, J. R. (2016). The Natural Resources Conservation Service land resource hierarchy and ecological sites. *Soil Science Society of America Journal*, *80*(1), 1-9.

Sheffield, J., Goteti, G., Wen, F., & Wood, E. F. (2004). A simulated soil moisture based drought analysis for the United States. Journal of Geophysical Research: Atmospheres, 109(D24).

Shepard, C., Schaap, M. G., Crimmins, M. A., Van Leeuwen, W. J., & Rasmussen, C. (2015). Subsurface soil textural control of aboveground productivity in the US Desert Southwest. Geoderma Regional, 4, 44-54.

Sheppard, P. R., Comrie, A. C., Packin, G. D., Angersbach, K., & Hughes, M. K. (2002). The climate of the US Southwest. Climate Research, 21(3), 219-238.

Simunek, J., Sejna, M., Van Genuchten, M. T., Šimůnek, J., Šejna, M., Jacques, D., & Sakai, M. (1998). HYDRUS-1D. Simulating the one-dimensional movement of water, heat, and multiple solutes in variably-saturated media, version, 2.

Simunek, J., Van Genuchten, M. T., & Sejna, M. (2005). The HYDRUS-1D software package for simulating the one-dimensional movement of water, heat, and multiple solutes in variably-saturated media. University of California-Riverside Research Reports, 3, 1-240.

Sugg, M., Runkle, J., Leeper, R., Bagli, H., Golden, A., Handwerger, L. H., ... & Woolard, S. (2020). A scoping review of drought impacts on health and society in North America. Climatic Change, 162(3), 1177-1195.

Svoboda, M., LeComte, D., Hayes, M., Heim, R., Gleason, K., Angel, J., ... & Stephens, S. (2002). The drought monitor. Bulletin of the American Meteorological Society, 83(8), 1181-1190.

Ukkola, A. M., De Kauwe, M. G., Roderick, M. L., Abramowitz, G., & Pitman, A. J. (2020). Robust future changes in meteorological drought in CMIP6 projections despite uncertainty in precipitation. Geophysical Research Letters, 47(11), e2020GL087820.

Van Lanen, H. A. J., & Peters, E. (2000). Definition, effects and assessment of groundwater droughts. In Drought and drought mitigation in Europe (pp. 49-61). Springer, Dordrecht.

Van Loon, A. F. (2015). Hydrological drought explained. Wiley Interdisciplinary Reviews: Water, 2(4), 359-392.

Weiss, J. L., Castro, C. L., & Overpeck, J. T. (2009). Distinguishing pronounced droughts in the southwestern United States: Seasonality and effects of warmer temperatures. Journal of Climate, 22(22), 5918-5932.

Wilcox, B. P., Seyfried, M. S., Breshears, D. D., Stewart, B., & Howell, T. (2003). The water balance on rangelands. Encyclopedia of water science, 791(4).

Wilhite, D. A., & Glantz, M. H. (1985). Understanding: the drought phenomenon: the role of definitions. Water international, 10(3), 111-120.

Williamson, J. C., Bestelmeyer, B. T., & Peters, D. P. (2012). Spatiotemporal patterns of production can be used to detect state change across an arid landscape. Ecosystems, 15(1), 34-47.

Wythers, K. R., Lauenroth, W. K., & Paruelo, J. M. (1999). Bare-soil evaporation under semiarid field conditions. Soil Science Society of America Journal, 63(5), 1341-1349.

APPENDIX B

DEFINING THE MULTISCALAR INDEX TIMESCALE - SOIL WATER DEPTH CONTINUUM FOR THE SOUTHWESTERN UNITED STATES

Trevor T. McKellar[*1]

[*]Corresponding Author

[1]Department of Environmental Science

1177 E. 4th St.

Tucson, AZ 85721, USA

Phone: +1 (520) 621-1646

Email: envs-dept@arizona.edu

Targeted for Publication in Journal of Geophysical Research: Atmospheres

ABSTRACT

Drought monitoring in the semi-arid Southwestern United States poses unique challenges, as distinguishing water deficits from background aridity can be difficult due to potential evapotranspiration being significantly greater than precipitation. Southwestern vegetation has become adapted to the seasonal timing and magnitude of precipitation for soil water recharge, which is the primary control on vegetation productivity. The lack of long-term reliable *in-situ* soil moisture datasets have led land managers to use multiscalar meteorological drought indices, like the Standardized Precipitation Index (SPI) and Standardized Precipitation-Evapotranspiration Index (SPEI), as proxies for soil water availability. However, objectively identifying the index and timescale that best represents soil water availability in semi-arid environments remains a significant gap for applying available climate information to land management action. In this study, we conduct a regional analysis of the Southwest to define the relationship between multiscalar index timescale and soil water availability of different depths. By coupling soil modeling with site-specific soils information and high resolution, spatially continuous datasets, we simulate daily matric potential values at 5cm intervals for 0-200cm from 1979-2020 for the purpose of creating a new matric potential index (MPI). Time series of MPI values at each depth are correlated with SPI and SPEI timescales from 1-24 months. Results indicate the relationship between the highest correlating index timescale and MPI depth operates roughly on a 1:1 step progression at shallow depths (<80cm). Below 80cm, the timescale-depth relationship becomes less linear with a shallower slope. Analysis of the timescale-depth continuum by soil type shows that clay loam soils produce shallower sloped relationships than sandy soils. Furthermore, higher correlation and lower RMSE values are observed when using the SPI or SPEI in clay loam soils then sandy soils. However, the SPI produces higher

correlations and lower RMSE with the MPI overall compared to the SPEI due to the SPEI's use of potential evapotranspiration, which is often much greater than actual evapotranspiration in the Southwest. Therefore, this study recommends SPI usage for shallow (<80cm) soil water monitoring on Southwestern drylands, with a general rule that the relationship between timescale and depth scales linearly in a 1:1 progression. However, if land managers have access to local soils information, it should be consulted given the impacts of soil type on the timescale-depth relationship.

INTRODUCTION

Drylands of the Southwestern United States are an important ecosystem, managed for multiple uses, including forage for livestock, habitat conservation, and open space (Salley et al. 2016). Southwestern climate is arid to semi-arid and characterized by short pulses of moisture and extend periods of dryness (Lauenroth and Bradford 2006), which can create complex drought impacts and monitoring challenges. Dryland managers can benefit from drought monitoring strategies that help them anticipate and respond to changing drought conditions (Gremer et al. 2015, Bodner and Robles 2017). Numerous multiscalar drought indices based on temperature and precipitation data are readily available and commonly used by dryland managers to monitor drought conditions (McKee et al. 1993, Vicente-Serrano et al. 2010; Svoboda and Fuchs 2016). While the multiscalar aspect of these indices can be used to represent different water sources (McKee et al. 1993), objectively identifying the index and timescale that best represent drought conditions of dryland ecosystems remains a significant gap for applying available climate information to land management action. As increased heat wave frequency and drought duration from climate change create extreme stress on areas with water scarcity issues, the need for improved drought monitoring techniques over the coming decades is an important area of future research (Romero-Lankao et al. 2014).

Dryland vegetation productivity is dependent on the timing and magnitude of seasonal precipitation for soil water recharge, which can be used as an indication of overall ecosystem health (Hadley and Szarek 1981; Neilson et al. 1992; Wilcox et al. 2003; Shepard et al. 2015). While monitoring soil water recharge via *in-situ* methods would be ideal, soil moisture probe calibration, maintenance, and expense issues, and the lack of long-term reliable datasets turn many dryland managers toward using meteorological drought indices to approximate soil water

availability (Robock et al. 2000; Robock et al. 2005; Dorigo et al. 2011; Dorigo et al. 2012). Meteorological drought indices are numerical time series of drought severity that convey the probability of occurrence of meteorological drought indicators – such as changes in precipitation, temperature, snowpack, or reservoir levels – compared to the historical record (Svoboda and Fuchs 2016). Two commonly used meteorological drought indices are the Standardized Precipitation Index (SPI) and Standardized Precipitation-Evapotranspiration Index (SPEI), which communicate frequency and magnitude of precipitation and water balance, respectively (McKee et al. 1993, Vicente-Serrano et al. 2010). The SPI and SPEI are multiscalar, allowing for drought conditions of various water sources to be evaluated by calculating index values at different monthly timescale lengths. Choosing the appropriate timescale length is important for monitoring drought conditions as water movement rates vary between water sources (McKee et al. 1993). For example, shorter timescales can be used to approximate shallow soil moisture (Sims et al. 2002) and longer timescales can be used to approximate streamflow, surface reservoirs, or groundwater (Svoboda and Fuchs 2016). However, the complex relationship between Southwestern precipitation and soil water recharge presents unique challenges that prevent fully utilizing multiscalar drought indices as an effective drought monitoring strategy.

Aspects of Southwestern climatology prevent all falling precipitation at the surface from infiltrating into the soil profile. Most Southwestern precipitation is received as small events (<5mm), with short intervals in between (<10 days)(Loik et al. 2004). Many soil and climate factors influence the timing and amount of precipitation that will become available as plant accessible water. For example, low intensity precipitation events can be captured by tree canopy interception (Owens et al. 2006); soil infiltration rates can be limited by texture, compaction, and ground litter (Wythers et al. 1999; Newman et al. 1997; Madsen et al. 2008); soil burn from fire

can result in large scale runoff events, especially during high intensity precipitation from the North American Monsoon (Moody and Martin 2001; Adams and Comrie 1997; Grover 2021); and high temperatures can increase soil evaporation rates (Wythers et al. 1999; Newman et al. 1997; Weiss et al. 2009). Therefore, it is unclear how to apply multiscalar index information to land management action in the Southwest as not all precipitation can be assumed to impact soil water recharge.

Previous studies have established that multiscalar indices can be good indicators of soil water availability; however, these studies are often restricted to examining discrete depths, few locations, and few soil types due to limited data availability – rendering them unable to characterize the entire relationship between index timescale and depth (Sims et al. 2002; Wang et al. 2015). Recent advancements in hydrologic computer modeling have allowed for sophisticated simulation of water movement through a soil profile (Simunek et al. 2005). Studies have begun to couple hydrological models with spatially continuous, high resolution meteorological datasets to drive daily model outputs of soil water availability, allowing for the relationship between index timescale and soil depth to be explored at greater resolution and on more regional scales (Bradford et al. 2019; Koehn et al. 2021). Although located outside the Southwest, these studies have highlighted some potential issues of using multiscalar indices to monitor soil water availability in dryland environments – such as the SPEI being less successful monitoring spring soil water availability and longer index timescales in general struggling to quantify severe drought events (Sohrabi et al. 2015; Barnard et al. 2021). Furthermore, these studies have yet to quantify the impacts of subsurface soil type on the depth-timescale relationship, which is important for aboveground dryland vegetation productivity (Shepard et al. 2015). Thus, the relationship between index timescale and soil water availability at different depths warrants

further investigation for the Southwest. Understanding the relationship between multiscalar drought indices and soil water recharge affords the opportunity to utilize drought indices more effectively for land management purposes on Southwestern drylands.

Here, we investigate the relationship between multiscalar index timescale and different depths of soil water availability for six major soil types of the Southwestern United States. By combining 41 years (1979-2020) of meteorological data and site-specific soils information, daily matric potential estimates are simulated at 5cm intervals from 0-200cm at 240 locations using HYDRUS-1D (Simunek et al. 2005). A new matric potential index (MPI) is created and compared with two common multiscalar meteorological drought indices, the SPI and SPEI (hereby referred to as 'multiscalar indices' when discussed together). By evaluating the best correlating multiscalar index timescale at each MPI depth, we characterize a series of general depth-timescale relationships for the Southwest as a whole, and then further based on soil type. Case studies are used to evaluate differences between multiscalar indices and the MPI at various depths to understand how, when, and where misalignment between indices exists. This study aims to improve drought monitoring on Southwestern drylands by providing approximate 'rule of thumb' relationships for using multiscalar indices as effective drought monitoring practices of soil water availability.

MATERIALS AND METHODS

Study Region

This study defines the Southwestern United States, hereby referred to as "Southwest", as the Mojave, Sonoran, and Chihuahuan deserts. Specifically, this study focuses on the desert regions spanning from Southern California through West Texas that are north of the United States-Mexico border. The United States Department of Agriculture (USDA) divides land into a

hierarchy system based on land usage, resource management, environmental conservation, and agricultural planning (Salley et al. 2016). The primary organization unit of this hierarchy is the Major Land Resource Area (MLRA), which are geographically associated land units that share similar physiography, geology, climatology, hydrology, soils, biology, and land use (Austin 1965; Salley et al. 2016). MLRAs comprise large areas and are important for state and local level agricultural planning, resource conservation, and management decisions (Bestelmeyer et al. 2009). The United States is subdivided into 278 MLRAs, of which four cover the defined study region. Specifically, this study focuses on MLRA 30 (Sonoran Basin and Range), MLRA 40 (Central Arizona Basin and Range), MLRA 41 (Southeastern Arizona Basin and Range), and MLRA 42 (Southern Desertic Basins, Plains, and Mountains), which are part of the larger 'Western Range and Irrigated Region'.

The climatology of the study region can be characterized as having potential evapotranspiration often being significantly greater than precipitation, with each MLRA having a different modal precipitation distribution (Wilcox et al. 2003; McKellar et al. 2022a). The study region has a precipitation gradient from west to east, with western MLRAs (Mojave Desert, MLRA 30) mainly receiving unimodal precipitation during the cool season (fall and winter months) and eastern MLRAs (Chihuahuan Desert, MLRA 42) mainly receiving unimodal precipitation during the warm season (spring and summer months) via the North American Monsoon (NAM). Central areas of the study region (MLRA 40 and MLRA 41, Sonoran Desert) receive precipitation during both the cool and warm season, albeit in varying seasonal amounts, creating a bimodal precipitation distribution (McKellar et al. 2022a). This precipitation gradient gives the study region a good variety of soil water distributions, allowing for a more complete analysis of the relationship between multiscalar indices and modeled soil water availability

throughout the year. The study region contains six dominant soil types – sand, loamy sand, sandy loam, loam, sandy clay loam, and clay loam (Shepard et al. 2015) (figure 1). Given its control on dryland vegetation productivity, the subsurface soil texture was used as the basis for examining the impacts of soil type on the depth-timescale relationship (see section: *Modeling*).

Standardized Precipitation Index (SPI)

The Standardized Precipitation Index (SPI) is a time series of z-score values that represent the frequency and magnitude of *t*-month total precipitation compared to the historical distribution of those same *t*-months (McKee et al. 1993). Due to monthly precipitation data often not being normally distributed, values are transformed using a gamma function to take the shape of a standard normal distribution. This allows the relationship of precipitation probability during a certain time interval to be established. To accomplish this, the 'fitSCI' R-package was used, which removes seasonality from a time series of environmental data and forces it to take the shape of a standard normal distribution (Gudmundsson and Stagge 2016). The resulting time series of z-score values represents the number of standard deviation units an occurrence of total precipitation during a particular monthly interval lies from the historical mean. Furthermore, the SPI can be calculated at a variety of timescales of period t-months, summing precipitation values from the period (McKee et al. 1993).

SPI users can interpret monthly z-score values at various timescales to assess how surpluses or deficits in accumulated precipitation may impact the development or amelioration of drought conditions. Larger negative SPI values represent increasingly dry conditions and larger positive values represent increasingly wet conditions. Importantly, the standardized process allows for direct comparisons of SPI values from different locations. Thus, an SPI value of -2

from two locations indicates the same information about the frequency and magnitude of drought conditions.

Key strengths of the SPI lie with its simple calculation and use of monthly data (McKee et al. 1993; Svoboda and Fuchs 2016). Additionally, the flexibility of varying timescales allows the SPI to approximate water surpluses or deficits of different water sources, like shallow soil moisture or groundwater storage, in which water moves at different rates. However, SPI is limited by its exclusion of temperature, which impacts evapotranspiration rates, and inability to account for surface runoff. Despite these shortcomings, the SPI is an incredibly power tool for quantifying monthly drought occurrence (Svoboda and Fuchs 2016).

The Standardized Precipitation-Evapotranspiration Index (SPEI)

Building on the methodology of the SPI, the Standardized Precipitation-Evapotranspiration Index (SPEI) adds a temperature component to calculate potential evapotranspiration (PET) (Vicente-Serrano et al. 2010). By subtracting PET from precipitation, the SPEI uses a monthly water balance as the basis for it index values. The resulting time series of z-score values convey the frequency and magnitude of monthly water balance surpluses and deficits compared to the historical mean. Like the SPI, the SPEI is also multiscalar, giving more flexibility for approximating water storage of different reservoirs.

Monthly water balance values are often not normally distributed and must undergo a transformation process (Vicente-Serrano et al. 2010). This study uses the R-package 'fitSCI' for the transformation process, which removes seasonality from a time series of environmental data and forces it to take the shape of a standard normal distribution (Gudmundsson and Stagge 2016). Choosing the correct probability distribution is important when transforming monthly water balance data, as different distributions can lead to discrepancies between SPEI values

(Beguería et al. 2014; Stagge et al. 2015). The original authors of the SPEI recommended the use of a log-logistic probability distribution (Vicente-Serrano et al. 2010). However, there is debate about the correct probability distribution function to use (Stagge et al. 2015; Vicente-Serrano and Beguería 2016; Stagge et al. 2016). Shapiro-Wilk normality tests were conducted for different probability distributions available through the 'fitSCI' R package (Gudmundsson and Stagge 2016), with a generalized extreme value (gev) function found to best transform the data to fit a normal distribution.

An advantage of the SPEI compared to the SPI is the inclusion of PET, which allows it to evaluate the impacts of temperature on drought conditions (Vicente-Serrano et al. 2010); however, this comes at the expense of needing additional data and the choice of method used to estimate PET. The use of Thornthwaite, which only accounts for monthly mean temperature (Thornthwaite 1948), to estimate PET can be problematic, as inconsistencies between SPEI values calculated using different PET estimation methods has been observed (Beguería et al. 2014; Stagge et al. 2015). This study uses the Penman-Monteith method to estimate PET, which is more accurate than Thornthwaite due to its inclusion of wind, relative humidity, temperature, and solar radiation (Allen 1998; Majumder and Kumar, 2019).

Data

Soil physical parameters, latitude and longitude coordinates, and elevation data were downloaded using the 'soilDB' R-package, which extracts information from publicly available online soil databases (Beaudette et al. 2021). Data was acquired for all available soil profiles in MLRA 30, 40, 41, 42, which returned a total of 317 profiles. Previous research has found that six main subsurface soil types are common throughout the study region – sand, loamy sand, sandy loam, loam, sandy clay loam, and clay loam (Shepard et al. 2015). Given the importance of

subsurface soil texture on above ground vegetation production (Shepard et al. 2015), the acquired data was filtered to contain complete records of the necessary information needed for modeling (i.e. % sand, % silt, % clay, and soil physical parameters) for only these subsurface soil types. To ensure a representative sampling distribution of the study region and to maximize computational efficiency for the scope of this study, the remaining dataset was filtered so that an equal amount (n=10) of each subsurface soil type (n=6) were selected within each MLRA (n=4). Therefore, a total of 240 study sites were selected across the study region (i.e. 10 of each soil type x 6 soil types x 4 MLRAs = 240 study sites).

Using study-site-specific latitude and longitude coordinates acquired during the previous step, daily meteorological records were retrieved using the Gridded Surface Meteorological (gridMET) dataset (Abatzaglou 2013). GridMET combines gridded data from PRISM (Daly et al. 2008) with coarse regional reanalysis satellite data from the Land Data Assimilation System (LDAS) to produce a spatially and temporally continuous meteorological dataset for the United States at a 4x4km resolution. Notably, GridMET provides wind, relative humidity, and shortwave radiation at a daily scale, which are needed to estimate daily PET using the Penman-Monteith method in the HYDRUS model (Allen 1998). At each study site, daily records were downloaded from 1/1/1979 – 7/17/2021. The acquired GridMET variables are shown in Table 1.

Modeling

Daily matric potential data was simulated for all 240 locations using HYDRUS-1D, a deterministic modeling software designed for simulating water movement in a one-dimensional variably saturated porous media (Simunek et al. 2005). A unique modeling simulation was conducted at each study location using the acquired meteorological and soil profile information. Simulation profile simplifications were made to allow for more straightforward interpretation of

model output. A single, homogeneous soil layer extending from 0-200cm was used, with the soil type being based on the subsurface 'B-horizon' due to its regulation of vegetation production in dryland soils (Shepard et al. 2015). A generalized root profile based on typical dryland vegetation was used to simulate transpiration in the top 200cm of the soil, with root concentration declining in an exponential pattern with depth (Jackson et al. 1996). PET was estimated using the Penman-Monteith equation (Allen 1998). To account for initial conditions influencing model output, a 'spin-up' was included at the beginning of each model simulation that consisted of the first 10 years of gridMET data specific to each site (i.e. 1-1-1079 through 12-31-1988). These 10 years were removed from model output post simulation. For more information on model setup, see McKellar 2022.

Matric Potential Index (MPI)

Model output consisted of daily matric potential values at 5cm intervals ('depth node') from 0-200cm. A matric potential index (MPI) was created at each depth node using a similar methodology to the SPI and SPEI. Daily matric potential values were aggregated into monthly median values. To force these values to fit a standard normal distribution, a transformation was applied using a Pearson-III function from the 'fitSCI' R-package (Gudmundsson and Stagge 2016). The resulting time series of z-score values convey the monthly frequency and magnitude of matric potential surpluses and deficits at each depth node. Unlike the SPI and SPEI, the MPI is not multiscalar as it already contains the soil water memory inherent to soils at increasing depth. In other words, the MPI is always being calculated at a 1-month timescale.

Drought index – MPI Correlations

To study the relationship between multiscalar index timescale and soil water availability at different depths, each timescale of the SPI and SPEI were aligned with each depth of the MPI.

Conceptually, the depth-timescale relationship should be linear to some degree at shallow depths and become more non-linear at deeper depths (figure 2). At shallow depths, soil water availability will more closely match precipitation inputs. However, soil factors such as texture, root water uptake, and soil evaporation will impact infiltration and water movement through the profile. Thus, the linear timescales of the multiscalar indices will become more misaligned with the non-linear movement of soil water through the soil profile at deeper depths (figure 2).

Using the 'corr.test' function in R, Pearson correlation values were calculated between time series of the multiscalar indices at timescales of 1-24 months and time series of the MPI at 5cm intervals from 0-200cm for all study sites. The average (n=240) correlation between each multiscalar index timescale and MPI depth node was evaluated so a general relationship between timescale and depth could be defined. Furthermore, a linear model was fit between each time series of the multiscalar indices at timescales of 1-24 months and each time series of the MPI at 5cm intervals from 0-200cm for all study sites. For this, the SPI or SPEI were treated as the independent variable and the MPI as the dependent variable. The root mean squared error (RMSE) was computed from each study site's linear regression model was used to evaluate bias of the multiscalar indices. The average (n=240) RMSE and MBE for all study sites was used to characterize the role of error and bias when using different multiscalar index timescale to approximate different MPI depths. The role of soil type was characterized using the same correlation and linear model methodology described. However, study sites were subsetted and averaged by soil type (n=60) instead of as all sites.

RESULTS AND DISCUSSION

Average Pearson correlation values between the multiscalar indices and MPI for all study locations (n=240) are shown in Figure 3. Each box of the gridded layout is color coded to

represent the average correlation value between the y-depth MPI and x-timescale SPI (figure 3a) or SPEI (figure 3b) at all 240 study sites. The black-dashed line is plotted through the highest correlating timescale at each depth, hereby referred to as the Highest Correlation Line (HCL). Boxes are only plotted for correlations where p-values <0.05. Grey boxes toward the bottom of figure 3a and 3b indicate that no strong relationship between the MPI-SPI and MPI-SPEI exists at these depths.

Observing the HCL between the SPI and MPI reveals a negatively sloped relationship, where the highest correlating SPI timescale increases with MPI depth (figure 3a). At shallow depths and short timescales, this relationship is highly linear (i.e. 1:1). At depths below 80cm and timescales longer than 14 months, the HCL is still linear but with a shallower slope. The highest average (n=240) correlating value with $p<0.05$ along the HCL is 0.73 and occurs between the 5cm MPI and 2mo SPI. The lowest average correlating value with $p<0.05$ along the HCL is 0.68 and occurs between the 95cm MPI and 24mo SPI. Therefore, a 0.05 decline in correlation values is observed between the best and worst correlating timescales along the HCL.

A negatively sloped relationship is also observed for the HCL between the MPI and SPEI (figure 3b). However compared to the SPI, the HCL slope is steeper and less linear at shallow depths (i.e. not 1:1). At depths below 80cm and timescales longer than 13 months, the HCL is still linear but has shallower slope. The highest average (n=240) correlating value with $p<0.05$ occurs between the 5cm MPI and 2mo SPEI with a value of 0.73. The lowest average correlating value with $p<0.05$ occurs between the 105cm MPI and 24mo SPEI with a value of 0.62. Therefore, a 0.11 decline in correlation values is observed along the HCL between the highest and lowest correlating timescale-depth pairing.

Along the HCL, correlation differences between the SPI-MPI and SPEI-MPI are small. When comparing differences between figure 3a and 3b (i.e. [MPI-SPI] – [MPI-SPEI]), the SPI produces equal to slightly higher correlation values (0 ~ 0.06) with the MPI at all timescale-depth pairings along the respective HCL compared to the SPEI. Notably, SPEI-MPI correlation values are slightly weaker than those of the SPI-MPI. However, when comparing the SPI-HCL and SPEI-HCL across the same depth, the SPEI tends to correlate at slightly shorter timescales than the SPI (figure 3a and 3b).

For both the SPI and SPEI, the timescale-depth relationship is fairly linear from the surface to about 80cm. Maximum correlation values between multiscalar index timescales and MPI depths occur at almost a 1:1 step progression. Thus, at shallow depths, timescales of the drought indices scale linearly with each additional month to a deeper depth of soil water. These scaling results are consistent with previous studies that have attempted to align multiscalar indices with soil water of different depths (McEvoy et al. 2012; Sohrabi et al. 2015; Barnard et al. 2021).

Error analysis between the multiscalar indices and MPI showed that average RMSE values along the HCL were lower (0.05~0.1) for the SPI than the SPEI, indicating that the SPI does a slightly better job fitting the MPI. Average (n=240) values of mean bias difference (MBD), which is the time series sum of the difference between daily multiscalar index and MPI values (sum[daily SPI – daily MPI]), showed that both the SPI and SPEI tend to slightly overestimate the MPI, and that differences increase with depth along the HCL. However, the SPEI produces near-zero bias (MBD = 0 ~ 0.01) at shallow depths and short timescales, while the SPI shows slight positive bias (MBD = ~ 0.07). While these differences are small, the fact that residual RMSE values for the SPEI are high indicate that bias differences between monthly

SPEI and MPI values are more random at shallow depths and short timescales. Conversely, lower residual RMSE values for the SPI indicate that the SPI more closely matches the MPI time series, but with slight positive bias between monthly SPI and MPI values.

It is interesting to note that the inclusion of temperature through the PET term in the SPEI calculation should in theory produce a more closely related monthly value to the MPI, which also includes evapotranspiration through the HYDRUS-1D model. However, it is clear from the correlation results that the inclusion of temperature does not improve the relationship with soil water availability compared to the SPI in the semi-arid Southwest. This is likely due to the SPEI using *potential* instead of *actual* evapotranspiration (AET). Average annual PET in the Southwest is about 2000 mm/year, while AET is closer to MAP (about 200 ~ 400 mm/year depending on MLRA). The MPI incorporates AET through the HYDRUS modeling by the use of a sink term, which is a function of the ratio of PET. The SPI effectively operates as if PET is equal to 0, which is closer to AET in the Southwest compared to PET. Thus, the SPI produces higher correlation values with the MPI compared to the SPEI in the semi-arid Southwest. This result is confirmatory with Afshar et al. 2022, who compared the SPI and SPEI with a satellite derived soil moisture index. However, it may be that the SPEI correlates higher with the MPI during specific seasons, as was noted by Barnard et al. 2021, but this was not examined during this study. Therefore, the higher correlation values between the SPI and MPI overall lead this study to recommend SPI usage for soil water monitoring on Southwestern drylands.

Results by Soil Type

Pearson correlation values between the multiscalar indices and MPI were analyzed by soil type to evaluate the impacts of clay percentage on timescale-depth relationships. The HCL between the SPI-MPI (figure 4a) and SPEI-MPI (figure 4b) for a sand (dotted) and clay loam

(solid) soil are shown. The HCL for loamy sand, sandy loam, loam, and sandy clay loam soil types are not shown for simplification reasons, as they plot between the sand and clay loam HCLs. Each timescale-depth pairing along the HCL is colored to represent the average correlation value between the soil-type-specific MPI (n=40) and multiscalar index.

Results show that soils with less clay content produce steeper sloped and less linear (i.e. not 1:1) timescale-depth relationships then soils with higher clay content (figure 4). At deeper depths (below 80cm), the timescale-depth relationship is less linear for both soil types. However, clay loam HCLs have shallower slopes below 80cm compared to sand HCLs. Correlation values for both SPI-MPI and SPEI-MPI weaken with depth for both soil types. Comparing across the same depth shows soils with more clay content correlate higher and at longer timescales with the MPI than soils with less clay content. Additionally, comparing between the same soil type, the SPI produces equal to higher correlation values than the SPEI.

Analyzing mean RMSE values by soil type shows at shallow depths (<10cm), both the SPI and SPEI produces approximate equal residual errors when fitting sand and clay loam MPIs (~0.7 RMSE). However, below 10cm, both the SPI and SPEI produces less error (lower RMSE values) with clay loam MPIs then sand MPIs. For the SPI, a 0.24 and 0.04 increase in RMSE value is observed along the HCL for sand and clay loam, respectively. For the SPEI, a 0.26 and 0.1 increase in RMSE value is observed along the HCL for sand and clay loam, respectively. Thus, when comparing the same soil type, the SPI produces less error with the soil-type-MPI than the SPEI. However, both the SPI and SPEI produce less error with clay loam MPIs then sand MPIs. Evaluating MBD values shows that both the SPI and SPEI produce larger positive bias for sand MPIs compared to clay loam MPIs and these biases increase with depth.

Correlation results by soil type demonstrate that soil type impacts the relationship between timescale and depth. Furthermore, error analysis indicates that soil type plays a role in controlling RMSE and bias. Differences in soil properties, such as hydraulic conductivity, between sands and clay loams are the likeliest explanation for timescale-depth relationship differences. Larger pore size, distribution, and interconnectivity allows for faster infiltration rates of sandy soils. Faster infiltrations rates will lead to shorter multiscalar index timescales correlating with sand MPIs then clay loam MPIs when comparing across the same depth (figure 4). Additionally, faster infiltration rates in sandy soils will produce steeper sloped HCL relationships compared to clay loams (figure 4). However, faster infiltration rates create misalignment with the linearity of multiscalar index timescales, resulting in increased error and lower correlation values with deeper depth MPIs.

Examining Differences Between Multiscalar Indices and MPI Time Series

Case studies were conducted to better understand the differences between the drought indices and MPI time series produced after aligning the highest correlating multiscalar index timescale with the appropriate MPI depth. Monthly precipitation was aligned with time series of the SPI, SPEI, and MPI. An example case study for a clay loam in MLRA 40 (model #213) is shown in figure 5, where the 30cm MPI is aligned with the respective highest correlating multiscalar index timescales, 7-month SPI (corr=0.77) and 5-month SPEI (corr=0.66), based on the results from figure 4. Three examples of differences between the multiscalar indices and MPI are discussed (figure 5a – 5c).

The documented uncertainty of estimating transformation parameters for a meteorological time series encountering a high number of consecutive zero precipitation months to fit a standard distribution is present in some SPI case studies (Gudmundsson and Stagge 2013;

Stagg et al. 2015). Within the 'fitSCI' R-package, a mixed distribution (p_0=TRUE) can be used during the parameter estimation process to accommodate for this issue (Gudmundsson and Stagge 2013). However, uncertainty in the fitting parameters can persist when greater than 75% of months included in the SPI timescale are zero, leading to an unrealistic index value (Stagg et al. 2015). An example of this is shown in figure 5b, where a dry winter during 1981-82 led to two consecutive months (November and December 1981) where the SPI calculation contained greater than 75% (6 of 7 months) zeros in the timescale. This caused the SPI to differ from the MPI by greater than 1 stand deviation. For this case, increasing the SPIs timescale can correct for the fit parameter issue, but may lower the overall correlation with the MPI. Furthermore, the SPEI's use of a monthly water balance removes the chance of encountering multiple zeros and thus does not suffer from this fit parameter issue.

Both the SPI and SPEI are limited by their timescale length when examining a single time series, which can restrict their ability to match the soil water memory inherent to the MPI. This is especially evident at shallow depths, where timescales are limited to shorter durations of months. During periods of drought, multiscalar indices utilizing short timescales can become optimistic of drought cessation before the MPI due to recent months of above average precipitation. An example of this occurred during the summer of 1990 (Figure 5c), where the MPI was still indicating moderate drought conditions due to a previous dry spell that was no longer included in the SPI and SPEI timescale (7- and 5-months, respectively). For both multiscalar indices, above average precipitation during the summer of 1990 indicated drought cessation, with the SPI and SPEI overestimating the MPI by +1.5 and +2.5 standard deviations, respectively. Additionally, below average PET during this period caused the SPEI to

overestimate the MPI more than the SPI. The MPI would not indicate drought cessation until January 1991.

Conversely, both the SPI and SPEI can indicate drought onset when an above average precipitation month is dropped from the moving timescale, but the MPI is still registering wet conditions. Such was the case during the spring of 2014, where both multiscalar indices indicated moderate drought onset following a dry winter, however the MPI remained normal due to an above average November 2013 (Figure 5d). In this example, both multiscalar indices began to indicate moderate drought onset once November was dropped from the 5mo. SPEI and 7mo. SPI timescales (April and June, respectively). The inherent soil water memory of the MPI still accounted for November 2013 and never signaled drought conditions.

Comparing case study results of difference errors from a clay loam and sand indicate that both multiscalar indices can struggle matching wet conditions in soils with lower clay content due to faster infiltration rates. However, the same timescale issues described above persist. Furthermore, the unimodal and bimodal precipitation distributions of the Southwest introduce additional complexities, as short timescales may struggle with 1) bimodal MLRAs that receive a below average season following an above average season, inconsistent annual monsoon precipitation (i.e. MLRA 40), or an unseasonable precipitation event being dropped from the multiscalar index timescale.

CONCLUSION

This study sought to understand the relationship between multiscalar meteorological indices and soil water availability across the Southwestern United States. A new modeled matric potential index (MPI) was compared with two multiscalar meteorological indices, the SPI and SPEI, across 240 study sites to evaluate regional timescale-depth relationships. The highest

correlating multiscalar index timescale at each depth of the MPI, referred to as the highest correlation line (HCL), was characterized, allowing for the full index-timescale to MPI-depth continuum to be defined. Furthermore, the impacts of soil type on these relationships were assessed, resulting in unique soil type HCLs. Differences between time series of the highest correlating multiscalar index timescale and MPI at different depths were analyzed to understand the errors that can exist between multiscalar indices and matric potential. For simplicity, conclusions from this study are limited to discussing the highest correlating multiscalar index timescale for each depth of the MPI, referred to as the highest correlation line (HCL).

At shallow depths (<80cm), maximum correlating values of each MPI depth occur at almost a 1:1 step progression with multiscalar index timescales. Therefore, at shallow depths, timescales of the drought indices scale linearly with each additional month to a deeper depth of soil water. These scaling results are consistent with previous studies that have attempted to align multiscalar indices with soil water of different depths (McEvoy et al. 2012; Sohrabi et al. 2015; Barnard et al. 2021). At depths below 80cm, the slope of the relationship between timescale and depth becomes less linear and shallower as the linear timescales of the multiscalar indices struggle to match the non-linear complexities of water movement at deeper depths.

On average across all sites, the SPI produces equal to higher correlation values and equal to lower RMSE values for all depth-timescale pairings along the HCL compared to the SPEI. Assessing error bias shows that both the SPI and SPEI produce near zero to slight positive bias compared to the MPI and that bias increases with depth. This analysis indicates that the SPI better matches MPI variability compared to the SPEI. Lower correlation values between the SPEI and MPI are attributed to the SPEI using potential instead of actual ET.

Soil type impacts the relationship between timescale and depth. Both the SPI and SPEI produce higher correlation values and lower RMSE values when aligned with clay loam MPIs than sand MPIs. However, the SPI produces higher correlations overall with the MPI than the SPEI when comparing between the same soil type. A more linear relationship (i.e. 1:1) between multiscalar index timescales and MPI depth is observed for clay loam soils compared to sandy soils. Furthermore, the HCL slope of sandy soils is steeper than that of clay loam soils. This change in slope is attributed to the difference in infiltration rates between sand and clay loam soils. It should be noted that the HCL of other soil types lie in between the steepest sloped HCL (sand) and shallowest sloped HCL (clay). Therefore, the slope of the relationship between timescale and depth decreases (i.e. becomes shallower) with increasing clay content.

Case studies revealed that difference errors produced by the SPI and SPEI were caused by timescales being unable to match the inherent soil water memory of the MPI. Common negative errors (underestimation) occur when both multiscalar indices begin to signal drought onset while the MPI does not due to an above average precipitation month being removed from the index calculation. Conversely, common positive errors (overestimation) occur when both multiscalar indices signal drought cessation following a long dry spell due to the addition of above average precipitation months introduced into the index calculation. These scenarios can lead to both positive and negative errors, explaining why bias is near zero. However, the slight positive bias lean means more instances of overestimation.

Overall, correlation results from this study indicate that both the SPI and SPEI can match soil water availability at shallow depths when using the appropriate timescale. However, the SPI correlates higher and produce less error with the MPI than the SPEI. This finding is consistent when observed by soil type. Thus, it is clear that the inclusion of temperature through the PET

component in the SPEI calculation does not improve the ability to approximate soil water availability in the semi-arid Southwest compared to using just monthly precipitation totals. This is due to the SPEI's use of potential ET, which is often much greater than actual ET in the Southwest. The SPI, which excludes potential ET (i.e. PET=0), produces higher correlations with the MPI due to the MPI incorporating actual ET (which is closer to 0 than potential ET) through the HYDRUS modeling. However, McEvoy et al. 2012 concluded that the SPEI showed slightly higher correlations over the SPI when used to evaluate streamflow, lake, and reservoir levels. These water sources operate on longer timescales (18 to 48 months) than the shallow soil water evaluated for this study, explaining the differences in conclusions. It is therefore that this study recommends SPI usage for shallow (<80cm) soil water monitoring on Southwestern drylands.

This study laid the groundwork for understanding the relationship between multiscalar meteorological drought index timescales and soil water availability at different depths for the Southwestern United States. Further research is needed to evaluate changes of the timescale-depth relationship for 1) the of introduction of multiple soil layers into the modeling soil profile, 2) impacts of runoff on precipitation inputs, and 3) vegetation changes on PET estimation. Future work will also need to investigate the relationship between the multiscalar indices and MPI by the modal precipitation distribution of each MLRA. During our investigation, we found evidence that not only did the timescales of the multiscalar indices vary by depth, but also by month. Future work will need to investigate if using a single timescale is the optimum strategy for best matching soil water availability or if more flexible approach that allows timescales to vary monthly is needed. Regardless, results from this study show that the use of a single index timescale can be a good proxy of shallow soil water values for the Southwest.

Given their common usage for drought monitoring for the Southwestern United States, it is important to understand the relationship between multiscalar meteorological drought index timescale and soil water availability at different soil depths. This study contributed to this effort by showing the timescale-depth relationship operates on a 1:1 step progression for shallow depths. This result will allow for improved versatility and useability of the SPI and SPEI when evaluating drought conditions in dryland ecosystems. Furthermore, the findings of how soil type impacts the timescale-depth relationship will aid index users in making better informed decisions about land management activities. As future climate change exacerbates drought duration and intensity in the Southwest, making better use of readily available and simple to use indices, like the SPI and SPEI, is important for drought planning, mitigation, and adaptation.

FIGURES AND TABLES

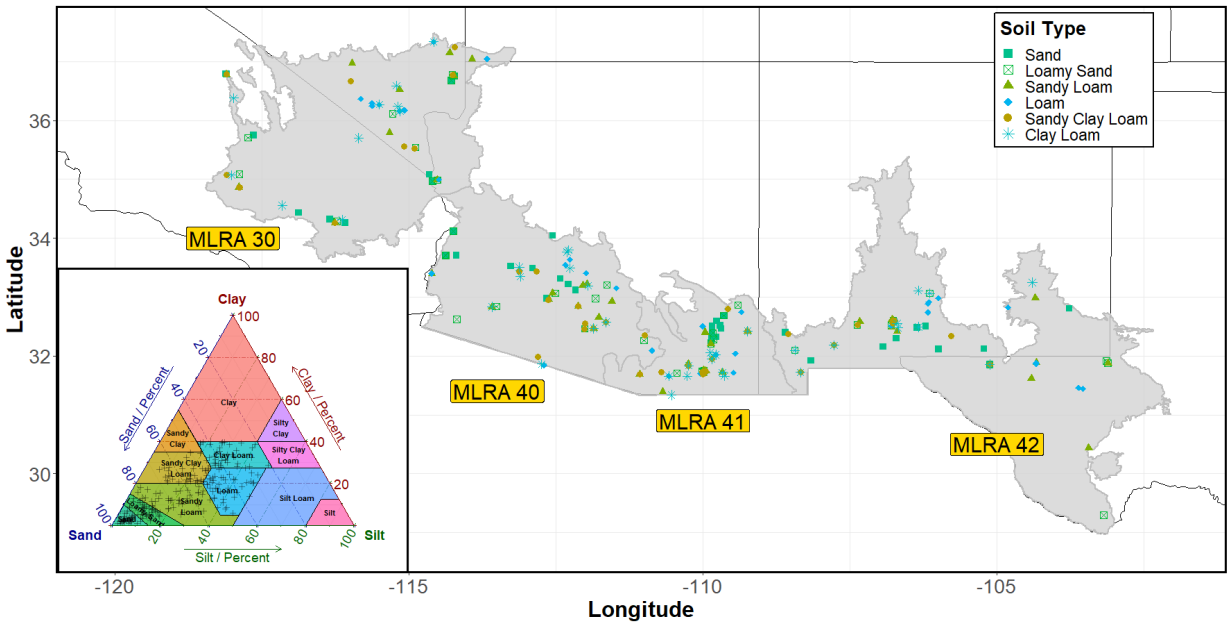

Figure 1: Subsurface soil type for each study location (n=240) acquired using the 'soilDB' R-package (Beaudette et al. 2021). Subsurface soil types were selected based on their regional popularity and control over dryland vegetation productivity (Shepard et al. 2015). A total of 10 of each soil type were selected from each MLRA.

Table 1: Downloaded gridMET Variables Used In HYDRUS-1D Modeling		
Meteorological Variable	*Download GridMET Unit*	*Converted HYDRUS Unit*
Precipitation	mm	cm
Temperature	K	C
Wind	m/s	km/day
Relative Humidity	%	%
Mean Shortwave Radiation	W/m^2	$MJ/m^2/day$

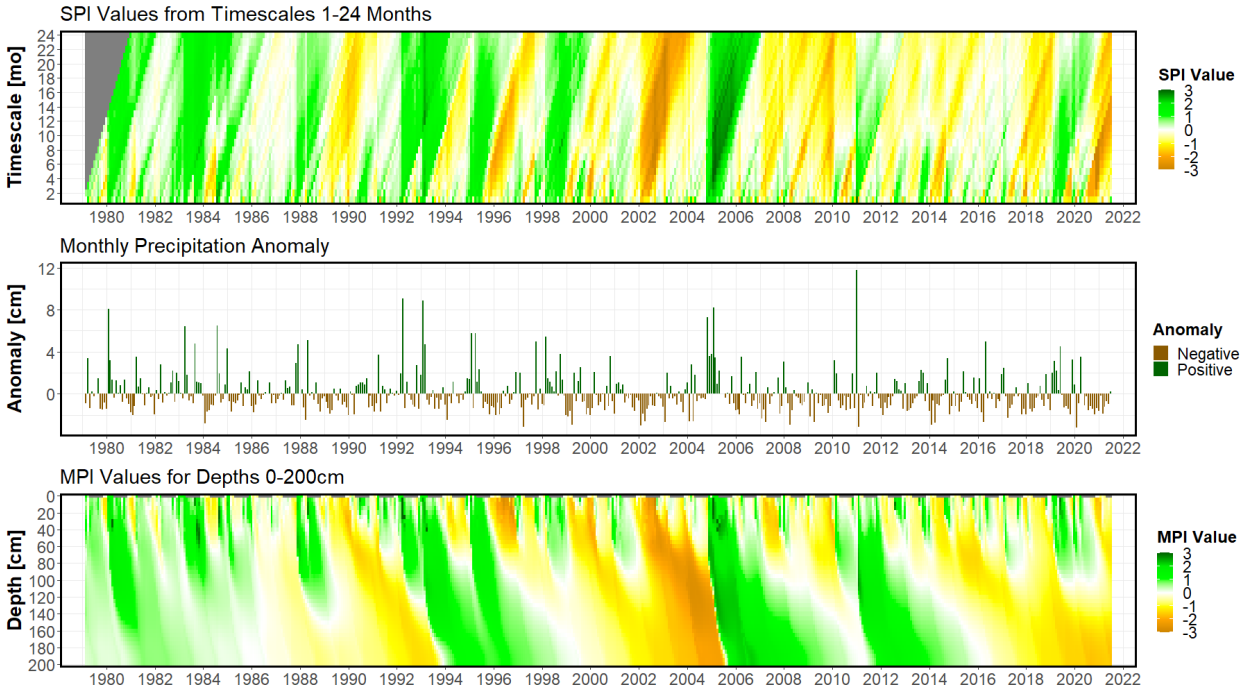

Figure 2: Conceptual figure demonstrating the alignment of linear SPI timescales (top) with non-linear depths of the MPI (bottom) for a loam soil (model #121; MLRA 30). At shallow depths, the MPI should correlate highly with short timescales in a more linear fashion. At deeper depths, the MPI should align with longer SPI timescales but with lower correlation values as the linear index timescales struggle to match the non-linearity of water movement in the soil profile. The same concept applies between the MPI and SPEI.

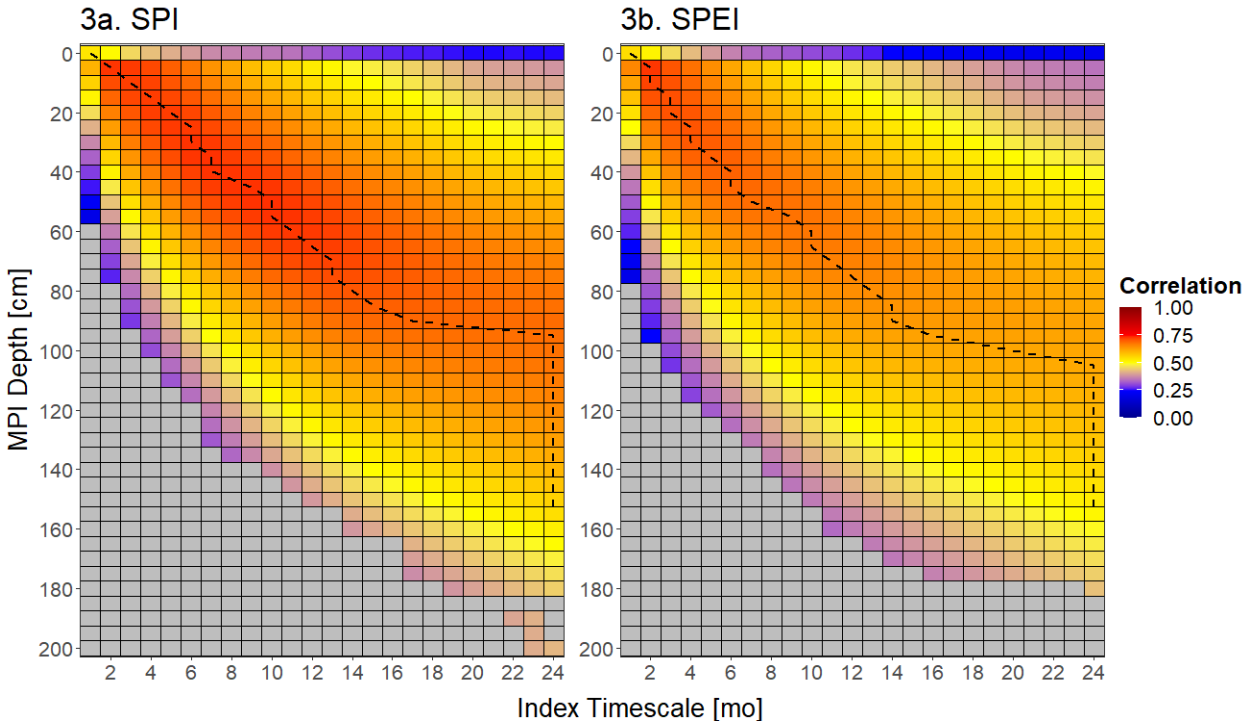

Figure 3: General timescale-depth relationship between the SPI – MPI (left) and SPEI – MPI (right). Each grid cell represents the mean Pearson correlation value between the time series of the *X*-timescale SPI or SPEI and time series of the *Y*-depth MPI of all 240 study locations. Grayed-out grid cells represent instances when the resulting p-value from the Pearson correlation between the multiscalar index timescale and MPI was not statistically significant ($p>0.05$).

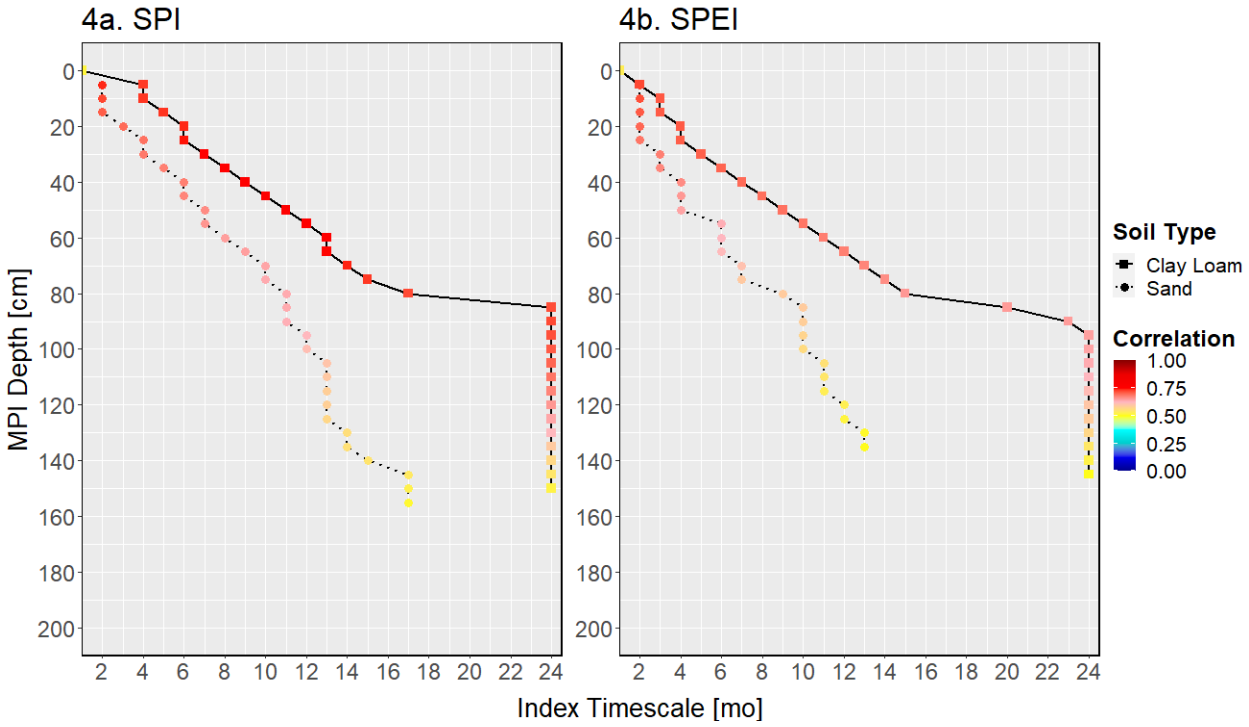

Figure 4: The highest correlation line for sand (dotted) and clay loam (solid) variants of the MPI and the SPI (4a) and SPEI (4b). The HCL for loamy sand, sandy loam, loam, and sandy clay loam are not plotted for simplification, as they plot between the sand and clay loam HCL. Each depth-timescale point along the HCL is the mean correlation value (n=40) between the soil type variant MPI (circle = sand; square = clay loam) and SPI (4a) or SPEI (4b).

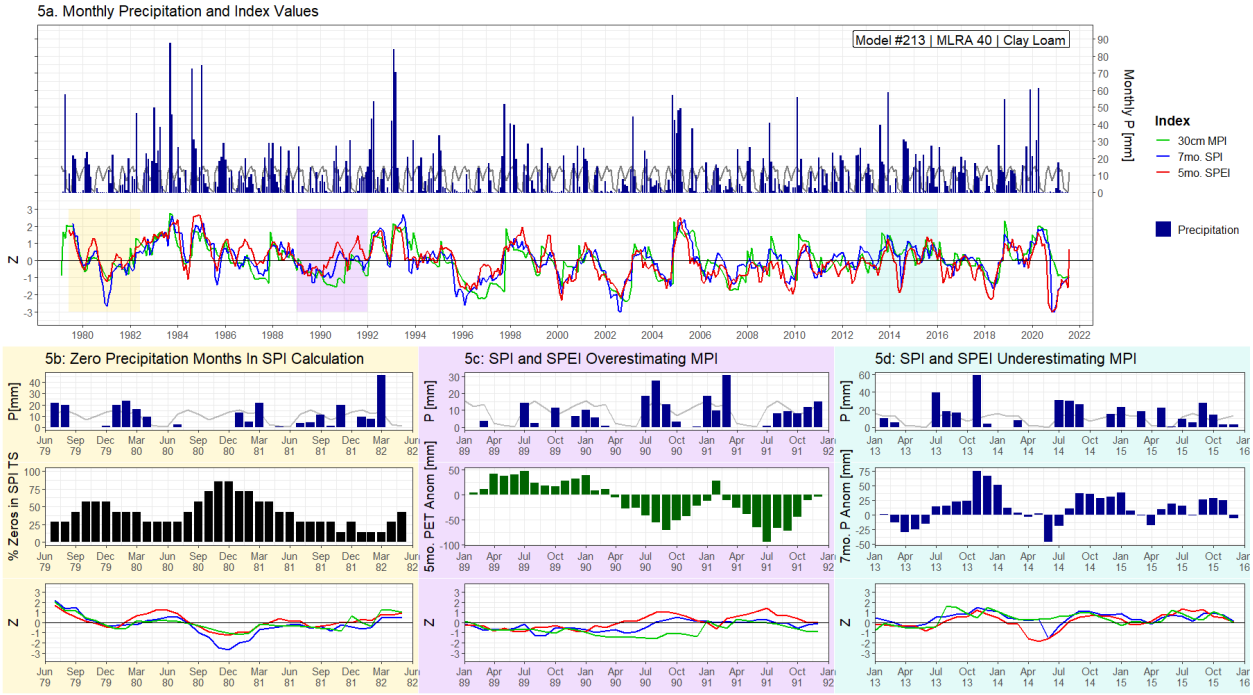

Figure 5: Case study examining remaining errors produced after aligning the 7mo. SPI and 5mo. SPEI with the 30cm MPI for a clay loam (model #213; MLRA 40). Monthly precipitation and index values are shown in figure 5a. Three examples of errors between the multiscalar indices and MPI are highlighted. When the SPI encounters consecutive months with greater than 75% zeros in its index calculation, an unrealistic value can occur (5b). Additionally, the timescale length can limit the multiscalar indices' ability to properly capture drought cessation when a previous dry spell is dropped from the moving timescale (5c). Furthermore, the timescale length can cause the multiscalar indices to signal drought onset when a previous above average precipitation month is dropped from the moving timescale (5d).

REFERENCES

Abatzoglou, J. T. (2013). Development of gridded surface meteorological data for ecological applications and modelling. International Journal of Climatology, 33(1), 121-131.

Adams, D. K., & Comrie, A. C. (1997). The north American monsoon. Bulletin of the American Meteorological Society, 78(10), 2197-2214.

Allen, R. G., Pereira, L. S., Raes, D., & Smith, M. (1998). Crop evapotranspiration-Guidelines for computing crop water requirements-FAO Irrigation and drainage paper 56. Fao, Rome, 300(9), D05109.

Barnard, D. M., Germino, M. J., Bradford, J. B., O'Connor, R. C., Andrews, C. M., & Shriver, R. K. (2021). Are drought indices and climate data good indicators of ecologically relevant soil moisture dynamics in drylands?. Ecological Indicators, 133, 108379.

Beaudette, D. E., Skovlin, J., Roecker, S., & Beaudette, M. D. (2022). Package 'soilDB'.

Beguería, S., Vicente-Serrano, S. M., Reig, F., & Latorre, B. (2014). Standardized precipitation evapotranspiration index (SPEI) revisited: parameter fitting, evapotranspiration models, tools, datasets and drought monitoring. International journal of climatology, 34(10), 3001-3023.

Bestelmeyer, B. T., Tugel, A. J., Peacock Jr, G. L., Robinett, D. G., Shaver, P. L., Brown, J. R., ... & Havstad, K. M. (2009). State-and-transition models for heterogeneous landscapes: a strategy for development and application. Rangeland Ecology & Management, 62(1), 1-15.

Bodner, G. S., & Robles, M. D. (2017). Enduring a decade of drought: Patterns and drivers of vegetation change in a semi-arid grassland. Journal of Arid Environments, 136, 1-14.

Bradford, J. B., Schlaepfer, D. R., Lauenroth, W. K., Palmquist, K. A., Chambers, J. C., Maestas, J. D., & Campbell, S. B. (2019). Climate-driven shifts in soil temperature and moisture regimes suggest opportunities to enhance assessments of dryland resilience and resistance. Frontiers in Ecology and Evolution, 358.

Daly, C., Neilson, R. P., & Phillips, D. L. (1994). A statistical-topographic model for mapping climatological precipitation over mountainous terrain. Journal of Applied Meteorology and Climatology, 33(2), 140-158.

Dorigo, W. A., Wagner, W., Hohensinn, R., Hahn, S., Paulik, C., Xaver, A., ... & Jackson, T. (2011). The International Soil Moisture Network: a data hosting facility for global in situ soil moisture measurements. Hydrology and Earth System Sciences, 15(5), 1675-1698.

Dorigo, W., de Jeu, R., Chung, D., Parinussa, R., Liu, Y., Wagner, W., & Fernández-Prieto, D. (2012). Evaluating global trends (1988–2010) in harmonized multi-satellite surface soil moisture. Geophysical Research Letters, 39(18).

Gremer, J. R., Bradford, J. B., Munson, S. M., & Duniway, M. C. (2015). Desert grassland responses to climate and soil moisture suggest divergent vulnerabilities across the southwestern United States. Global Change Biology, 21(11), 4049-4062.

Grover, H. 2021. Mitigating Postfire Runoff and Erosion in the Southwest using Hillslope and Channel Treatments. ERI Working Paper No. 44. Ecological Restoration Institute, Northern Arizona University. 11 pp

Gudmundsson, L., & Stagge, J. H. (2016). Package "SCI": Standardized Climate Indices Such as SPI, SRI or SPEI, v1. 0-2, CRAN [code].

Hadley, N. F., & Szarek, S. R. (1981). Productivity of desert ecosystems. BioScience, 31(10), 747-753.

Jackson, R. B., Canadell, J., Ehleringer, J. R., Mooney, H. A., Sala, O. E., & Schulze, E. D. (1996). A global analysis of root distributions for terrestrial biomes. Oecologia, 108(3), 389-411.

Koehn, C. R., Petrie, M. D., Bradford, J. B., Litvak, M. E., & Strachan, S. (2021). Seasonal precipitation and soil moisture relationships across forests and woodlands in the southwestern united states. Journal of Geophysical Research: Biogeosciences, 126(4), e2020JG005986.

Lauenroth, W. K., & Bradford, J. B. (2006). Ecohydrology and the partitioning AET between transpiration and evaporation in a semiarid steppe. Ecosystems, 9(5), 756-767.

Loik, M. E., Breshears, D. D., Lauenroth, W. K., & Belnap, J. (2004). A multi-scale perspective of water pulses in dryland ecosystems: climatology and ecohydrology of the western USA. Oecologia, 141(2), 269-281.

Madsen, M. D., Chandler, D. G., & Belnap, J. (2008). Spatial gradients in ecohydrologic properties within a pinyon-juniper ecosystem. Ecohydrology: Ecosystems, Land and Water Process Interactions, Ecohydrogeomorphology, 1(4), 349-360.

Majumder, D., & Kumar, B. (2019). Estimation of monthly average pet by various methods and its relationship with pan evaporation at Bhagalpur, Bihar. Journal of Pharmacognosy and Phytochemistry, 8(1), 2481-2484.

McEvoy, D. J., Huntington, J. L., Abatzoglou, J. T., & Edwards, L. M. (2012). An evaluation of multiscalar drought indices in Nevada and Eastern California. Earth Interactions, 16(18), 1-18.

McKee, T. B., Doesken, N. J., & Kleist, J. (1993, January). The relationship of drought frequency and duration to time scales. In Proceedings of the 8th Conference on Applied Climatology (Vol. 17, No. 22, pp. 179-183).

Moody, J. A., & Martin, D. A. (2001). Post-fire, rainfall intensity–peak discharge relations for three mountainous watersheds in the western USA. Hydrological processes, 15(15), 2981-2993.

Neilson, R. P., King, G. A., & Koerper, G. (1992). Toward a rule-based biome model. Landscape Ecology, 7(1), 27-43.

Newman, B. D., Campbell, A. R., & Wilcox, B. P. (1997). Tracer-based studies of soil water movement in semi-arid forests of New Mexico. Journal of Hydrology, 196(1-4), 251-270.

Owens, M. K., Lyons, R. K., & Alejandro, C. L. (2006). Rainfall partitioning within semiarid juniper communities: effects of event size and canopy cover. Hydrological Processes: An International Journal, 20(15), 3179-3189.

Robock, A., Mu, M., Vinnikov, K., Trofimova, I. V., & Adamenko, T. I. (2005). Forty-five years of observed soil moisture in the Ukraine: No summer desiccation (yet). Geophysical Research Letters, 32(3).

Robock, A., Vinnikov, K. Y., Srinivasan, G., Entin, J. K., Hollinger, S. E., Speranskaya, N. A., ... & Namkhai, A. (2000). The global soil moisture data bank. Bulletin of the American Meteorological Society, 81(6), 1281-1300.

Romero-Lankao, P., Smith, J. B., Davidson, D. J., Diffenbaugh, N. S., Kinney, P. L., Kirshen, P., ... & Villers Ruiz, L. (2014). North America. Climate Change 2014: impacts, adaptation, and vulnerability part B: regional aspects contribution of working group II to the Fifth Assessment Report of the Intergovernmental Panel of Climate Change.

Salley, S. W., Talbot, C. J., & Brown, J. R. (2016). The Natural Resources Conservation Service land resource hierarchy and ecological sites. *Soil Science Society of America Journal*, *80*(1), 1-9.

Shepard, C., Schaap, M. G., Crimmins, M. A., Van Leeuwen, W. J., & Rasmussen, C. (2015). Subsurface soil textural control of aboveground productivity in the US Desert Southwest. Geoderma Regional, 4, 44-54.

Sims, A. P., Niyogi, D. D. S., & Raman, S. (2002). Adopting drought indices for estimating soil moisture: A North Carolina case study. Geophysical Research Letters, 29(8), 24-1.

Simunek, J., Sejna, M., Van Genuchten, M. T., Šimůnek, J., Šejna, M., Jacques, D., & Sakai, M. (1998). HYDRUS-1D. Simulating the one-dimensional movement of water, heat, and multiple solutes in variably-saturated media, version, 2.

Simunek, J., Van Genuchten, M. T., & Sejna, M. (2005). The HYDRUS-1D software package for simulating the one-dimensional movement of water, heat, and multiple solutes in variably-saturated media. University of California-Riverside Research Reports, 3, 1-240.

Sohrabi, M. M., Ryu, J. H., Abatzoglou, J., & Tracy, J. (2015). Development of soil moisture drought index to characterize droughts. Journal of Hydrologic Engineering, 20(11), 04015025.

Stagge, J. H., Tallaksen, L. M., Gudmundsson, L., Van Loon, A. F., & Stahl, K. (2015). Candidate distributions for climatological drought indices (SPI and SPEI). International Journal of Climatology, 35(13), 4027-4040.

Stagge, J. H., Tallaksen, L. M., Gudmundsson, L., Van Loon, A. F., & Stahl, K. (2016). Response to comment on 'candidate distributions for climatological drought indices (SPI and SPEI)'. International Journal of Climatology, 36(4), 2132-2138.

Stagge, J. H., Tallaksen, L. M., Xu, C. Y., & Van Lanen, H. A. (2014). Standardized precipitation-evapotranspiration index (SPEI): Sensitivity to potential evapotranspiration model and parameters. In Hydrology in a changing world (Vol. 363, pp. 367-373).

Svoboda, M. D., & Fuchs, B. A. (2016). Handbook of drought indicators and indices (pp. 1-44). Geneva, Switzerland: World Meteorological Organization.

Thornthwaite, C. W. (1948). An approach toward a rational classification of climate. Geographical review, 38(1), 55-94.

Vicente-Serrano, S. M., & Beguería, S. (2016). Comment on 'Candidate distributions for climatological drought indices (SPI and SPEI)'by James H. Stagge et al. International Journal of Climatology, 36(4), 2120-2131.

Vicente-Serrano, S. M., Beguería, S., & López-Moreno, J. I. (2010). A multiscalar drought index sensitive to global warming: the standardized precipitation evapotranspiration index. Journal of climate, 23(7), 1696-1718.

Wang, H., Rogers, J. C., & Munroe, D. K. (2015). Commonly used drought indices as indicators of soil moisture in China. Journal of Hydrometeorology, 16(3), 1397-1408.

Weiss, J. L., Castro, C. L., & Overpeck, J. T. (2009). Distinguishing pronounced droughts in the southwestern United States: Seasonality and effects of warmer temperatures. Journal of Climate, 22(22), 5918-5932.

Wilcox, B. P., Seyfried, M. S., Breshears, D. D., Stewart, B., & Howell, T. (2003). The water balance on rangelands. Encyclopedia of water science, 791(4).

Wythers, K. R., Lauenroth, W. K., & Paruelo, J. M. (1999). Bare-soil evaporation under semiarid field conditions. Soil Science Society of America Journal, 63(5), 1341-1349.

APPENDIX C

A TIME-VARYING APPROACH TO USING MULTISCALAR INDICES FOR SOIL WATER APPROXIMATION IN THE SEMI-ARID SOUTHWESTERN UNITED STATES

Trevor T. McKellar[*1]

[*]Corresponding Author

[1]Department of Environmental Science

1177 E. 4th St.

Tucson, AZ 85721, USA

Phone: +1 (520) 621-1646

Email: envs-dept@arizona.edu

Targeted for Publication in International Journal of Climatology

ABSTRACT

Seasonal precipitation timing and magnitude are important for soil water recharge, which is the primary control on vegetation production in the Southwestern United States ('Southwest'). Land managers can utilize multiscalar meteorological drought indices, like the Standardized Precipitation Index (SPI) or Standardized Precipitation-Evapotranspiration Index (SPEI), to approximate water movement in shallow soils. However, the SPI and SPEI's use of a single timescale is unlikely to fully represent the intra-annual variability of soil water at different profile depths and a more robust approach is needed. Here, we create a timescale-varying drought index based on the SPI and SPEI to improve drought monitoring of soil water in semi-arid climates with precipitation seasonality. By coupling sophisticated computer modeling, site-specific soils information, and spatially continuous, high resolution meteorological datasets, we create a Matric Potential Index (MPI) at 5cm, 30cm, and 60cm for 240 sites throughout the Southwest. A composite index for the SPI and SPEI ('composite indices') is created that varies the timescale length during each calendar month based on the highest correlating timescale with the MPI during that same month. For all depths and soil types, correlation values between time series of the composite indices and MPI were compared with correlation values between time series of the SPI- and SPEI- using a traditional single timescale ('single indices') and MPI. Results show that both the composite-SPI and composite-SPEI significantly ($p<0.05$) improve correlation values with the MPI compared to when using a single timescale for all depths and soil types. Higher correlation values were observed between the MPI and composite-SPI compared to the composite-SPEI. Significant differences ($p<0.05$) were observed between soil types for shallow and deep depths, with greater improvement observed for clay loam composite indices at shallow depths and greater improvement for sand composite indices at deeper depths. This

approach demonstrates that accounting for seasonal precipitation distribution allows the SPI and SPEI to better approximate soil water availability over the use of a single timescale. Land managers can benefit from this approach by understanding general seasonal relationships between timescale length and soil water availability. As climate change increases water stress on semi-arid ecosystems, seasonal optimization of multiscalar index timescales is important for fully applying drought monitoring strategies to land management action.

INTRODUCTION

The semi-arid climate of the Southwestern United States creates unique challenges for drought monitoring, as distinguishing background aridity from abnormally dry conditions can be difficult due to potential evapotranspiration often being greater than precipitation (Wu et al. 2007; Crimmins et al. 2017; Wilcox et al. 2003). Furthermore, drought impacts dryland ecosystems in complex ways, with southwestern U.S. climate characterized as having extended periods of dryness intermixed with short pulses of moisture (Loik et al. 2004; Lauenroth and Bradford 2006). This leads to distinctive short and long-term drought onset and cessation patterns in soils that are tied to seasonal precipitation distribution (McKellar et al. 2022a). Land managers working in dryland ecosystems can benefit from using a suite of drought monitoring strategies to evaluate soil drought conditions and aid decision making (Gremer et al. 2015, Crausbay et al. 2017). Multiscalar meteorological drought indices, such as the Standardized Precipitation Index (SPI) or Standardized Precipitation-Evapotranspiration Index (SPEI), are drought monitoring tools commonly used due to simple calculation and minimal data requirements (McKee et al. 1993, Vicente-Serrano et al. 2009; Svoboda and Fuchs, 2016). Analyzing SPI and SPEI values communicates information about the timing, magnitude, and frequency of drought events. Notably, these indices are multiscalar, allowing for index indicator values to be totaled over varying monthly timescale lengths. The multiscalar aspect of these indices allows for the use of a single timescale to approximate water movement through different water sources (McKee et al. 1999), including shallow soil moisture (Sims et al. 2002; Barnard et al. 2021; McKellar et al. 2022b). However, given the importance of seasonal precipitation timing, magnitude, and frequency for plant productivity (Jenerette et al 2010; Hottenstein et al. 2015; Li et al. 2022), the use of a single timescale is unlikely to fully represent the seasonal

variability of soil water at depth and a more robust approach is needed (McKellar 2022a; McKellar 2022b). Climate change is projected to increase water stress on dryland ecosystems, and thus understanding the relationship between multiscalar index timescales and intra-annual precipitation variability is important for making full use of these drought monitoring strategies (Romero-Lankao et al. 2014).

Seasonal precipitation timing and magnitude are important for soil water recharge, which is the primary control on vegetation dynamics in dryland ecosystems (Noy-Meir 1973; Hadley and Szarek 1981; Neilson et al. 1992; Wilcox et al. 2003; Jenerette et al. 2010; Hottenstein et al. 2015). Tracking soil water availability at different depths is thus key for understanding overall ecosystem health (Lauenroth and Bradford 2006; Schlaepfer et al. 2012; Biederman et al. 2018; Barnard et al. 2021). The lack of long-term, reliable *in-situ* soil moisture datasets (Robock et al. 2005; Dorigo et al. 2011) have led to alternative approaches for tracking soil water availability, including the use of multiscalar drought indices (Sims et al. 2002; Wang et al. 2015). Recent studies have combined hydrological modeling with spatially continuous, high temporal resolution climate datasets to simulate soil water availability at different depths on a more regional scale, allowing for broader analysis of the soil water depth – multiscalar index timescale continuum (Barnard et al. 2021; McKellar et al. 2022b). These studies have established the general relationship between multiscalar index timescale and soil water availability at different depths, but have been limited to using a single timescale at each depth (Barnard et al. 2021; McKellar et al. 2022b). With seasonal precipitation distributions controlling drought patterns across the southwestern United States (McKellar et al. 2022a), the use of a single timescale can restrict the ability of multiscalar indices to accurately portray soil water availability during

specific seasons (McKellar et al. 2022b). Thus, matching multiscalar index timescales with monthly timing of precipitation can benefit drought monitoring efforts on drylands.

Here, we evaluate an approach to create a monthly composite multiscalar index for the SPI and SPEI, respectively, to better approximate intra-annual soil water variability for 240 study locations across the Southwestern United States. By allowing the drought index timescale length to vary from month to match to match a locations seasonal precipitation distribution, the composite index can theoretically better track soil water variability at specific depths. To approximate soil water availability, daily matric potential values are simulated by coupling sophisticated computer modeling, site-specific soils information, and spatially continuous, high resolution meteorological datasets at 240 study locations throughout the Southwest. A monthly Matric Potential Index (MPI) is created for 5cm, 30cm, and 60cm at each study site and correlated with SPI and SPEI time series for timescales of 1-24 months. A composite index is created that uses the highest correlating timescale with the MPI for each month. Correlation values between the multiscalar composite indices and MPI are compared with correlation values of the multiscalar indices using a single timescale and MPI. Results are evaluated by index, depth, and soil type. Lastly, error differences between the MPI, composite multiscalar indices, and single timescale multiscalar indices are evaluated.

MATERIALS AND METHODS

Study Area

The study defines the Southwestern United States, hereby referred to as the ‘Southwest’, as the Mohave, Sonoran, and Chihuahuan deserts, which stretch from southern California to southwest Texas and north of the United States-Mexico border. The United States Department of Agriculture (USDA) divides land into a hierarchy system based on land usage, resource

management, environmental conservation, and agricultural planning (Salley et la. 2016). The primary organization unit of this hierarchy is the Major Land Resource Area (MLRA), which are geographically associated land units that share similar physiography, geology, climatology, hydrology, soils, biology, and land use (Austin 1965; Salley et al. 2016). The United States is subdivided into 278 MLRAs, which encompass large areas and are important for state and local level agricultural planning, drought monitoring, and ecosystem management. This study specifically focuses on MLRA 30 (Sonoran Basin and Range), MLRA 40 (Central Arizona Basin and Range), MLRA 41 (Southern Arizona Basin and Range), and MLRA 42 (Southern Desertic Basins, Plains, and Mountains), hereby referred to as the 'study region', – which together are part of LRR D (Western Range and Irrigated Region) (Austin 1965).

The study region can be characterized as having short pulses of moisture followed by extended periods of dryness, with potential evapotranspiration often being significantly greater than precipitation (Wilcox et al. 2003; Lauenroth and Bradford 2006). Each MLRA within the study region has a unique seasonal precipitation distribution that creates a gradient from west to east (figure 1). Western areas (MLRA 30) receive most precipitation during the 'cool season' (fall and winter months) (figure 1, dark grey) and eastern areas (MLRA 42) receive most precipitation during the 'warm season' (spring and summer months) (figure 1, light grey), resulting in a unimodal precipitation distribution (figure 2a and 2d). Central areas (MLRA 40 and 41) receive precipitation during both cool and warm seasons, creating a bimodal precipitation distribution (figure 2b and 2c). Each MLRA receives different mean annual precipitation totals (MAP), with MLRA 41 receiving the highest MAP (370mm) and MLRA 30 receiving the lowest MAP (197.5mm) (figure 2a-d). MAP and seasonal precipitation distribution

of each MLRA control drought onset and cessation patterns (McKellar et al. 2022a), and thus it is important to account for these factors when using different drought monitoring tools.

The study region is comprised of six main soil types – sand, loamy sand, sandy loam, loam, sandy clay loam, and clay loam (Shepard et al. 2015) (figure 1). Due to subsurface soil texture being a primary control on aboveground vegetation productivity, we assign the subsurface 'B-horizon' from each study location's soil profile as the primary soil type during modeling (see section *Modeling*). Previous work has established that soil type influences the relationship between multiscalar index timescale and soil water depth in the Southwest, with soils containing higher percentages of clay correlating at longer timescales (McKellar et al. 2022b). It is therefore important to account for soil type when creating the composite index to accurately represent differences in soil water availability.

Data

Soils information, elevation, and latitude and longitude coordinates were acquired for the MLRA 30, 40, 41, and 42 using the 'soilDB' R-package, which collects information from openly available online soil databases (Beaudette et al. 2022). A total of 317 complete soil pedons were returned with necessary records of percent sand, silt, and clay, and soil hydraulic parameters needed for modeling. To ensure a representative sampling distribution of the study region and to maximize computational efficiency for the scope of this study, the remaining dataset was filtered so that an equal amount (n=10) of each subsurface soil type (n=6) were selected within each MLRA (n=4). Therefore, a total of 240 study sites were selected across the study region (i.e. 10 of each soil type x 6 soil types x 4 MLRAs = 240 study sites).

The latitude and longitude coordinates associated with each soil profile were used to acquire meteorological information using the Gridded Surface Meteorological (gridMET) dataset

(Abatzaglou 2013). By combining gridded data from PRISM (Daly et al. 1994) with coarse regional reanalysis satellite data from the Land Data Assimilation System (LDAS), gridMET produces spatially and temporally continuous meteorological dataset for the United States at a 4x4km resolution. Daily records of precipitation, temperature, wind, relative humidity, and mean shortwave radiation were downloaded for each study location from 1/1/1979 – 7/17/2021. Notably, gridMET contains the necessary information to estimate daily PET using the Penman-Monteith method (Allen 1998), which allows for more accurate water balance calculations during soil moisture modeling.

The Standardized Precipitation Index (SPI)

The Standardized Precipitation Index (SPI) uses monthly precipitation totals to convey the frequency of wet and dry periods as a time series of z-score values, where positive values represent water surplus and negative values represent water deficits (McKee et al. 1993). The SPI can be calculated at a variety of timescales for period t-months, which sums monthly precipitation totals during for the chosen interval (McKee et al. 1993). This 'multiscalar' aspect allows the SPI to approximate water movement through different hydrologic reservoirs (i.e. soil or ground water) depending on the timescale length, with shorter timescales representing soil water and longer timescales representing ground water (Svoboda and Fuchs 2016).

Due to monthly precipitation totals often not being normally distributed, data must undergo a transformation process to better approximate a standard normal distribution before an index time series is produced. This study uses the 'fitSCI' R-package, which forces time series of environmental data to take the shape of a standard normal distribution by estimating fit parameters for different available maximum likelihood probability distributions (Gudmundsson and Stagge 2016). Monthly precipitation values for timescales from 1-24 months were entered

into the ‘fitSCI’ function to estimate the transformation parameters needed to approximate a gamma distribution. The found parameters for each timescale were entered into the ‘transformSCI’ function, which applied the transformation to the precipitation data. The output of z-score values represents the number of standard deviation units an occurrence of t-month total precipitation falls from the historical mean. Thus, at each study location, a total of 24 SPI time series were created with each representing a timescale of 1-24 months.

The simple calculation and use of monthly precipitation makes the SPI an attractive option for land managers looking to approximate drought conditions but are limited by data availability (Svoboda and Fuchs 2016). Furthermore, the standardization process allows SPI values from different locations to be compared, as both values represent the same probability of a precipitation event occurring with respect to the period of record (McKee et al. 1993). However, the SPIs exclusion of temperature, which is important for PET and monthly water balance, can sometimes limit the comparison of SPI values from different locations that occurred under different temperature scenarios (Svoboda and Fuchs 2016). Additionally, uncertainty when estimating transformation parameters during the standardization process can occur when a high number of zero precipitation months are included in the SPI timescale, resulting in an unrealistic SPI value being portrayed (Gudmundsson and Stagge 2016; Stagg et al. 2015; Wu et al. 2007). The ‘fitSCI’ R-package allows for a mixed distribution (p_0=TRUE) to be used during the transformation parameter estimation process to accommodate for this issue, however uncertainty can still exist when greater than 75% zeros are included in the SPI timescale (Gudmundsson and Stagge 2013; Stagg et al. 2015). Despite these deficiencies, the SPI is a powerful tool that is easy to use and has the multiscalar flexibility to evaluate drought of different hydrological reservoirs (Svoboda and Fuchs 2016).

The Standardized Precipitation Evapotranspiration Index (SPEI)

Building on the SPI, the Standardized Precipitation Evapotranspiration Index (SPEI) adds a temperature component to the index calculation, allowing for the impacts of PET on drought conditions to be evaluated (Vicente-Serrano et al. 2009). By using monthly mean temperature values, PET can be estimated using the Thornthwaite method (Thornthwaite 1948). A monthly water balance is calculated by subtracting PET from precipitation, which the SPEI uses as the basis for the index input (Vicente-Serrano et al. 2009). The resulting time series of z-score values represents the frequency and magnitude of wet and dry periods, where positive values represent water surplus and negative values represent water deficits. The SPEI can be calculated at a variety of t-month timescales, which sum water balance totals for the chosen t-interval (Vicente-Serrano et al. 2009). This allows the SPEI to evaluate water balances of different hydrologic reservoirs, like shallow soil water or groundwater (Svoboda and Fuchs 2016).

The SPEI uses a similar methodology to the SPI to calculate index values. Due to water balance values not often being normally distributed, a transformation process must be applied using the 'fitSCI' R-package (Gudmundsson and Stagge 2016). Monthly water balance values for timescales from 1-24 months were entered into the 'fitSCI' function to estimate the transformation parameters needed to approximate a generalized extreme value (gev) distribution. Parameters for each timescale were then entered into the 'transformSCI' function, which applied the transformation to the water balance data. The resulting z-score values represent the number of standard deviation units an occurrence of t-month total water balance falls from the historical mean. At each study locations, 24 SPEI time series were created, each representing a timescale of 1-24 months.

While the inclusion of PET allows the SPEI to evaluate the impacts of temperature on drought conditions (Vicente-Serrano et al. 2009), it comes at the expense of needing additional data and the choice of method used to estimate PET. Inconsistencies between SPEI values has been observed when using different methods of PET estimation (Stagge et al. 2014, Beguería et al. 2014). Here, we use the Penman-Monteith method to estimate PET, with its inclusion of wind, relative humidity, temperature, and solar radiation allow it to more accurately estimate PET compared to other methods (Allen 1998; Majumder and Kumar 2019). Furthermore, the Penman-Monteith method was used during soil modeling, which allows for more direct comparison between SPEI and MPI values (see section *Modeling*).

HYDRUS-1D Modeling

HYDRUS-1D, a deterministic modeling software designed for simulating water movement in a one-dimensional variably saturated porous media (Simunek et al. 2005), was used to simulate daily soil water availability at each study location. Each model consisted of a single, homogeneous layer of soil from 0-200cm, which was based on the subsurface 'B-horizon' at each location due to its control on dryland vegetation dynamics (Shepard et al. 2015). A generalized southwestern root profile, based on Jackson et al. 1996, used to simulate transpiration, with root concentration declining in an exponential pattern from 0-200cm. Using the acquired girdMET data, PET was estimated using the Penman-Monteith method (Allen 1998). Daily records of the acquired gridMET were entered into the model. Model output consisted of daily matric potential values from 1/1/1979 – 7/17/2021. For more information on model setup, see (McKellar 2022d).

The Matric Potential Index (MPI)

Using the same methodology as the SPI and SPEI, a new Matric Potential Index (MPI) was created for 5cm, 30cm, and 60cm at all 240 study locations. Model output of daily matric potential values were aggregated into monthly median values. Like monthly precipitation and water balance values of the SPI and SPEI, respectively, monthly matric potential values are not normally distributed and must undergo a transformation process to fit a stand normal distribution. Using the 'fitSCI' R-package, monthly matric potential values for each depth were entered into the 'fitSCI' function. Of the probability distributions available through the 'fitSCI' R-package, it was determined a Pearson Type-III distribution produced optimum normality for monthly matric potential values. The transform parameters for each depth were entered into the 'transformSCI' function, which applied the transformation to the monthly matric potential data. The resulting time series of z-score values (hereby referred to as the 5cm-MPI, 30cm-MPI, and 60cm-MPI) represents the number of standard deviation units an occurrence of monthly median matric potential lies from the mean. Unlike the SPI and SPEI, the MPI is not multiscalar due to soil memory being incorporated into HYDRUS-1D modeling. In other words, the MPI is always being calculated at a '1-month' timescale.

Composite Timescale Multiscalar Drought Index – MPI Correlations

At each location, a monthly composite multiscalar index was created for the SPI and SPEI, hereby referred to as the composite-SPI and composite-SPEI, or 'composite indices' when referred to together, which are designed to better track intra-annual precipitation variability within each MLRA (figure 2). Time series of SPI and SPEI values from 1-24 months were aligned with time series of the 5cm, 30cm, and 60cm MPI. Pearson correlation values were calculated between monthly values of each multiscalar index timescale and depth of MPI. For

example, a Pearson correlation value was calculated between the January values of the 5cm MPI and 1mo SPI (*or SPEI*); and next for January values of the 5cm MPI and 2mo SPI, and so forth for timescales up to 24 months. The highest correlating timescale of those 24 months was chosen for January and the process was repeated for the remaining months through December. This methodology resulted in a unique multiscalar index timescale for each calendar month that best represented the associated monthly MPI values (figure 2). Next, 12 SPI time series, were computed using the highest correlating timescales for each month found during the previous step. Using a monthly timestep, a new 'composite' time series was constructed that selected the corresponding monthly multiscalar index value from each time series. This creates a complete timescale-varying drought index time series for the study period of record.

Monthly correlation values between the SPI at timescales from 1-24 months and clay loam MPIs at 5cm (2e-h) and 60cm (2i-l) are shown with each MLRAs climatology (2a-d) in figure 2. The single-SPI (dashed) and composite-SPI (solid) show the differences in approach to using multiscalar indices with a single timescale and monthly varying timescale (i.e. composite). At each study location, the single highest correlating SPI and SPEI timescale from 1-24 months, hereby referred to as the single-SPI and single-SPEI, was recorded for the 5cm, 30cm, and 60cm MPI. These correlation values were compared with correlation values between the composite indices and 5cm, 30cm, and 60cm MPI to evaluate improvement.

RESULTS AND DISCUSSION

Correlation values from each study location (n=240) between the single indices, composite indices, and MPI at 5cm, 30cm, and 60cm are shown in figure 3. Higher correlation values are observed for the composite-SPI and composite-SPEI compared to the single-SPI and single-SPEI, respectively. Paired Wilcoxon tests were performed to evaluate significance

differences between group median values. Both the composite-SPI and composite-SPEI significantly improve ($p<0.05$) correlation values with the MPI at all observed depths compared to when using a single timescale (figure 3). It should be noted that median correlation values increase with depth when observing the single-SPI; however, this is not observed for the single-SPEI, which produces lower median correlation values with increased depth. Decreased variability amongst MPI values at 30cm and 60cm can lead to closer alignment with longer multiscalar index timescales, producing higher correlations at a site-to-site comparison (McKellar et al. 2022b). Additionally, the SPI produces higher correlations with MPI at deeper depths compared to the SPEI; furthermore, the SPEI produces more error at deeper depths compared to the SPI (McKellar et al. 2022b). These factors result in observed differences between median correlation values of the SPI and SPEI with the MPI at increased depth.

Differences between correlation values of the composite- and single- indices with the 5cm, 30cm, and 60cm MPI are shown in figure 4. Median correlation differences vary by depth when using the composite-SPI, with larger increases observed at shallow depths. Median correlation differences between the composite-SPI and single-SPI [Composite SPI – Single SPI] at 5cm and 60cm are 0.074 and 0.0367, respectively. Additionally, increased variance is observed in correlation differences between the composite and single SPI at 5cm, indicating larger variability in composite improvement compared to deeper depths. Conversely, no improvement in median correlation difference between depths is observed when using the composite-SPEI. Median correlation differences between the composite-SPEI and single-SPEI at 5cm and 60cm are 0.052 and 0.05, respectively. Increased variance is observed when using the composite-SPEI at 5cm, with outliers gaining as much as 0.18 correlation with the 5cm MPI.

Higher median correlation values are observed for the difference between the composite- and single-SPI compared to the composite- and single-SPEI at 5cm. Examining correlation values shows the SPI produces higher correlation values on a month-to-month comparison over the SPEI, allowing for greater improvement when using the composite-SPI. Additionally, the SPEI has lower correlation with the MPI at shallow depths (McKellar et al. 2022), which likely restricts composite-SPEI improvement at 5cm. At 30cm and 60cm, differences in soil hydraulic conductivity due to soil texture, seasonal precipitation frequency and timing, and root water uptake can distribute water throughout the soil profile. Furthermore, autocorrelation of longer timescales becomes a factor, as monthly overlap between timescales increases. Soil water distribution and autocorrelation lead to multiple timescale lengths producing high correlation values with the MPI (figure 2i-l). This limits the improvement in correlation value with the MPI when using the composite indices at these depths, as a single timescale will already include high correlating months (figure 2i-l, dashed). Thus, using the composite to represent these depths becomes less advantageous than at shallow depths (i.e. 5cm).

Boxplots of correlation differences between the composite- and single- indices for all observed depths subsetted by soil type are shown in figure 5. Differences in median correlation value between soil types varies by depth. Paired Wilcoxon tests were performed to evaluate significance differences between soil type median values at each depth. Significant differences ($p<0.05$) were observed between clay loam and sandy soil types for both the SPI and SPEI at 5cm, indicating that the composite index improves correlation values with the 5cm MPI more for soil types with higher clay percentages (figure 5). Additionally, significant differences ($p<0.05$) were observed between sand and clay loam soil types for both the SPI and SPEI at 60cm,

indicating that the composite index improves correlation values with the 60cm MPI more for soil types with less clay content (figure 5).

Soil type impacts correlation values between the single timescale multiscalar index and MPI, with soils that have higher percentages of clay producing higher correlations on a depth-to-depth comparison (McKellar et al. 2022b). Comparing month-to-month correlation values of clay loam and sand MPIs at 5cm shows that clay loam soils produces higher correlation values over sandy soils (figure 2e-h and figure 6e-h). This leads to clay loam composite indices using higher correlation values overall when building the composite time series compared to sand composites. At deeper depths, temporal autocorrelation is greater for clay loam soils compared to sandy soils across all months, meaning that a broader range of drought index timescales correlate similarly with clay loam MPI time series compared to sand MPI time series (figure 2i-l and figure 6i-l). Thus, using a single timescale to represent clay loam soils at 60cm can produce a higher correlation value for the single indices and restrict composite indices improvement (figure 2i-l). Conversely, using a single timescale to represent soil water availability of sandy soils force timescales with low correlation values to be included into the time series, reducing overall correlation with the 60cm MPI (figure 6i-l). Using the composite of sandy soil types can thus lead to greater improvement at 60cm over clay loam soil types.

In general, the use of a single timescale to approximate MPI values is often not sensitive enough to capture the intra-annual precipitation variability of each MLRA (figure 2). Using a single timescale forces months that are less representative of MPI values (i.e. June, figure 2f) to be incorporated into the single timescale time series, producing overall lower correlation values with the MPI. The composite's ability to vary timescale monthly allows for better temporal resolution of soil water availability and improves correlations with the MPI for both the SPI and

SPEI. However, choice of multiscalar index, depth, and soil type can impact the increase in correlation value with the MPI when using the composite over a single timescale. Overall, the composite works best when used with the SPI, at shallow depths, and with soils that contain higher percentages of clay. At deeper depths, analyzing composite improvements are more nuanced as soil water distribution and autocorrelation become factors. Soil types with less clay content are less impacted by these factors at deeper depths and can thus gain more from composite usage.

Comparison of Composite-indices, Single-indices, and MPI Time Series

Examining the composite indices performance against the single indices shows that by varying the timescale monthly, the composite indices can track soil moisture variability more realistically than when using a single timescale (figure 7). The 5cm MPI, 4-month single-SPI (highest correlating single timescale for this depth and site), and composite-SPI from July 1992 through July 1994 are shown for a clay loam soil site in MLRA 40 (figure 7a). In July 1993, the 4-month single-SPI produced a z-score value that was -2.5 standard deviations less than 5cm MPI (figure 7d). During July, the 4-month single-SPI no longer represents precipitation from the cool season (fall and winter), which accounts for 55% of MAP in MLRA 40 (figure 2b). Furthermore, NAM precipitation is historically inconsistent in MLRA 40, which can lead to misrepresentation of drought conditions during the early monsoon and produce uncertainty when selecting the highest correlating timescale with the MPI during these months (i.e. June, figure 2f). In years when below average monsoon precipitation is observed in MLRA 40, shorter index timescales will cause overrepresentation of drought conditions (figure 7d) during the fore-summer months (figure 7b). Conversely, longer index timescale will be less impacted by dry summer fore-months, as these timescale lengths will still represent cool season precipitation

(figure7c). In this case, the composite-SPI, which used a 6-month timescale during July, still represented precipitation from the 1992-1993 cool season (figure 7c). This caused less impact of absent precipitation during early monsoon (i.e. July 1993) on the composite-SPI value, which allowed the composite-SPI to better represent 5cm MPI values (figure 7d).

The 60cm MPI, 7-month single-SPI, and composite-SPI from June 2007 through December 2009 are shown for a sand soil in MLRA 30 (figure 7h). On two separate occasions during September 2008 and 2009, the 7-month single-SPI underrepresented 60cm MPI values (figure 7f), with the 2009 occurrence being greater than -1 standard deviation lower. MLRA 30 has a unimodal precipitation distribution, with 70% of precipitation occurring during the cool season (figure 2a). On both occasions, the previous year's cool season precipitation was dropped from the 7-month single-SPI timescale during September (figure 7f), causing underestimation of 60cm MPI values. The composite-SPI, which uses an 11-month timescale during September (figure 7g), still captures cool season precipitation and thus better represents 60cm MPI values.

As previously mentioned, the SPI can produce unrealistic negative z-score values when encountering consecutive months with greater than 75% zeros included in the timescale (Gudmundsson and Stagge 2013; Stagg et al. 2015). By varying timescale length monthly, the composite-SPI can reduce the occurrence for this issue. The 5cm MPI, 6-month single-SPI, and composite-SPI for a clay loam soil in MLRA 40 are shown in figure 8d. During September, October, and November of 2020, the SPI encountered three consecutive months with greater than 75% zeros included in the 6-month timescale (figure 8b), causing unrealistic single-SPI values that were -3 standard deviations less the 5cm MPI (figure 8d). The composite-SPI, which used a 7-, 8-, and 10-month timescale during September, October, and November, respectively, never

encounter consecutive months of greater than 75% zeros in a monthly timescale (figure 8c) and thus better represented 5cm MPI values.

It should be noted that the composite-SPI did encounter two consecutive months with greater than 75% zeros in its monthly timescales during April and May 2021 (figure 8c). During these months, the composite used a 2- and 3- month timescale, respectively. In MLRA 40, spring months are commonly dry, and thus the 2- and 3- month timescales containing 100% zeros is not abnormal. Therefore, for the Southwest, it should be amended that the issue related to the SPI encountering zero precipitation months is relative to the season and timescale length being used (Wu et al. 2007).

While the composite often corrects for the SPI-zeros issue, instances do occur when the composite-SPI produces unrealistic z-score values. The 30cm MPI, 7-month single-SPI, and composite-SPI from January 1999 through January 2001 are shown for a loam soil in MLRA 30 (figure 8h). Above average summer precipitation during 1999 was followed by a dry fall (figure 8e). The composite-SPI used a 4-month timescale during December and January (figure 8g), respectively, to better represent intra-annual precipitation variability in MLRA 30 (figure 2a). In this case, as 4-month timescale no longer represented above average summer precipitation during 1999 (figure 8e), causing multiple zeros to be included into the composite-SPI timescale (figure 8g) and produce an unrealistic value (figure 8h). The single-SPI, which used a 7-month timescale (figure 8f), still captured summer 1999 precipitation, and did not encounter consecutive months with greater than 75% zero precipitation – allowing for better approximation of 30cm MPI values.

Cases involving the composite-SPI producing unrealistic values due to the zero's- issue are rare and often circumstantial, being the result of the composite-SPI using an equal or shorter

timescale than the single-SPI (figure 8e-h). Nevertheless, instances due occur despite overall correlations between the composite-SPI and MPI being higher. Whether using the single-SPI or composite-SPI, instances related to the zero's-issue are the result of some previous wet period being dropped from the index's timescale, causing more recent dry conditions to be overrepresented compared to MPI values. Furthermore, instances of the composite indices being more closely aligned with MPI values compared to the single indices are the result of some previous wet or dry period being dropped from the single indices timescale, leading to overrepresentation of current conditions (figure 7). A future 'smart-composite' will need to identify a process of extending the timescale during these cases.

Although not detailed here, the composite-SPEI also corrects for issues related to above or below average PET values causing errors between MPI and single-SPEI values. In these cases, varying monthly timescales of the composite-SPEI can better capture PET trends compared to the single-SPEI. In some cases, the composite-SPEI can produce higher correlations with the MPI over the composite-SPI (see outliers, figure 4). However, these cases are not the norm, and the composite-SPI still produces higher correlations with the MPI overall (figure 3).

CONCLUSION

This study created a monthly composite multiscalar index for the SPI and SPEI, respectively, to better approximate soil water availability at different depths for the Southwestern United States. Correlation values between the composite multiscalar indices and MPI were compared with correlation values between the single timescale multiscalar indices and MPI at 5cm, 30cm, and 60cm for six different soil types across the 240 study locations. Results show that both the composite-SPI and composite-SPEI significantly ($p<0.05$) improve correlation values with the MPI compared to when using a single timescale for all depths and soil types.

However, both composite indices see varying amounts of improvement over the use of a single timescale depending on depth and soil type chosen.

Higher correlations are observed between MPI values and the composite-SPI compared to the composite-SPEI. This is due to the SPI producing higher correlations and less error with the MPI compared to the SPEI (McKellar et al. 2022b). At shallow depths, closer alignment with annual precipitation distributions produce higher monthly correlation values between the composite indices and MPI, allowing for greater improvement when using the composite indices compared to deeper depths. At deeper depths, autocorrelation between timescales restricts composite index improvement over the use of a single timescale.

Composite correlation improvement with the MPI is also impacted by soil type. Significant differences were observed between soil types between shallow and deep depths based on clay percentage. Clay loam composite indices observer greater improvement at shallow depths due to higher monthly correlation values with the MPI compared to sandy soils. At deeper depths, autocorrelation between MPI values and multiscalar index timescales is higher in clay loam soils, leading to greater improvement between sand composite indices and single timescales.

Time series analysis demonstrated the usefulness of the composite index's ability to vary timescale length and better represent soil water availability compared to using a single timescale. Cases showed that errors produced between single-SPI and MPI values were caused by previous wet or dry periods being dropped from the moving timescale. By varying timescale length monthly, the composite index was able to still include these periods, producing values more aligned with the MPI. Additionally, the composite can correct for instances when the SPI depicts an unrealistic value due to consecutive months of greater than 75% zeros being included in the

single timescale. Although rare, instances can still occur when the composite is unable to correct for this issue, often being the result of the composite-SPI using a shorter monthly timescale than the single-SPI. Despite this, the composite most often corrects for discrepancies between the MPI and multiscalar indices, significantly improving correlations across all depths and soil types.

Overall, the approach of developing a timescale varying drought index has the potential to improve tracking soil water drought signals in climates with precipitation seasonality. This could enhance drought monitoring activities where tracking potential soil moisture drought impacts is critical. To fully optimize the composite indices, future work will need to focus on developing a smart-composite index that can better account for the remaining errors produced between composite and MPI values. Current errors between the composite indices are mainly caused by previous wet and dry periods being dropped from the moving timescale that have persisting effects on soil moisture values at a specified depth. Additionally, the composite-SPI, specifically, can still encounter instances when the moving timescale contains consecutive values of which greater than 75% are zeros. A smart-composite will need to recognize the occurrences that produce these errors and extend the timescale length accordingly. Furthermore, this study did not investigate the impacts of multiple soil horizons, different vegetation types, and runoff. Future work will need to focus on these issues to fully understand differences between composite and MPI values. Regardless, a timescale varying composite drought index does offer a simple way of enhancing the utility of the numerous efforts and platforms that already offer real time depictions of indices like the SPI and SPEI (e.g. Westwide Drought Tracker).

Accounting for the seasonal precipitation distribution allowed the composite indices to better approximate soil water availability over the use of a single timescale. While the composite indices varied timescale length during each month, dryland managers can make better use of the

SPI and SPEI by understanding general seasonal relationships between timescale length and soil water availability. By using shorter timescales during rainy seasons and longer timescales during dry seasons, dryland managers in the Southwest can make better informed decisions about land management activities. Accounting for soil type and depth will further improve the ability of the SPI and SPEI to accurately approximate soil water availability. Given the additional stress that climate change will create on dryland ecosystems, fully utilizing multiscalar index timescales during different seasons is key to applying drought monitoring strategies to management action.

FIGURES

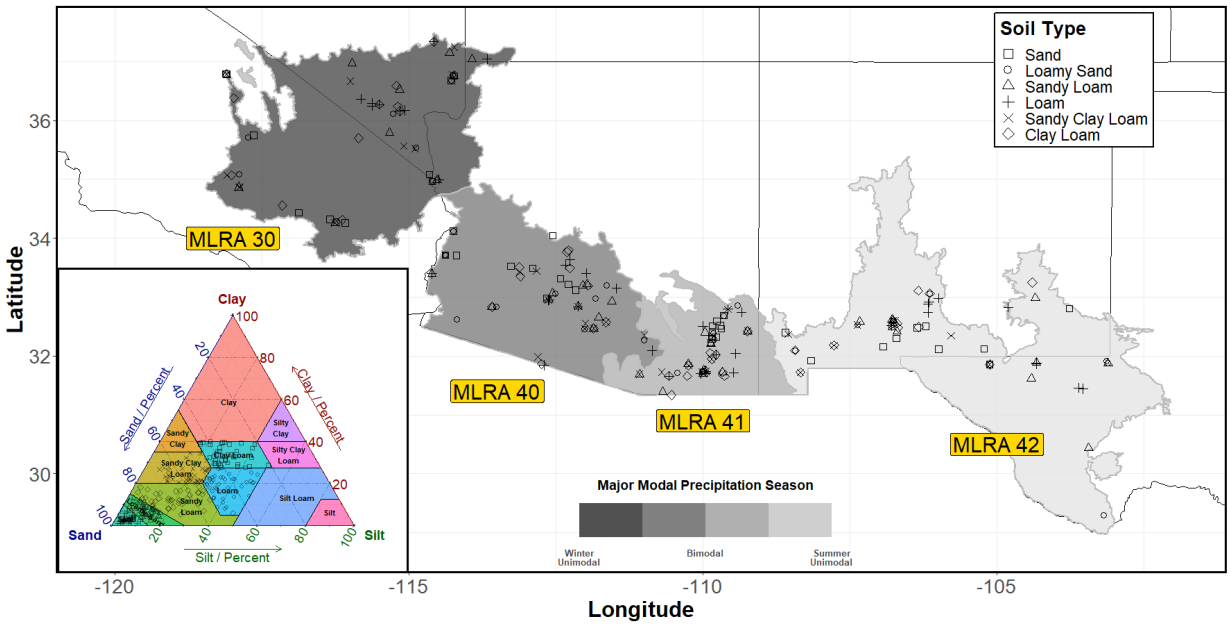

Figure 1: Major modal precipitation season and soil type for all 240 study locations. MLRAs across the study region receive most precipitation during either one (unimodal) or both (bimodal) seasons (cool and warm), reflected by the grey color scale. Study location point shape represents soil type. The percent sand, silt, and clay from each study site is shown on the soil ternary diagram in the bottom left.

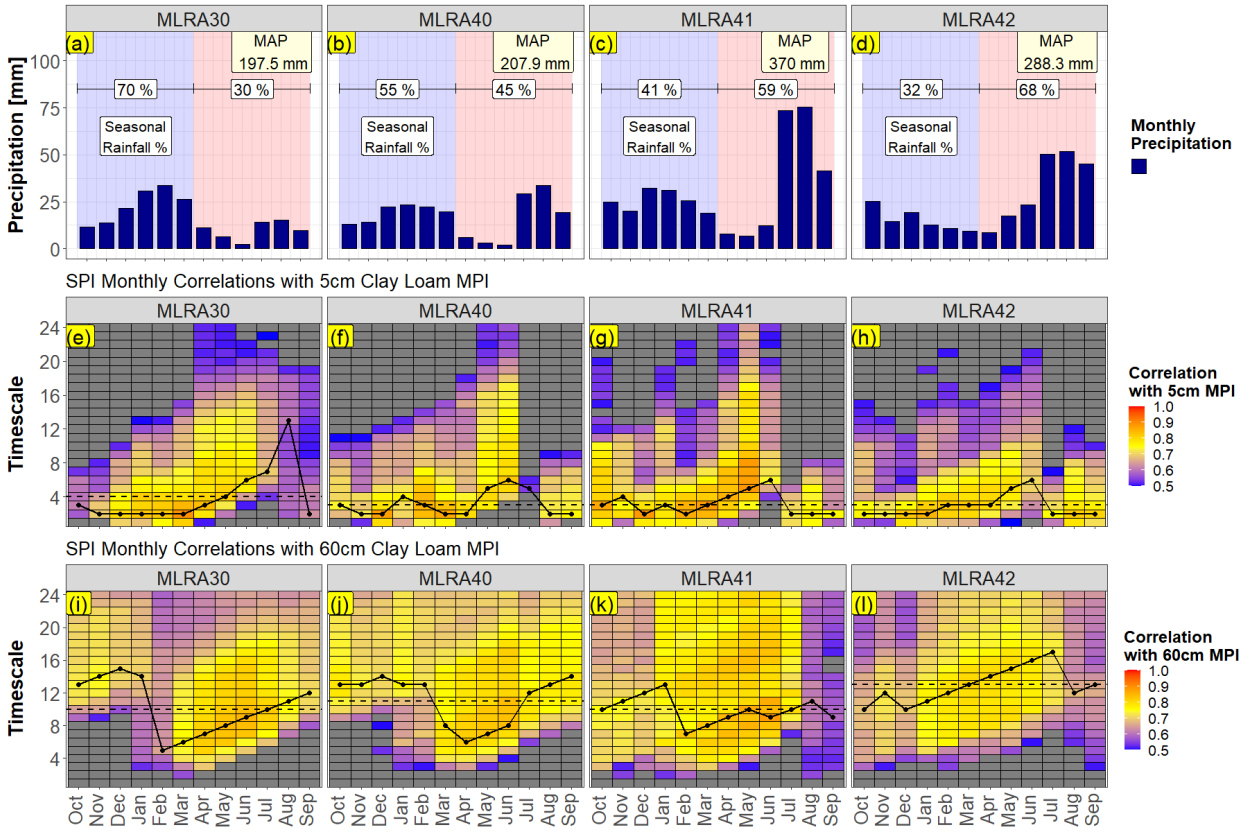

Figure 2: Monthly precipitation, mean annual precipitation (MAP), and seasonal rainfall percent of each MLRA (a-d). Mean monthly correlation values between the SPI and 5cm clay loam MPI (n=10) for each MLRA (e-h). Mean monthly correlation values between the SPI and 60cm clay loam MPI (n=10) for each MLRA (i-l). The composite-SPI (solid) plots through the highest correlating timescale at each month, while the single-SPI (dashed) plots through the average best annual correlating timescale. Grey boxes represent correlation values that are less than 0.5 or where $p>0.05$.

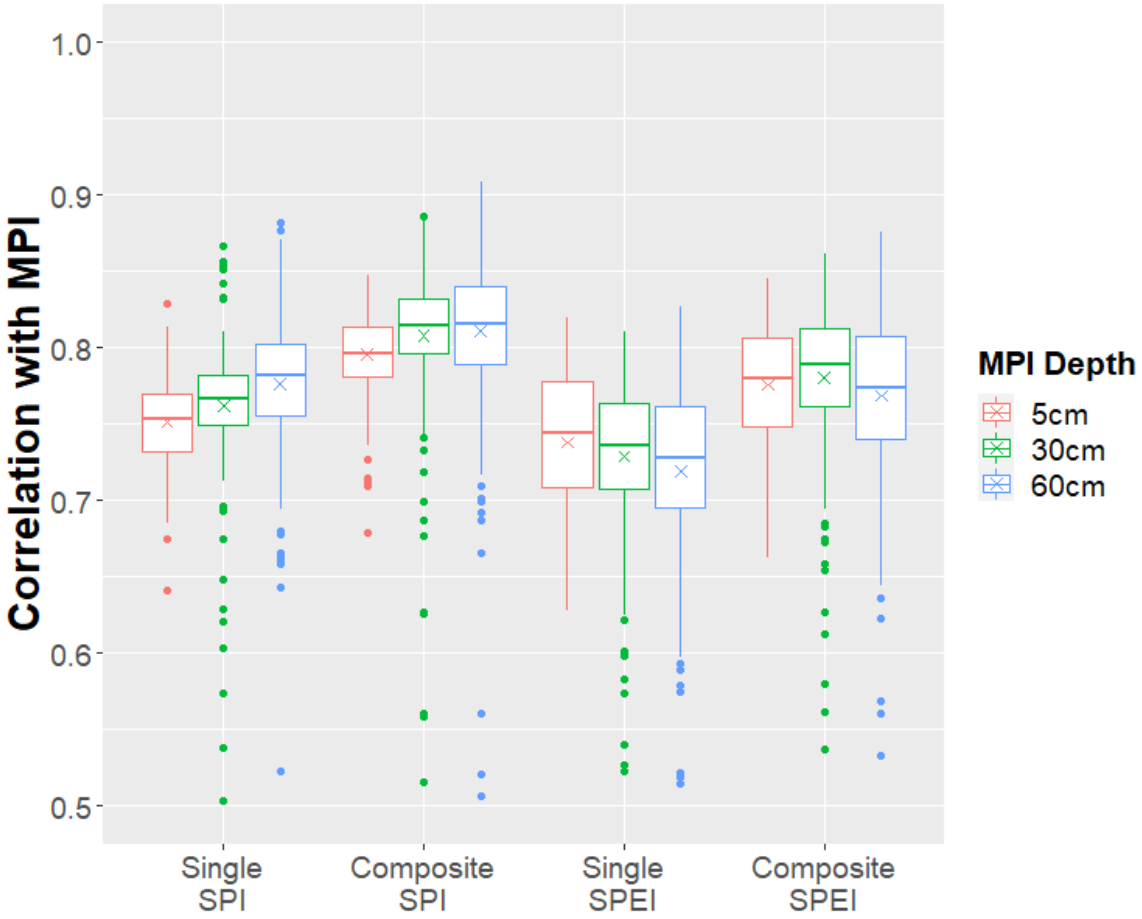

Figure 3: Pearson correlation values for all study sites (n=240) between the single indices and composite indices with the 5cm, 30cm, and 60cm MPI.

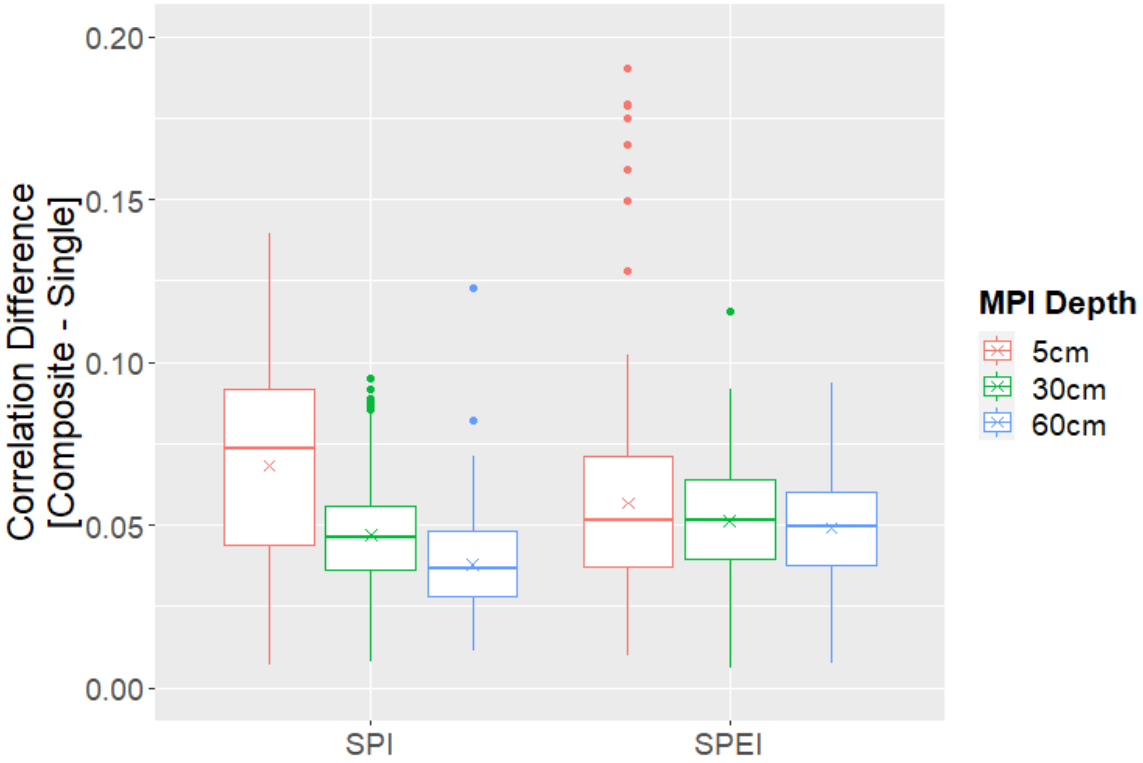

Figure 4: Pearson correlation differences between the composite and single indices [difference = composite – single] with the 5cm, 30cm, and 60cm MPI.

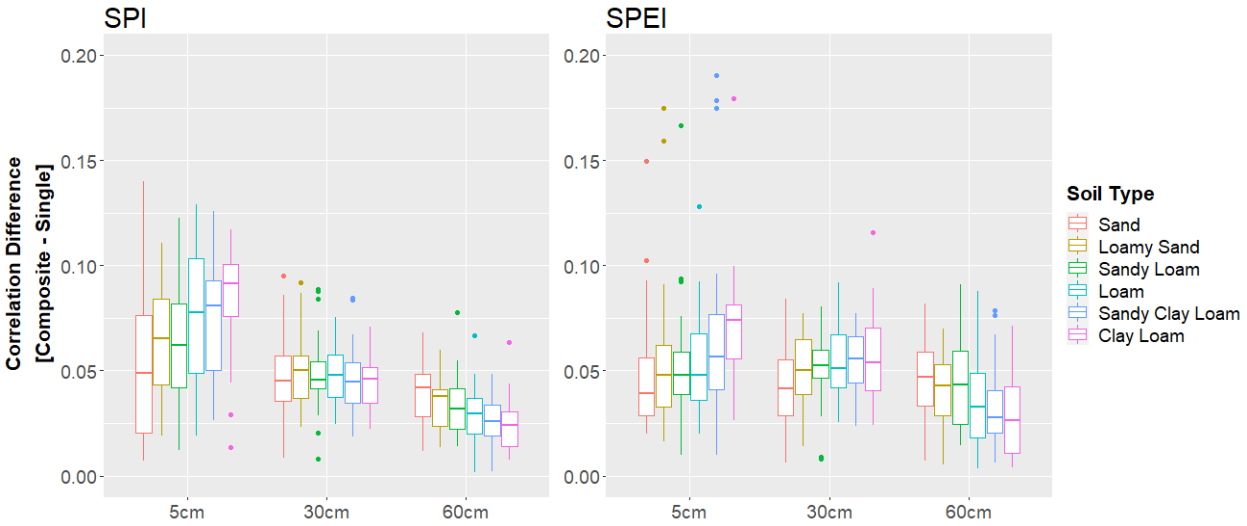

Figure 5: Pearson correlation differences between the composite and single indices with the 5cm, 30cm, and 60cm MPI by soil type.

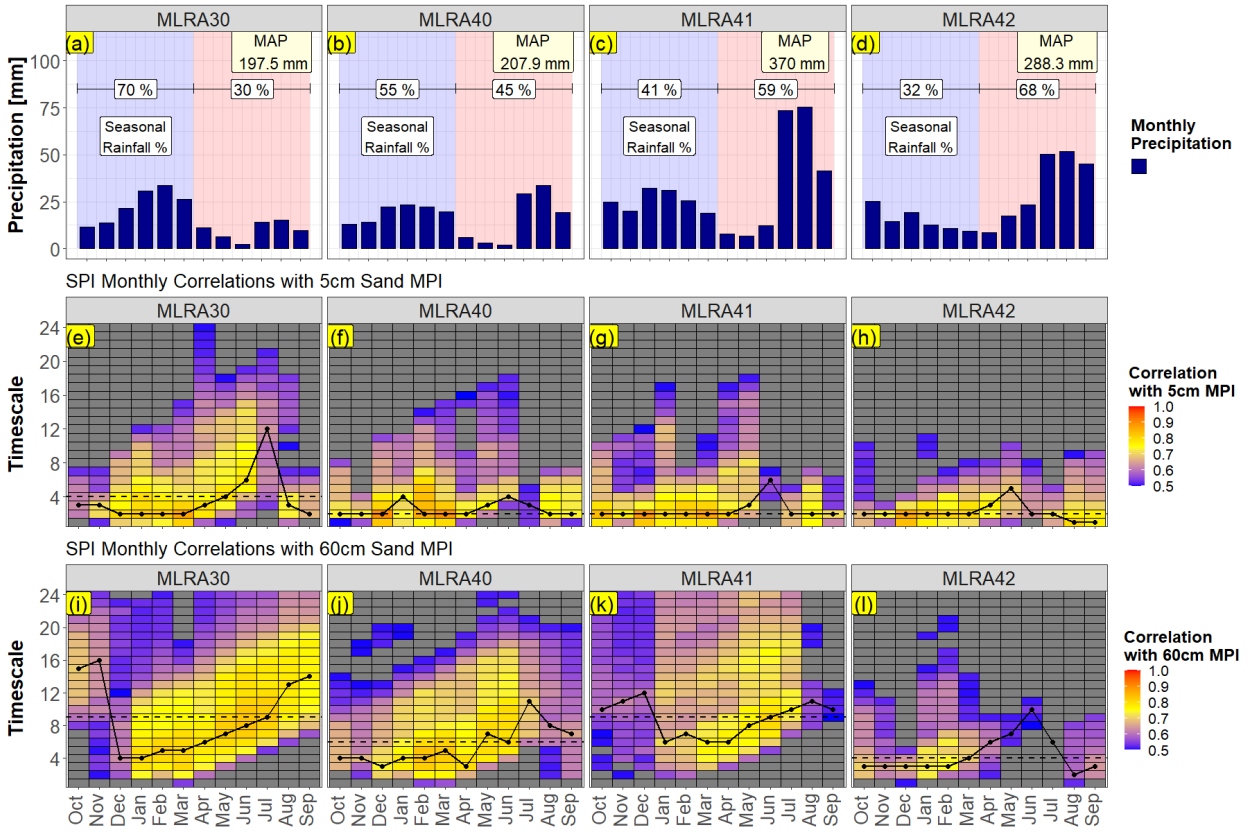

Figure 6: Monthly precipitation, mean annual precipitation (MAP), and seasonal rainfall percent of each MLRA (a-d). Mean monthly correlation values between the SPI and 5cm sand MPI (n=10) for each MLRA (e-h). Mean monthly correlation values between the SPI and 60cm sand MPI (n=10) for each MLRA (i-l). The composite-SPI (solid) plots through the highest correlating timescale at each month, while the single-SPI (dashed) plots through the average best annual correlating timescale. Grey boxes represent correlation values that are less than 0.5 or where $p>0.05$.

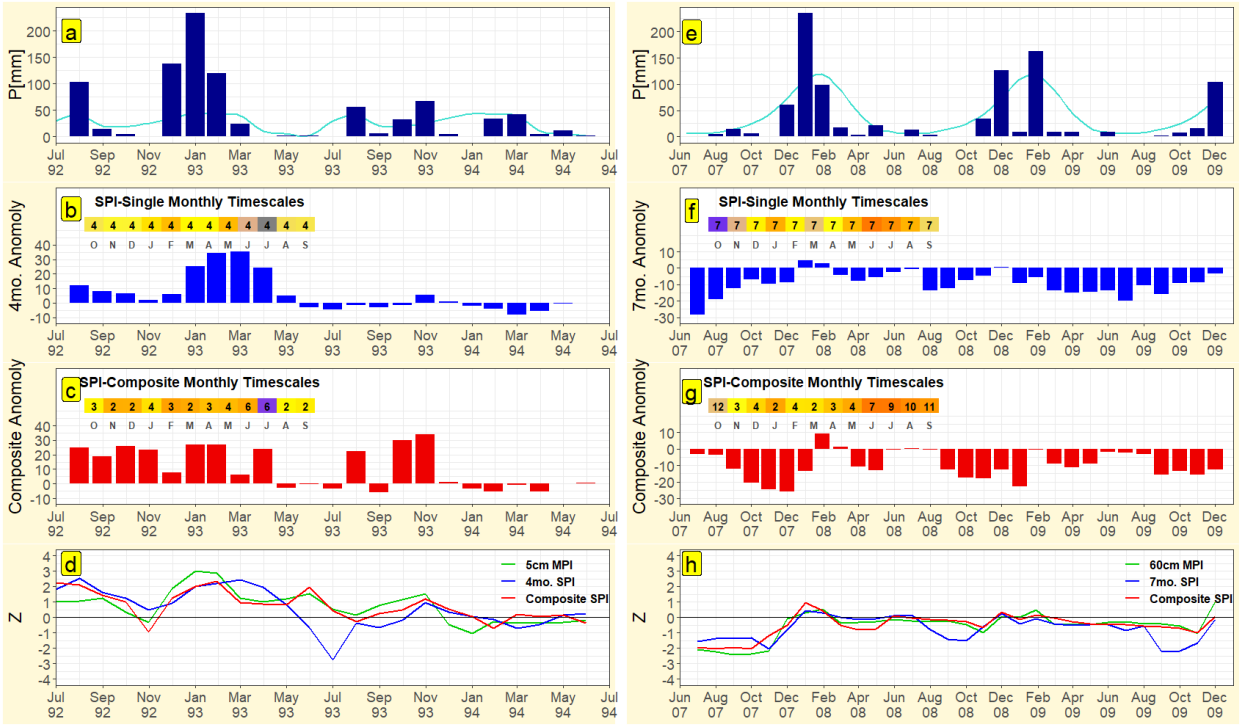

Figure 7: Monthly precipitation (a and e), SPI precipitation anomaly (b and f), composite precipitation anomaly (c and g). The 5cm MPI, 4-month single-SPI, and composite-SPI from July 1992 through July 1994 are shown for a clay loam soil in MLRA 40 (d). The 60cm MPI, 7-month single-SPI, and composite-SPI from June 2007 through December 2009 is shown for a sand soil in MLRA 30 (h). Highest correlating timescale lengths for each month used by the single-SPI (b and f) and composite-SPI (c and g), with color representing correlation value with MPI (red = 1, blue = 0.5, grey < 0.5).

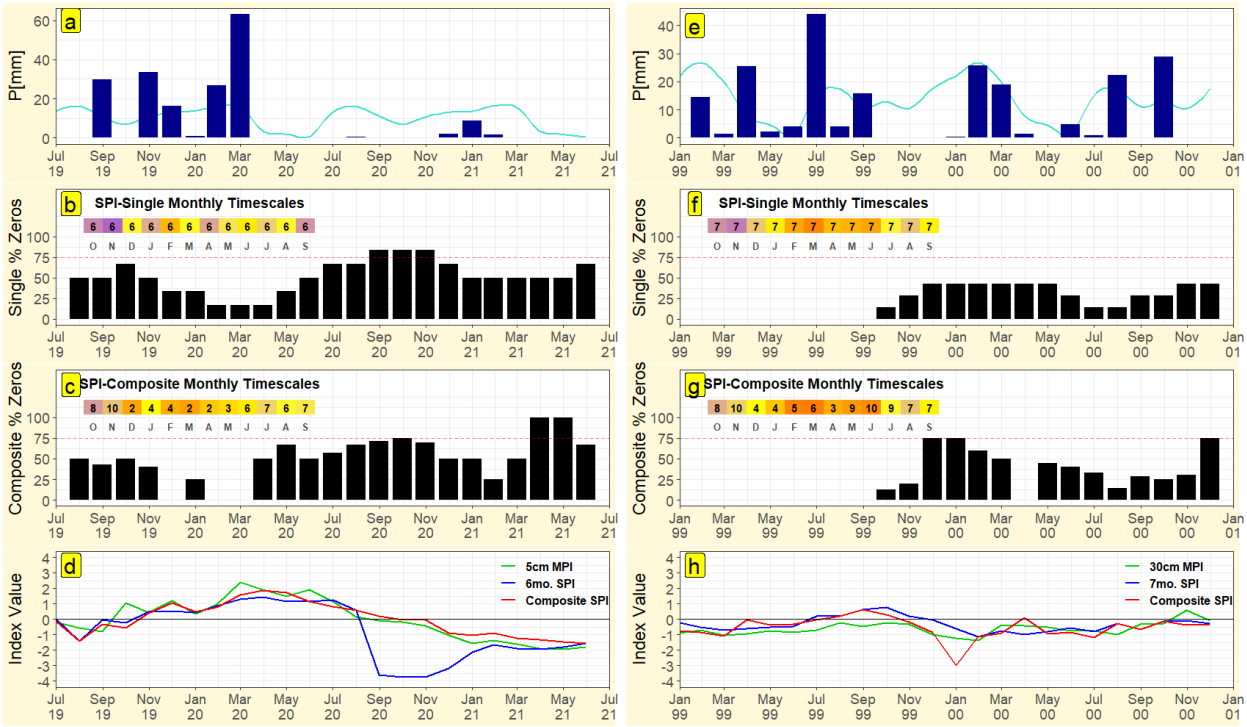

Figure 8: Monthly precipitation (a and e), the percent of zeros in the single-SPI timescale (b and f), percent of zeros in the composite-SPI timescale (c and g). The 5cm MPI, 6-month single-SPI and composite-SPI from July 2019 through July 2021 are shown for a clay loam soil in MLRA 40 (d). The 30cm MPI, 7-month single-SPI, and composite-SPI from January 1999 through January 2001 are shown for a loam soil in MLRA 30 (h). Highest correlating timescale lengths for each month used by the single-SPI (b and f) and composite-SPI (c and g), with color representing correlation value with MPI (red = 1, blue = 0.5, grey < 0.5).

REFERENCES

Abatzoglou, J. T. (2013). Development of gridded surface meteorological data for ecological applications and modelling. International Journal of Climatology, 33(1), 121-131.

Allen, R. G., Pereira, L. S., Raes, D., & Smith, M. (1998). Crop evapotranspiration-Guidelines for computing crop water requirements-FAO Irrigation and drainage paper 56. Fao, Rome, 300(9), D05109.

Austin, M. E. (1965). *Land resource regions and major land resource areas of the United States (exclusive of Alaska and Hawaii)* (No. 296-301). Soil Conservation Service, US Department of Agriculture.

Barnard, D. M., Germino, M. J., Bradford, J. B., O'Connor, R. C., Andrews, C. M., & Shriver, R. K. (2021). Are drought indices and climate data good indicators of ecologically relevant soil moisture dynamics in drylands?. Ecological Indicators, 133, 108379.

Beaudette, D. E., Skovlin, J., Roecker, S., & Beaudette, M. D. (2022). Package 'soilDB'.

Beguería, S., Vicente-Serrano, S. M., Reig, F., & Latorre, B. (2014). Standardized precipitation evapotranspiration index (SPEI) revisited: parameter fitting, evapotranspiration models, tools, datasets and drought monitoring. International journal of climatology, 34(10), 3001-3023.

Biederman, J. A., Scott, R. L., Arnone III, J. A., Jasoni, R. L., Litvak, M. E., Moreo, M. T., ... & Vivoni, E. R. (2018). Shrubland carbon sink depends upon winter water availability in the warm deserts of North America. Agricultural and Forest Meteorology, 249, 407-419.

Crausbay, S. D., Ramirez, A. R., Carter, S. L., Cross, M. S., Hall, K. R., Bathke, D. J., ... & Sanford, T. (2017). Defining ecological drought for the twenty-first century. Bulletin of the American Meteorological Society, 98(12), 2543-2550.

Crimmins, M. A., Ferguson, D. B., Meadow, A. M., & Weiss, J. L. (2017). Discerning "flavors" of drought using climate extremes indices. Journal of Applied Meteorology and Climatology, 56(4), 989-1001.

Daly, C., Neilson, R. P., & Phillips, D. L. (1994). A statistical-topographic model for mapping climatological precipitation over mountainous terrain. Journal of Applied Meteorology and Climatology, 33(2), 140-158.

Dorigo, W. A., Wagner, W., Hohensinn, R., Hahn, S., Paulik, C., Xaver, A., ... & Jackson, T. (2011). The International Soil Moisture Network: a data hosting facility for global in situ soil moisture measurements. Hydrology and Earth System Sciences, 15(5), 1675-1698.

Gremer, J. R., Bradford, J. B., Munson, S. M., & Duniway, M. C. (2015). Desert grassland responses to climate and soil moisture suggest divergent vulnerabilities across the southwestern United States. Global Change Biology, 21(11), 4049-4062.

Gudmundsson, L., & Stagge, J. H. (2016). Package "SCI": Standardized Climate Indices Such as SPI, SRI or SPEI, v1. 0-2, CRAN [code].

Hadley, N. F., & Szarek, S. R. (1981). Productivity of desert ecosystems. BioScience, 31(10), 747-753.

Hottenstein, J. D., Ponce-Campos, G. E., Moguel-Yanes, J., & Moran, M. S. (2015). Impact of varying storm intensity and consecutive dry days on grassland soil moisture. Journal of Hydrometeorology, 16(1), 106-117.

Jenerette, G. D., Scott, R. L., & Huete, A. R. (2010). Functional differences between summer and winter season rain assessed with MODIS-derived phenology in a semi-arid region. Journal of Vegetation Science, 21(1), 16-30.

Lauenroth, W. K., & Bradford, J. B. (2006). Ecohydrology and the partitioning AET between transpiration and evaporation in a semiarid steppe. Ecosystems, 9(5), 756-767.

Li, L., Qian, R., Liu, W., Wang, W., Biederman, J. A., Zhang, B., ... & Wang, Y. (2022). Drought timing influences the sensitivity of a semiarid grassland to drought. Geoderma, 412, 115714.

Loik, M. E., Breshears, D. D., Lauenroth, W. K., & Belnap, J. (2004). A multi-scale perspective of water pulses in dryland ecosystems: climatology and ecohydrology of the western USA. Oecologia, 141(2), 269-281.

Majumder, D., & Kumar, B. (2019). Estimation of monthly average pet by various methods and its relationship with pan evaporation at Bhagalpur, Bihar. Journal of Pharmacognosy and Phytochemistry, 8(1), 2481-2484.

McKee, T. B., Doesken, N. J., & Kleist, J. (1993, January). The relationship of drought frequency and duration to time scales. In Proceedings of the 8th Conference on Applied Climatology (Vol. 17, No. 22, pp. 179-183).

Neilson, R. P., King, G. A., & Koerper, G. (1992). Toward a rule-based biome model. Landscape Ecology, 7(1), 27-43.

Noy-Meir, I. (1973). Desert ecosystems: environment and producers. Annual review of ecology and systematics, 4(1), 25-51.

Robock, A., Mu, M., Vinnikov, K., Trofimova, I. V., & Adamenko, T. I. (2005). Forty-five years of observed soil moisture in the Ukraine: No summer desiccation (yet). Geophysical Research Letters, 32(3).

Romero-Lankao, P., Smith, J. B., Davidson, D. J., Diffenbaugh, N. S., Kinney, P. L., Kirshen, P., ... & Villers Ruiz, L. (2014). North America. Climate Change 2014: impacts, adaptation, and vulnerability part B: regional aspects contribution of working group II to the Fifth Assessment Report of the Intergovernmental Panel of Climate Change.

Salley, S. W., Talbot, C. J., & Brown, J. R. (2016). The Natural Resources Conservation Service land resource hierarchy and ecological sites. Soil Science Society of America Journal, 80(1), 1-9.

Schlaepfer, D. R., Lauenroth, W. K., & Bradford, J. B. (2012). Ecohydrological niche of sagebrush ecosystems. Ecohydrology, 5(4), 453-466.

Shepard, C., Schaap, M. G., Crimmins, M. A., Van Leeuwen, W. J., & Rasmussen, C. (2015). Subsurface soil textural control of aboveground productivity in the US Desert Southwest. Geoderma Regional, 4, 44-54.

Sims, A. P., Niyogi, D. D. S., & Raman, S. (2002). Adopting drought indices for estimating soil moisture: A North Carolina case study. Geophysical Research Letters, 29(8), 24-1.

Simunek, J., Sejna, M., Van Genuchten, M. T., Šimůnek, J., Šejna, M., Jacques, D., & Sakai, M. (1998). HYDRUS-1D. Simulating the one-dimensional movement of water, heat, and multiple solutes in variably-saturated media, version, 2.

Stagge, J. H., Tallaksen, L. M., Gudmundsson, L., Van Loon, A. F., & Stahl, K. (2015). Candidate distributions for climatological drought indices (SPI and SPEI). International Journal of Climatology, 35(13), 4027-4040.

Stagge, J. H., Tallaksen, L. M., Xu, C. Y., & Van Lanen, H. A. (2014). Standardized precipitation-evapotranspiration index (SPEI): Sensitivity to potential evapotranspiration model and parameters. In Hydrology in a changing world (Vol. 363, pp. 367-373).

Svoboda, M. D., & Fuchs, B. A. (2016). Handbook of drought indicators and indices (pp. 1-44). Geneva, Switzerland: World Meteorological Organization.

Thornthwaite, C. W. (1948). An approach toward a rational classification of climate. Geographical review, 38(1), 55-94.

Vicente-Serrano, S. M., & Beguería, S. (2016). Comment on 'Candidate distributions for climatological drought indices (SPI and SPEI)'by James H. Stagge et al. International Journal of Climatology, 36(4), 2120-2131.

Wang, H., Rogers, J. C., & Munroe, D. K. (2015). Commonly used drought indices as indicators of soil moisture in China. Journal of Hydrometeorology, 16(3), 1397-1408.

Wilcox, B. P., Seyfried, M. S., Breshears, D. D., Stewart, B., & Howell, T. (2003). The water balance on rangelands. Encyclopedia of water science, 791(4).

Wu, H., Svoboda, M. D., Hayes, M. J., Wilhite, D. A., & Wen, F. (2007). Appropriate application of the standardized precipitation index in arid locations and dry seasons. International Journal of Climatology: A Journal of the Royal Meteorological Society, 27(1), 65-79.